TR-792-8-306

NUMERICAL SOLUTION OF FLOW FIELDS SURROUNDING SATURN TYPE VEHICLES

Nortronics-Huntsville Technical Report No. 382

June 1968

by

J. W. Hooie
T. J. Thomas
F. B. Tatom
Dr. J. C. Williams III

PREPARED FOR:

NATIONAL AERONAUTICS AND SPACE ADMINISTRATION
GEORGE C. MARSHALL SPACE FLIGHT CENTER
AERO-ASTRODYNAMICS LABORATORY

under contract **NAS8-20409**

N68 28309

Reviewed and Approved by

F. B. Tatom

F. B. Tatom, Aero/Thermodynamics Branch

W. G. Eaton

W. G. Eaton, Director, Space Sciences Section

NORTRONICS - HUNTSVILLE
HUNTSVILLE, ALABAMA

FOREWORD

This report presents the results of the work performed by Nortronics-Huntsville under Contract NAS8-20409 with the Aero-Astrodynamics Laboratory, Marshall Space Flight Center. Technical coordination was provided by Mr. Joseph L. Sims of the Fluid Mechanics Research Office, Aerophysics Division, Aero-Astrodynamics Laboratory, George C. Marshall Space Flight Center.

SUMMARY

Nortronics-Huntsville, under Contract NAS8-20409 with the Aero-Astrodynamics Laboratory, George C. Marshall Space Flight Center, has developed numerical techniques and computer programs which can be used to predict the entire steady-state flow field around Saturn-type vehicles at zero angle of attack.

The basic guidelines that were used in this research effort are:

(1) The bodies were restricted to bodies of revolution.

(2) An ideal, inviscid gas with a supersonic free-stream velocity was used.

(3) All shock waves in the flow field were treated as discrete discontinuities.

(4) Separated flow phenomena were not considered.

Because of the geometry of the bodies and the flow conditions, both subsonic and supersonic flow regions were considered. Each such region was treated separately after which the resulting flow fields were coupled together. A time-dependent finite-difference technique similar to that developed by Moretti and Abbett was used to compute the subsonic flow region behind detached bow shocks of blunt- and sharp-nose bodies. The technique treats the shock wave as a movable discrete discontinuity while the boundary conditions advance in time by the use of a quasi-one-dimensional method of characteristics. In a similar manner, the flow field about an expanding frustum with a slope too large to support supersonic flow was computed by a time-dependent finite-difference technique. A Taylor-Maccoll numerical integration technique was used to compute the flow around a sharp-nose body when the shock wave was attached. The supersonic flow regions around the cylindrical sections of the body were computed with a two-dimensional method of characteristics.

The techniques used in this research effort should prove to be valuable tools for predicting the complete inviscid, steady-state flow field around Saturn-type vehicles. The techniques developed for the calculation of the subsonic field around a frustum is the only known means available for this type of calculation. However, due to the lack of available data for comparison, the results for the frustum have not been validated.

TABLE OF CONTENTS

LIST OF ILLUSTRATIONS

LIST OF ILLUSTRATIONS (Concluded)

LIST OF SYMBOLS

Symbol	Title
ENGLISH	
A	Lowest node point on shock wave.
A1	A point in the grid system at time T_o found by the intersection of a characteristic issued from point Q1 and the time T_o plane.
A2	A point in the grid system determined by the intersection of a characteristic issued at point Q2 and the time T_o plane.
A3	A point in the grid mesh determined by the intersection of a characteristic issued from point Q3 and the time T_o plane.
a	The nondimensional speed of sound.
B	Lowest node point on body.
B3	A point in the grid mesh determined by the intersection of a characteristic issued from point Q3 and the time T_o plane.
b	Horizontal distance from Blunt Body axes to body surface.
C	Uppermost node point on shock wave.
C_v	Specific heat of gas.
D	Uppermost node point on body.
D	A convenient grouping of terms in a coordinate transformation $[(v_z - \xi W + v_r E)/\delta]$.
D'	The sonic point on the rounded shoulder of a frustum.
D''	A point downstream of the location of the intersection of the limiting characteristic and the frustum shoulder.
E	Point of intersection of a limiting characteristic and the body.
E	A convenient grouping of terms in a coordinate transformation $[(\xi-1) \cot \phi - \xi \cot \theta]$.
F	If the grid system extends above the body, the grid point that is located at the intersection of the uppermost horizontal grid line and the vertical (transformed) grid line which includes the body.
g	Any fluid property.
H	The right-hand side of the compatibility equation for the shock characteristics. H contains the forcing terms resulting from the cross flow superimposed on the characteristics.

LIST OF SYMBOLS (Continued)

I	A node point index in the horizontal direction.
J	A node point index in the vertical direction.
K	The right-hand side of the compatibility equation for the body characteristics. K contains the forcing terms resulting from the cross flow superimposed on the characteristics.
L_o	A reference length.
M	Mach number.
N	The right-hand side of a compatibility equation for frustum flow. N includes the effects due to a superimposed cross flow.
P	Some point within the grid system.
P	The natural log of the pressure ratio.
p	Nondimensional pressure of gas (see Subsection 2.2.2.1).
Q	A node point on the shock at time T_o.
Q	In frustum flow, a grid point located on the cylinder preceeding the frustum at time T_o.
Q1	A node point on the shock at time $T_o + \Delta T$.
Q2	A node point on the body.
Q3	In frustum flow, a node point located on the cylinder at time $T_o + \Delta t$.
R	Nondimensional radial coordinate for Blunt Body formulation (see Subsection 2.2.2.1).
R	The natural log of the density ratio.
R_L	The radius of the cylindrical section immediately preceeding a frustum.
r	Nondimensional radial coordinate for Blunt Body formulation (see Subsection 2.2.2.1).
s	Nondimensional entropy of gas (see Subsection 2.2.2.1).
T	Nondimensional time in transformed plane (identically equal to t).
T_o	Some initial time when all fluid properties are known at all of the grid points.
t	Nondimensional time (see Subsection 2.2.2.1).
U	The nondimensional velocity component along the σ axis.
V	The nondimensional free stream velocity.
V	The nondimensional velocity component along the υ axis.
$\bar{V}$	The nondimensional velocity vector at point P.
v_r	Nondimensional radial gas velocity component (see Subsection 2.2.2.1).

LIST OF SYMBOLS (Continued)

v_z Nondimensional axial gas velocity component (see Subsection 2.2.2.1).

W The nondimensional horizontal shock velocity.

Z Nondimensional axial coordinate for master polar coordinate system (see Subsection 2.2.2.1).

z Nondimensional axial coordinate in Blunt Body formulation (see Subsection 2.2.2.1).

GREEK

γ The specific heat ratio of the gas.

ΔT The nondimensional time step in the transformed plane. Identically equal to Δt.

Δt The nondimensional time step in the real plane for advancing the flow values in time.

$\Delta\eta$ The nondimensional vertical distance between the transformed vertical node points.

$\Delta\xi$ The nondimensional horizontal distance between the transformed node points.

δ Horizontal distance between shock and body.

η Transformed vertical coordinate.

θ The angle between a tangent to the shock and horizontal.

ν An axis of a coordinate system used such that ν is either

1. Tangential to the shock
2. Tangential to the body
3. Perpendicular to the z axis (frustum only).

ξ Trnasformed horizontal coordinate.

ρ Nondimensional density of gas (see Subsection 2.2.2.1).

σ An axis of a coordinate system used such that σ is either

1. Perpendicular to the shock
2. Perpendicular to the body
3. Parallel to the z axis (frustum only).

ϕ The angle between a tangent to the body and horizontal.

SUPERSCRIPTS

' A prime denotes a dimensional flow property.

SUBSCRIPTS

A1 Pertaining to point A1.

A2 Pertaining to point A2.

LIST OF SYMBOLS (Concluded)

A3	Pertaining to point A3.
B3	Pertaining to point B3.
Q	Pertaining to point Q.
Q1	Pertaining to point Q1.
Q2	Pertaining to point Q2.
Q3	Pertaining to point Q3.
∞	Free stream conditions.

Section I

INTRODUCTION

Prediction of flow fields around space vehicles during atmospheric flight has received increased interest due to the rapid advancement in space flight technology. Analytical determination of the flow conditions characteristic of a vehicle during flight is necessary because successful design of space systems cannot be obtained without prior knowledge of these flow conditions. Development of an accurate and practical method of predicting or describing this flow field has been and continues to be a challenge to the aerospace industry.

Nortronics-Huntsville, Huntsville, Alabama, under Contract NAS8-20409 with the Aero-Astrodynamics Laboratory of Marshall Space Flight Center, has been engaged in a research effort concerned with developing techniques and computer programs capable of describing the entire flow field about Saturn-type bodies at zero angle of attack.

Section II of this report provides a detailed discussion of the techniques for solving the governing differential equations of motion for the flow field. The computer programs into which these techniques have been incorporated are discussed in Section III. Discussion of the results of this research effort is given in Section IV. Section V summarizes the pertinent conclusions derived from this investigation and suggests various possibilities for future improvements.

Section II

TECHNICAL DISCUSSION

2.1 NATURE OF THE PROBLEM

The steady-state flow field around Saturn-type vehicles consists of subsonic and supersonic flow regions with shock waves. The flow problems under specific consideration may be classified as follows:

(1) An ideal, inviscid, supersonic free stream of gas flowing around a blunt-nose body of revolution consisting of cylindrical sections and conical frustums. The frustums have slopes that are too large to support supersonic flow.

(2) An ideal, inviscid, supersonic free stream of gas flowing around a sharp-nose body of revolution consisting of cylindrical sections and conical frustums which do not support supersonic flow.

These two flow fields can be further divided into flow regions according to the type of flow and the geometry of portions of the vehicle. The specific regions investigated are

(1) Blunt-nose body (subsonic)
(2) Sharp-nose body (subsonic or supersonic)
(3) Cylindrical section of body (supersonic)
(4) Frustum (subsonic).

The entire flow field around a Saturn-type vehicle can be predicted by proper coupling of these four flow regions.

The subsonic regions are governed by differential equations of motion that are elliptic in nature, while the supersonic regions are governed by hyperbolic differential equations. Because the solution of this set of mixed equations can not generally be obtained by one single mathematical technique, the subsonic and supersonic flow fields must be treated separately. The computed flow regions must then be joined together in a manner which does not alter the adjoining flow regions. Figure 2-1 illustrates the relative size and location of the different types of flow regions for a Saturn-type vehicle with a blunt-nose body. Notice should be taken that the frustum of Figure 2-1 has a slope too large to support supersonic flow.

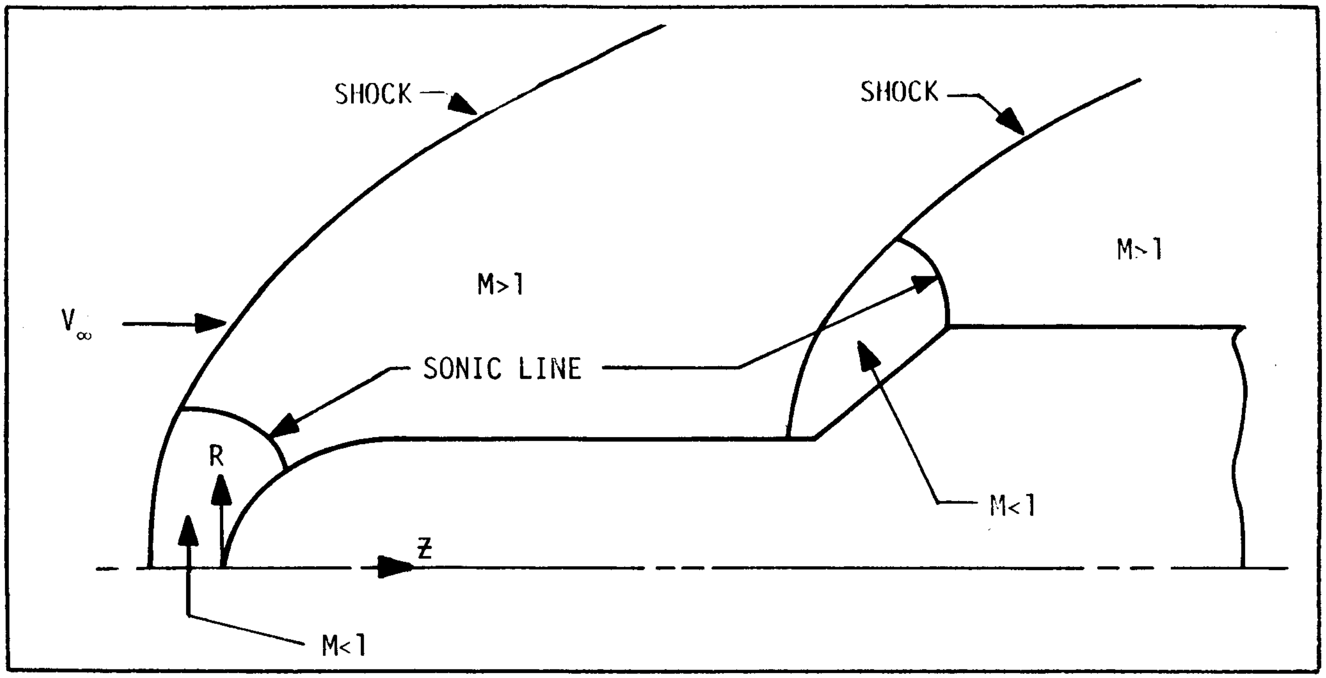

Figure 2-1. BLUNT-NOSE BODY FLOW FIELD

2.2 BLUNT BODY

2.2.1 Selection of Techniques

A number of approaches have been proposed for solving the steady-state, two-dimensional flow field around a blunt body with a detached shock wave. Van Dyke (ref. 1) has shown that existing analytical solutions are not sufficiently accurate to predict the details of the flow field and recent efforts have centered on numerical techniques for determining the flow field. Investigations of two-dimensional flow fields around blunt bodies have utilized various numerical techniques such as inverse methods (ref. 2), series expansions (ref. 3), perturbation of coordinates (ref. 4), artificial viscosity (ref. 5), strip (ref. 6), and time-dependent finite differences (refs. 7 through 10). Each of these techniques has advantages and disadvantages characteristic of the particular approach.

After a study of a number of these techniques, Moretti and Abbett (ref. 9) developed a time-dependent finite difference technique. The unsteady motion process of Moretti and Abbett is governed by a set of differential equations that are hyperbolic. The steady-state condition is approached asymptotically as the computation progresses. Some of the desirable characteristics of this technique are:

(1) It is a direct method in the sense that the body geometry is prescribed and controls the subsequent computation.

(2) The desired accuracy of the solution is set by the input spatial grid size, and not by a reformulation of the analysis. However, the relative short computation time required on a high speed computer increases with the desired increase in accuracy.

(3) The method is not restricted to a simplified thermodynamical model.

(4) The shock wave is considered a discrete discontinuity, which is more realistic than one several mesh-sizes thick, as assumed in some of the other techniques.

In general, the technique of Moretti and Abbett appears to offer the best method for obtaining a rapid, accurate solution to the blunt-body problem. Accordingly, the method adopted and described in subsequent subsections for the blunt body is essentially the same as that described in reference 9.

2.2.2 Interior Points

2.2.2.1 Development of Governing Differential Equations - A body-fixed polar coordinate system (Figure 2-2) is used in the blunt-nose body and frustum formulations. However, a master polar coordinate system, which originates at the nose of the vehicle (Figure 2-1), is used when the flow regions are coupled. The variables for a general flow problem are usually nondimensionalized so that the results are applicable to more than one particular body. The non-dimensional parameters used in this report are

$$v_z = v_z' \sqrt{\rho_\infty'/p_\infty'}$$

$$v_r = v_r' \sqrt{\rho_\infty'/p_\infty'}$$

$$s = \frac{s' - s_\infty'}{c_v}$$

$$p = p'/p_\infty'$$

$$\rho = \rho'/\rho_\infty'$$

$$t = \frac{t'}{L_o} \sqrt{p_\infty'/\rho_\infty'}$$

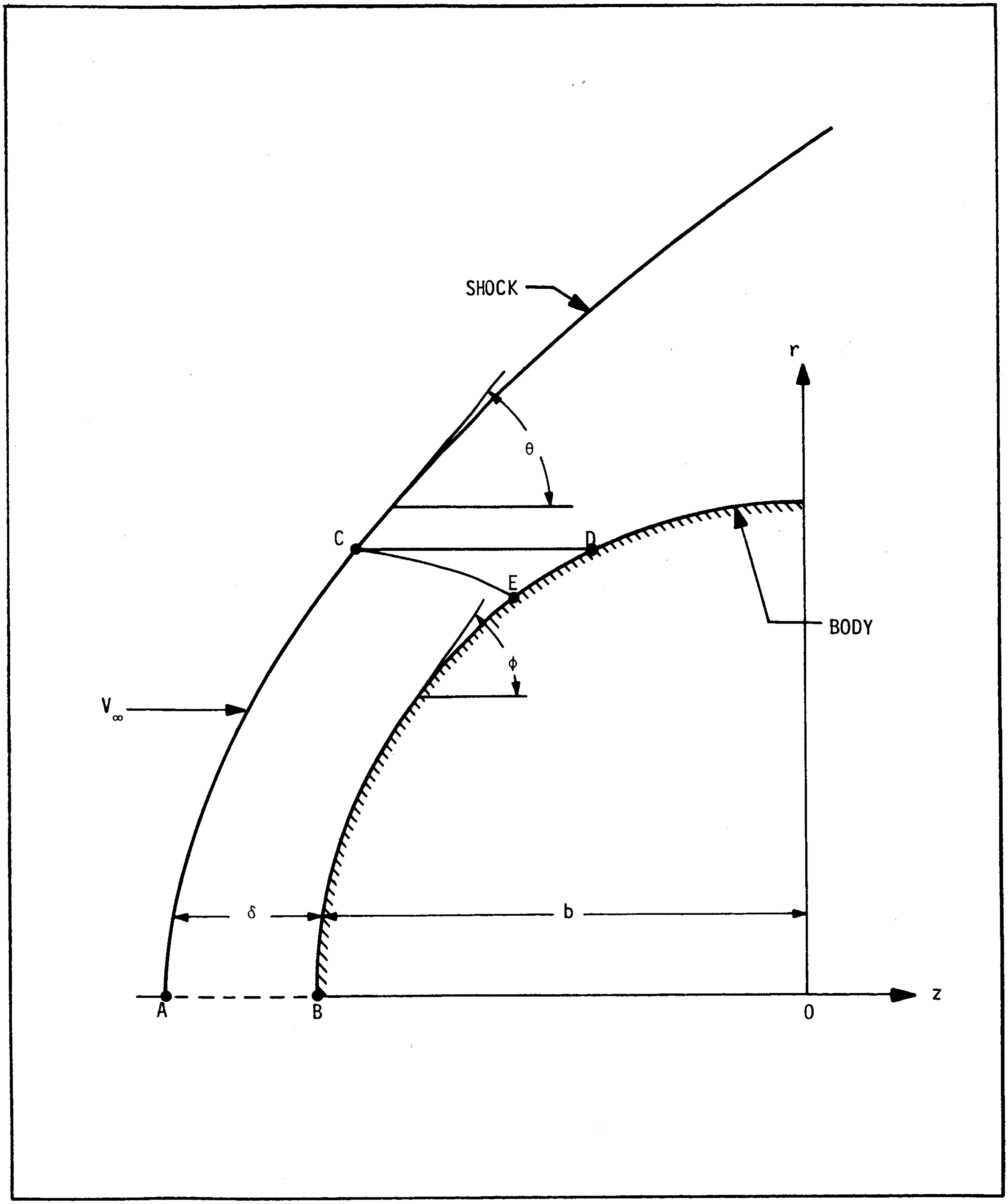

Figure 2-2. PHYSICAL PLANE

and all lengths are divided by L_o, a characteristic length.

The equations of motion in the physical plane, written in terms of dimensionless parameters, are

$$\frac{\partial \rho}{\partial t} + \frac{1}{r}\frac{\partial}{\partial r}(\rho v_r r) + \frac{\partial}{\partial z}(\rho v_z) = 0 \qquad (1)$$

$$\rho\left(\frac{\partial v_r}{\partial t} + v_r \frac{\partial v_r}{\partial r} + v_z \frac{\partial v_r}{\partial z}\right) + \frac{\partial p}{\partial r} = 0 \qquad (2)$$

$$\rho\left(\frac{\partial v_z}{\partial t} + v_r \frac{\partial v_z}{\partial r} + v_z \frac{\partial v_z}{\partial z}\right) + \frac{\partial p}{\partial z} = 0 \qquad (3)$$

$$\frac{\partial s}{\partial t} + v_r \frac{\partial s}{\partial r} + v_z \frac{\partial s}{\partial z} = 0 \qquad (4)$$

These equations are valid for axisymmetric flow fields composed of an ideal, inviscid gas with no heat addition.

Because a time-dependent finite-difference technique is used to compute the interior points (region inside ABCD of Figure 2-2) flow properties, a uniform mesh grid is desired for simplicity in formulating expressions for the partial derivatives. By means of a coordinate transformation the physical plane of Figure 2-2 can be molded into a rectangular region as shown in Figure 2-3.

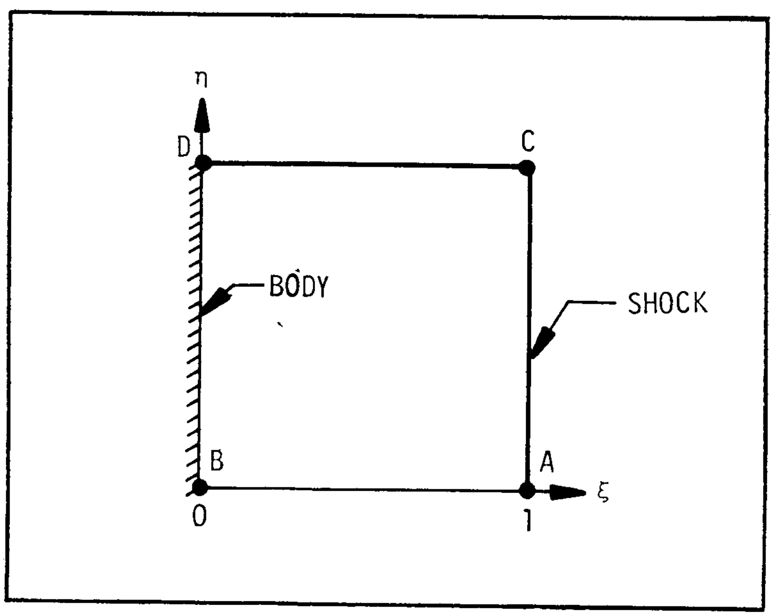

Figure 2-3. TRANSFORMED PLANE

The coordinate transformations which are used to transform equations (1) through (4) into the transformed plane are

$$\xi = \frac{z - b}{\delta}$$

$$\eta = r$$

$$T = t \quad .$$

This transformation allows the physical space between the shock and body to vary with time, while the transformed space is not affected. That is, the shock moves until the steady-state location of the shock is found. Thus, for a specified blunt-body shape, the corresponding shock wave configuration and location can be found for the steady-state condition.

Because of the coordinate transformation, it is necessary to develop equations relating the fluid properties in the physical plane to those of the transformed plane. Any fluid property $g(z, r, t)$ in the physical plane is related to a fluid property $g(\xi, \eta, T)$ in the transformed plane through the following three equations:

$$\frac{\partial g}{\partial z} = \frac{\partial g}{\partial \xi} \frac{1}{\delta} \tag{5}$$

$$\frac{\partial g}{\partial r} = \frac{\partial g}{\partial \xi} \frac{1}{\delta} \left\{ (\xi - 1) \cot \phi - \xi \cot \theta \right\} + \frac{\partial g}{\partial \eta} \tag{6}$$

$$\frac{\partial g}{\partial t} = \frac{\partial g}{\partial T} - \frac{\xi W}{\delta} \frac{\partial g}{\partial \xi} \tag{7}$$

The transformation equations [equations (5), (6), and (7)] are used in conjunction with equations (1) through (4) to produce the governing equations for the transformed plane. These equations are

$$\frac{\partial R}{\partial T} + D \frac{\partial R}{\partial \xi} + v_r \frac{\partial R}{\partial \eta} + \frac{E}{\delta} \frac{\partial v_r}{\partial \xi} + \frac{\partial v_r}{\partial \eta} + \frac{v_r}{\eta} + \frac{1}{\delta} \frac{\partial v_z}{\partial \xi} = 0 \tag{8}$$

$$\frac{\partial v_r}{\partial T} + D \frac{\partial v_r}{\partial \xi} + v_r \frac{\partial v_r}{\partial \eta} + \frac{Ep}{\delta \rho} \frac{\partial P}{\partial \xi} + \frac{p}{\rho} \frac{\partial P}{\partial \eta} = 0 \tag{9}$$

$$\frac{\partial v_z}{\partial T} + D\frac{\partial v_z}{\partial \xi} + v_r\frac{\partial v_z}{\partial \eta} + \frac{p}{\delta\rho}\frac{\partial P}{\partial \xi} = 0 \tag{10}$$

$$\frac{\partial P}{\partial T} - \gamma\frac{\partial R}{\partial T} + D\left(\frac{\partial P}{\partial \xi} - \gamma\frac{\partial R}{\partial \xi}\right) + v_r\left(\frac{\partial P}{\partial \eta} - \gamma\frac{\partial R}{\partial \eta}\right) = 0 \tag{11}$$

where

$$E = (\xi - 1)\cot\phi - \xi\cot\theta$$

$$D = (v_z - \xi W + v_r E)/\delta$$

$$R = \ln\rho$$

$$P = \ln p.$$

Notice should be taken that equation (11) represents the entropy equation based on the relationship

$$s = P - \gamma R \tag{12}$$

2.2.2.2 Numerical Solution of Interior Regions - The transient method of establishing the fluid properties for the interior region consists of expanding the fluid properties in a Taylor series with time as the variable. Lax and Wendroff (ref. 11), the principal investigators of this method, found that the term containing the second derivative was a necessary condition to insure convergence of the series. Basically this method utilizes the function (a fluid property) and the first and second derivatives of the function at time T_o to evaluate the function at time $T_o + \Delta T$. Written mathematically this statement is

$$g(T_o + \Delta T) = g(T_o) + \frac{\partial g}{\partial T}\Delta T + \frac{\partial^2 g}{\partial T^2}\frac{(\Delta T)^2}{2} \tag{13}$$

where the function g represents either R, P, v_z, or v_r. The first time derivative of g, expressed in terms of space derivatives, is obtained from equations (8) through (11). Differentiation of equations (8) through (11) with respect to time produces the second time derivatives of g as follows:

$$\frac{\partial^2 R}{\partial T^2} = -\left\{\frac{\partial D}{\partial T}\frac{\partial R}{\partial \xi} + D\frac{\partial^2 R}{\partial T\partial \xi} + \frac{\partial v_r}{\partial T}\frac{\partial R}{\partial \eta} + v_r\frac{\partial^2 R}{\partial T\partial \eta}\right.$$
$$+ \frac{1}{\delta}\left(\frac{\partial E}{\partial T} - \frac{E}{\delta}\frac{\partial \delta}{\partial T}\right)\frac{\partial v_r}{\partial \xi} + \frac{E}{\delta}\frac{\partial^2 v_r}{\partial T\partial \xi} + \frac{\partial^2 v_r}{\partial T\partial \eta}$$
$$\left. + \frac{1}{\eta}\frac{\partial v_r}{\partial T} + \frac{1}{\delta}\left(\frac{\partial^2 v_z}{\partial T\partial \xi} - \frac{1}{\delta}\frac{\partial v_z}{\partial \xi}\frac{\partial \delta}{\partial T}\right)\right\} \tag{14}$$

$$\frac{\partial^2 v_r}{\partial T^2} = -\left\{\frac{\partial D}{\partial T}\frac{\partial v_r}{\partial \xi} + D\frac{\partial^2 v_r}{\partial T\partial \xi} + \frac{\partial v_r}{\partial T}\frac{\partial v_r}{\partial \eta} + v_r\frac{\partial^2 v_r}{\partial T\partial \eta}\right.$$

$$+ \frac{Ep}{\rho\delta}\frac{\partial P}{\partial T}\frac{\partial P}{\partial \xi} + \frac{p}{\rho\delta}\frac{\partial E}{\partial T}\frac{\partial P}{\partial \xi} - \frac{pE}{\rho\delta}\frac{\partial R}{\partial T}\frac{\partial P}{\partial \xi}$$

$$- \frac{pE}{\rho\delta^2}\frac{\partial \delta}{\partial T}\frac{\partial P}{\partial \xi} + \frac{pE}{\rho\delta}\frac{\partial^2 P}{\partial T\partial \xi} + \frac{p}{\rho}\frac{\partial P}{\partial T}\frac{\partial P}{\partial \eta}$$

$$\left. - \frac{p}{\rho}\frac{\partial R}{\partial T}\frac{\partial P}{\partial \eta} + \frac{p}{\rho}\frac{\partial^2 P}{\partial T\partial \eta}\right\} \qquad (15)$$

$$\frac{\partial^2 v_z}{\partial T^2} = -\left\{\frac{\partial D}{\partial T}\frac{\partial v_z}{\partial \xi} + D\frac{\partial^2 v_z}{\partial T\partial \xi} + \frac{\partial v_r}{\partial T}\frac{\partial v_z}{\partial \eta} + v_r\frac{\partial^2 v_z}{\partial T\partial \eta}\right.$$

$$\left. + \frac{p}{\rho\delta}\left(\frac{\partial P}{\partial T} - \frac{\partial R}{\partial T} - \frac{1}{\delta}\frac{\partial \delta}{\partial T}\right)\frac{\partial P}{\partial \xi} + \frac{p}{\rho\delta}\frac{\partial^2 P}{\partial T\partial \xi}\right\} \qquad (16)$$

$$\frac{\partial^2 P}{\partial T^2} = \gamma\frac{\partial^2 R}{\partial T^2} - \left\{\frac{\partial D}{\partial T}\left(\frac{\partial P}{\partial \xi} - \gamma\frac{\partial R}{\partial \xi}\right) + D\left(\frac{\partial^2 P}{\partial T\partial \xi} - \gamma\frac{\partial^2 R}{\partial T\partial \xi}\right)\right.$$

$$\left. + \frac{\partial v_r}{\partial T}\left(\frac{\partial P}{\partial \eta} - \gamma\frac{\partial R}{\partial \eta}\right) + v_r\left(\frac{\partial^2 P}{\partial T\partial \eta} - \gamma\frac{\partial^2 R}{\partial T\partial \eta}\right)\right\} \qquad (17)$$

Equations (14) through (17) contain crossed time and space derivatives which can be expressed in terms of space derivatives by differentiating equations (8) through (11) with respect to ξ and η. These crossed derivatives in terms of space derivatives are

$$\frac{\partial^2 R}{\partial \xi\partial T} = -\left\{\frac{\partial D}{\partial \xi}\frac{\partial R}{\partial \xi} + D\frac{\partial^2 R}{\partial \xi^2} + \frac{\partial v_r}{\partial \xi}\left(\frac{\partial R}{\partial \eta} + \frac{1}{\delta}\frac{\partial E}{\partial \xi} + \frac{1}{\eta}\right)\right.$$

$$\left. + v_r\frac{\partial^2 R}{\partial \xi\partial \eta} + \frac{E}{\delta}\frac{\partial^2 v_r}{\partial \xi^2} + \frac{\partial^2 v_r}{\partial \xi\partial \eta} + \frac{1}{\delta}\frac{\partial^2 v_z}{\partial \xi^2}\right\} \qquad (18)$$

$$\frac{\partial^2 R}{\partial \eta\partial T} = -\left\{\frac{\partial D}{\partial \eta}\frac{\partial R}{\partial \xi} + D\frac{\partial^2 R}{\partial \eta\partial \xi} + \left(\frac{\partial R}{\partial \eta} + \frac{1}{\eta}\right)\frac{\partial v_r}{\partial \eta} + v_r\frac{\partial^2 R}{\partial \eta^2}\right.$$

$$+ \frac{1}{\delta}\left(\frac{\partial E}{\partial \eta} - \frac{E}{\delta}\frac{\partial \delta}{\partial \eta}\right)\frac{\partial v_r}{\partial \xi} + \frac{E}{\delta}\frac{\partial^2 v_r}{\partial \eta\partial \xi}$$

$$\left. + \frac{\partial^2 v_r}{\partial \eta^2} - \frac{v_r}{\eta^2} + \frac{1}{\delta}\left(\frac{\partial^2 v_z}{\partial \eta\partial \xi} - \frac{1}{\delta}\frac{\partial \delta}{\partial \eta}\frac{\partial v_z}{\partial \xi}\right)\right\} \qquad (19)$$

$$\frac{\partial^2 v_r}{\partial \xi \partial T} = - \left\{ \frac{\partial D}{\partial \xi} \frac{\partial v_r}{\partial \xi} + D \frac{\partial^2 v_r}{\partial \xi^2} + \frac{\partial v_r}{\partial \xi} \frac{\partial v_r}{\partial \eta} + v_r \frac{\partial^2 v_r}{\partial \xi \partial \eta} \right.$$

$$+ \frac{Ep}{\rho\delta} \left(\frac{\partial P}{\partial \xi}\right)^2 + \frac{p}{\rho\delta} \frac{\partial E}{\partial \xi} \frac{\partial P}{\partial \xi} - \frac{pE}{\rho\delta} \frac{\partial R}{\partial \xi} \frac{\partial P}{\partial \xi}$$

$$\left. + \frac{pE}{\rho\delta} \frac{\partial^2 P}{\partial \xi^2} + \frac{p}{\rho} \frac{\partial P}{\partial \xi} \frac{\partial P}{\partial \eta} - \frac{p}{\rho} \frac{\partial R}{\partial \xi} \frac{\partial P}{\partial \eta} + \frac{p}{\rho} \frac{\partial^2 P}{\partial \xi \partial \eta} \right\} \tag{20}$$

$$\frac{\partial^2 v_r}{\partial \eta \partial T} = - \left\{ \frac{\partial D}{\partial \eta} \frac{\partial v_r}{\partial \xi} + D \frac{\partial^2 v_r}{\partial \eta \partial \xi} + \left(\frac{\partial v_r}{\partial \eta}\right)^2 + v_r \frac{\partial^2 v_r}{\partial \eta^2} \right.$$

$$+ \frac{p}{\rho\delta} \left(E \frac{\partial P}{\partial \eta} + \frac{\partial E}{\partial \eta} - E \frac{\partial R}{\partial \eta} - \frac{E}{\delta} \frac{\partial \delta}{\partial \eta}\right) \frac{\partial P}{\partial \xi} + \frac{pE}{\rho\delta} \frac{\partial^2 P}{\partial \eta \partial \xi}$$

$$\left. + \frac{p}{\rho} \left(\frac{\partial P}{\partial \eta}\right)^2 - \frac{p}{\rho} \frac{\partial R}{\partial \eta} \frac{\partial P}{\partial \eta} + \frac{p}{\rho} \frac{\partial^2 P}{\partial \eta^2} \right\} \tag{21}$$

$$\frac{\partial^2 v_z}{\partial \xi \partial T} = - \left\{ \frac{\partial D}{\partial \xi} \frac{\partial v_z}{\partial \xi} + D \frac{\partial^2 v_z}{\partial \xi^2} + \frac{\partial v_r}{\partial \xi} \frac{\partial v_z}{\partial \eta} + v_r \frac{\partial^2 v_z}{\partial \xi \partial \eta} \right.$$

$$\left. + \frac{p}{\rho\delta} \left(\frac{\partial P}{\partial \xi} - \frac{\partial R}{\partial \xi}\right) \frac{\partial P}{\partial \xi} + \frac{p}{\rho\delta} \frac{\partial^2 P}{\partial \xi^2} \right\} \tag{22}$$

$$\frac{\partial^2 v_z}{\partial \eta \partial T} = - \left\{ \frac{\partial D}{\partial \eta} \frac{\partial v_z}{\partial \xi} + D \frac{\partial^2 v_z}{\partial \eta \partial \xi} + \frac{\partial v_r}{\partial \eta} \frac{\partial v_z}{\partial \eta} + v_r \frac{\partial^2 v_z}{\partial \eta^2} \right.$$

$$\left. + \frac{p}{\rho\delta} \left(\frac{\partial P}{\partial \eta} - \frac{1}{\delta} \frac{\partial \delta}{\partial \eta} - \frac{\partial R}{\partial \eta}\right) \frac{\partial P}{\partial \xi} + \frac{p}{\rho\delta} \frac{\partial^2 P}{\partial \eta \partial \xi} \right\} \tag{23}$$

$$\frac{\partial^2 P}{\partial \xi \partial T} = \gamma \frac{\partial^2 R}{\partial \xi \partial T} - \left\{ \frac{\partial D}{\partial \xi} \left(\frac{\partial P}{\partial \xi} - \gamma \frac{\partial R}{\partial \xi}\right) + D \left(\frac{\partial^2 P}{\partial \xi^2} - \gamma \frac{\partial^2 R}{\partial \xi^2}\right) \right.$$

$$\left. + \frac{\partial v_r}{\partial \xi} \left(\frac{\partial P}{\partial \eta} - \gamma \frac{\partial R}{\partial \eta}\right) + v_r \left(\frac{\partial^2 P}{\partial \xi \partial \eta} - \gamma \frac{\partial^2 R}{\partial \xi \partial \eta}\right) \right\} \tag{24}$$

$$\frac{\partial^2 P}{\partial \eta \partial T} = \gamma \frac{\partial^2 R}{\partial \eta \partial T} - \left\{ \frac{\partial D}{\partial \eta} \left(\frac{\partial P}{\partial \xi} - \gamma \frac{\partial R}{\partial \xi}\right) + D \left(\frac{\partial^2 P}{\partial \xi \partial \eta} - \gamma \frac{\partial^2 R}{\partial \xi \partial \eta}\right) \right.$$

$$\left. + \frac{\partial v_r}{\partial \eta} \left(\frac{\partial P}{\partial \eta} - \gamma \frac{\partial R}{\partial \eta}\right) + v_r \left(\frac{\partial^2 P}{\partial \eta^2} - \gamma \frac{\partial^2 R}{\partial \eta^2}\right) \right\} \tag{25}$$

Equations (8) through (11) and equations (18) through (25) can be used to evaluate the second time derivatives of g [equations (14) through (17)] solely as functions of space derivatives. The space derivatives occurring in the expressions for the first and second time derivatives can be closely approximated by finite differences. A standard central finite-difference scheme has been used for evaluating the partial derivatives. The first and second space derivatives of g in finite-difference form are

$$\frac{\partial g}{\partial \xi}(I,J) = [g(I+1,J) - g(I-1,J)]/2\Delta\xi \tag{26}$$

$$\frac{\partial g}{\partial \eta}(I,J) = [g(I,J+1) - g(I,J-1)]/2\Delta\eta \tag{27}$$

$$\frac{\partial^2 g}{\partial \xi^2}(I,J) = [g(I+1,J) + g(I-1,J) - 2g(I,J)]/(\Delta\xi)^2 \tag{28}$$

$$\frac{\partial^2 g}{\partial \eta^2}(I,J) = [g(I,J+1) + g(I,J-1) - 2g(I,J)]/(\Delta\eta)^2 \tag{29}$$

$$\frac{\partial^2 g}{\partial \eta \partial \xi}(I,J) = [g(I+1,J+1) - g(I+1,J-1) - g(I-1,J+1) + g(I-1,J-1)]/4\Delta\eta\Delta\xi \tag{30}$$

where I and J refer to the grid point in question, as shown in Figure 2-4.

The terms $\frac{\partial W}{\partial \eta}$, $\frac{\partial^2 \delta}{\partial \eta^2}$, and $\frac{d^2 b}{d\eta^2}$ are evaluated by the central finite-difference scheme. The remaining terms are evaluated as follows:

$$\frac{\partial \delta}{\partial \eta} = \cot\theta - \frac{db}{d\eta} \tag{31}$$

$$\frac{\partial \delta}{\partial T} = W \tag{32}$$

$$\frac{\partial E}{\partial \eta} = -\xi \frac{\partial^2 \delta}{\partial \eta^2} - \frac{d^2 b}{d\eta^2} \tag{33}$$

$$\frac{\partial E}{\partial \xi} = -\frac{\partial \delta}{\partial \eta} \tag{34}$$

$$\frac{\partial E}{\partial T} = -\xi \frac{\partial W}{\partial \eta} \tag{35}$$

$$\frac{\partial D}{\partial \eta} = - \frac{D}{\delta}\frac{\partial \delta}{\partial \eta} + \frac{1}{\delta}\left[- \xi \frac{\partial W}{\partial \eta} + E \frac{\partial \mathbf{v_r}}{\partial \eta} + \mathbf{v_r}\frac{\partial E}{\partial \eta} + \frac{\partial \mathbf{v_z}}{\partial \eta}\right] \tag{36}$$

$$\frac{\partial D}{\partial \xi} = \frac{1}{\delta}\left[-W + E \frac{\partial \mathbf{v_r}}{\partial \xi} + \mathbf{v_r}\frac{\partial E}{\partial \xi} + \frac{\partial \mathbf{v_z}}{\partial \xi}\right] \tag{37}$$

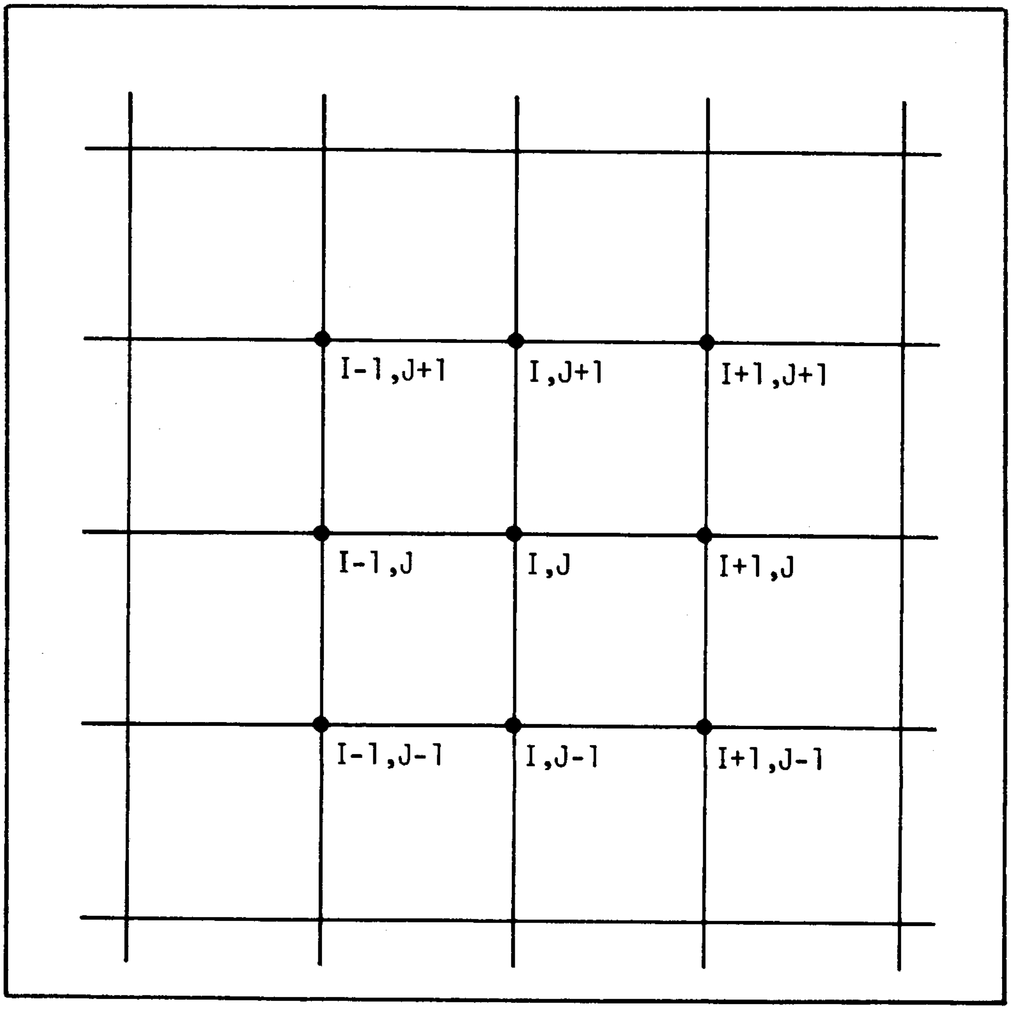

Figure 2-4. FINITE-DIFFERENCE MESH

$$\frac{\partial D}{\partial T} = \left[\frac{\partial v_z}{\partial T} - \xi \frac{\partial W}{\partial T} + \frac{\partial v_r}{\partial T} E + v_r \frac{\partial E}{\partial T}\right] \frac{1}{\delta}$$

$$- \frac{1}{\delta^2}\left[v_z - W\xi + v_r E\right] \frac{\partial \delta}{\partial T} \quad (38)$$

$$\frac{\partial W}{\partial T} = [W(T_o + \Delta T) - W(T_o)]/\Delta T \quad (39)$$

Equation (39) indicates that the shock velocity must be evaluated at each new time before the remaining fluid properties between the shock and body may be evaluated at that same time. Evaluation of the shock velocity will be discussed in detail in Subsection 2.2.3.

The time-dependent finite-difference technique will be stable if the Courant-Friedrichs-Lewy (ref. 12) criterion is satisfied. A safe or stable step size ΔT is taken as the minimum of $\Delta(\ )/1.5a(M+1)$, where $\Delta(\ )$ is the smallest of the intervals $\Delta\xi$ and $\Delta\eta$, a is the speed of sound, and M is the Mach number.

The procedure described can be programmed for a computer which will calculate the fluid properties (P, R, v_z, and v_r) at the new time step for the interior region between shock and body. However, the computation requires the boundary conditions at the old time step. These conditions are discussed in the next subsection.

2.2.3 Boundary Conditions

The points on the boundary, ABCD, of the blunt-body flow field (Figure 2-2) are computed differently from those of the interior region. The shock points are discussed first in detail since the body points are computed in a similar manner.

2.2.3.1 <u>Shock Points</u> - The Rankine-Hugoniot shock relations, which are used to compute the fluid properties on the downstream side of the shock at time $T_o + \Delta t$, are

$$U = \frac{(\gamma-1)(V_\infty-W)^2 \sin^2\theta + 2a_\infty^2}{(\gamma+1)(V_\infty-W)\sin\theta} + W \sin\theta \tag{40}$$

$$p = \frac{2(V_\infty-W)^2 \sin^2\theta - (\gamma-1)}{(\gamma+1)} \tag{41}$$

$$\rho = \frac{(\gamma+1)p + (\gamma-1)}{(\gamma+1) + (\gamma-1)p} \tag{42}$$

$$V = V_\infty \cos\theta \tag{43}$$

The only unknown parameters in the expressions for U, p, and ρ are W, the local shock velocity and θ, the local shock angle. These parameters are also needed for the solution to the set of differential equations governing the interior flow fields at time $T_o + \Delta t$. This implies that an initial shock velocity, location, and shape must be assumed to start the computational procedures.

Some technique must be developed which will insure that the correct shock velocity has been obtained at each time step, subsequent to the first, before the flow field calculations are made. This technique is developed through the use of an auxiliary set of cartesian coordinates fixed to a curvilinear shock wave with velocity W as shown in Figure 2-5. The ν-axis remains tangent to the shock wave at the point in question, Q1, while σ is normal to shock at the same point. The terms U and V are the σ and ν components of the velocity vector at any point P within the flow field. Thus, the equations of motion for the flow field can be written in the (σ, ν, t) space as given below.

$$\frac{\partial R}{\partial t} + U \frac{\partial R}{\partial \sigma} + \frac{\partial U}{\partial \sigma} = - \frac{\partial V}{\partial \nu} - V \frac{\partial R}{\partial \nu} - (V \sin\theta - U \cos\theta) \frac{1}{r} \tag{44}$$

$$\frac{\partial U}{\partial t} + U \frac{\partial U}{\partial \sigma} + \frac{p}{\rho} \frac{\partial P}{\partial \sigma} = - V \frac{\partial U}{\partial \nu} \tag{45}$$

$$\frac{\partial V}{\partial t} + U \frac{\partial V}{\partial \sigma} = - V \frac{\partial V}{\partial \nu} - \frac{p}{\rho} \frac{\partial P}{\partial \nu} \tag{46}$$

$$\frac{\partial P}{\partial t} - \gamma \frac{\partial R}{\partial t} + U \frac{\partial P}{\partial \sigma} - \gamma U \frac{\partial R}{\partial \sigma} = \gamma V \frac{\partial R}{\partial \nu} - V \frac{\partial P}{\partial \nu} \tag{47}$$

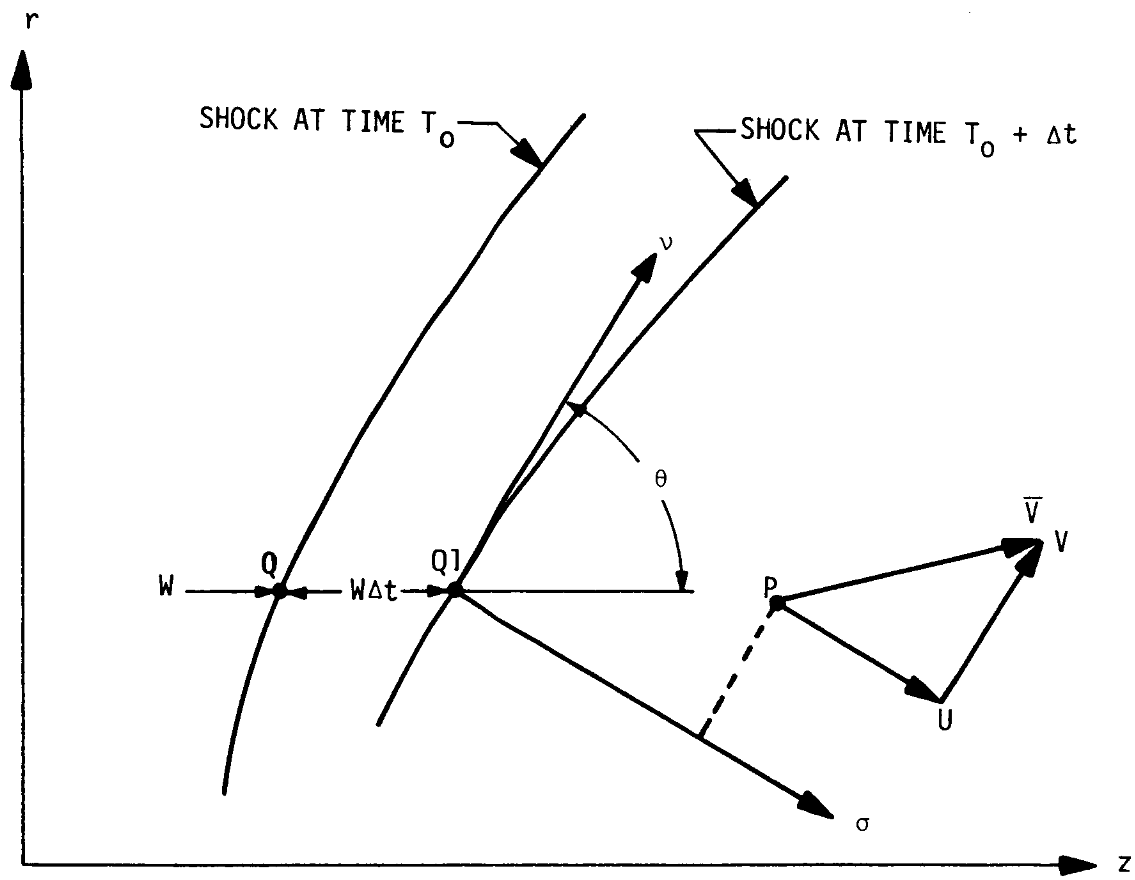

Figure 2-5. SHOCK POINT IN AXISYMMETRIC UNSTEADY FLOW

These equations are valid up to but not across the shock wave. However, it is well known that the ν-component of velocity is the same on both sides of the shock. Thus, in the neighborhood of a shock point, the significant parameters (ref. 9) are σ and U. Consequently, equations (44) through (46) are considered as quasi-one-dimensional equations modified by the forcing terms on the right-hand sides.

Equations (44) through (47) are hyperbolic differential equations for which real characteristics always exist for the subsonic flow region (ref. 13). This property of the equations is used to establish the technique necessary for calculating the correct shock velocity.

The exact differentials of the relevant fluid properties, with the assumption that the flow near the shock is quasi-one-dimensional, are

$$dU = \frac{\partial U}{\partial t}\, dt + \frac{\partial U}{\partial \sigma}\, d\sigma \tag{48}$$

$$dP = \frac{\partial P}{\partial t}\, dt + \frac{\partial P}{\partial \sigma}\, d\sigma \tag{49}$$

$$dR = \frac{\partial R}{\partial t}\, dt + \frac{\partial R}{\partial \sigma}\, d\sigma \tag{50}$$

Equations (44), (45), (47), and (48) through (50) can be used in a manner similar to the method discussed in reference 13 to obtain three characteristic equations in the (σ, t) plane. They are

$$\frac{d\sigma}{dt} = U - a \tag{51a}$$

$$\frac{d\sigma}{dt} = U + a \tag{51b}$$

$$\frac{d\sigma}{dt} = U \tag{51c}$$

These equations have immediate interpretation in terms of a quasi-one-dimensional flow. The compatibility equation along the first of these characteristics [equation (51a)], which extends from the shock to a point within the interior region, is

$$\frac{dU}{dt} - \frac{a}{\gamma}\frac{dP}{dt} = - V\frac{\partial U}{\partial \nu} + \frac{aV}{\gamma}\frac{\partial P}{\partial \nu} + a\frac{\partial V}{\partial \nu} + \frac{a}{r}(V \sin\theta - U\cos\theta) \qquad (52)$$

A characteristic with the slope $\frac{d\sigma}{dt} = (U - a)_{Q1}$ is drawn from point Q1 (new shock point based on an assumed horizontal shock velocity) in the (σ, t) plane as shown in Figure 2-6. The intersection point, A1, of the characteristic and the σ-axis at the old time T_o is contained in the physical plane. The complete flow field is known at time T_o and therefore, the fluid properties of point A1 are also known. However, point A1 is not likely to be a mesh point in the (ξ, η, T) plane and interpolation of the properties are usually necessary. Figure 2-6 shows the location of point A1 and also aids the subsequent discussion concerning the computational procedure for locating the point in the (ξ, η, T) plane at time T_o. The subscripts used in this figure refer to a particular point and are later used to indicate that the fluid property in question is evaluated at the point. The length of the characteristic curve, σ_{A1}, is

$$\sigma_{A1} = - \frac{d\sigma}{dt}\Delta t = - (U - a)\Delta t \quad .$$

The z coordinate of the shock point at time $T_o + \Delta t$, z_{Q1}, is expressed as

$$z_{Q1} = z_Q + W\Delta t \quad .$$

The z coordinate of point A1 is

$$z_{A1} = z_{Q1} + \sigma_{A1}\sin\theta$$

$$= z_Q + W\Delta t + \sigma_{A1}\sin\theta .$$

The z coordinate of point Q can be written in terms of variables which have already been defined as

$$z_Q = \delta_Q + b_Q \quad .$$

The transformed coordinate, ξ_{A1}, is obtained from the relation

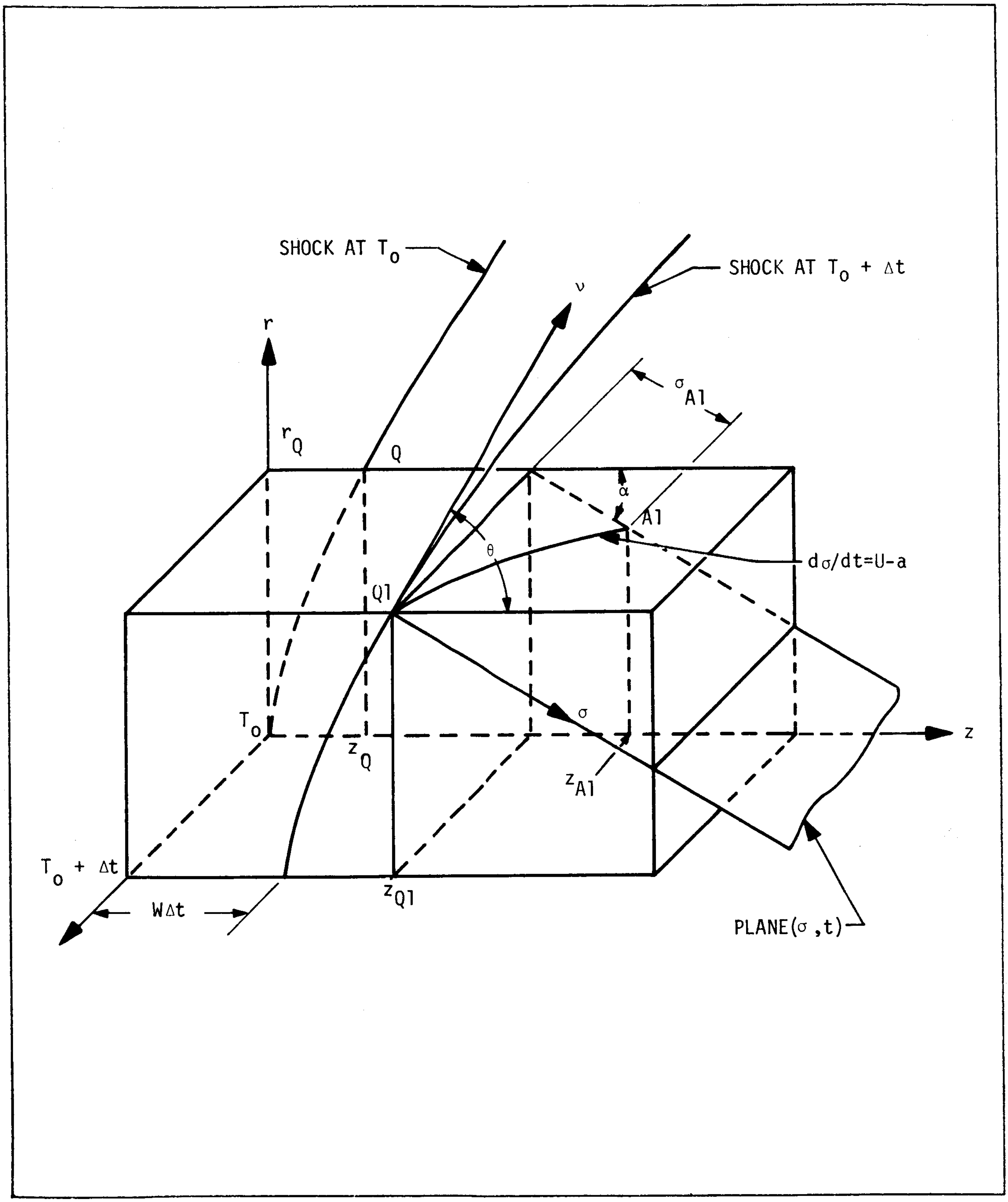

Figure 2-6. LOCATION OF POINT A1 IN PHYSICAL PLANE AT TIME T_o

$$\xi_{A1} = \frac{z_{A1} - b_{A1}}{\delta_{A1}} \quad .$$

z_{A1} is substituted into the expression for ξ_{A1} to yield

$$\xi_{A1} = \frac{\delta_Q + b_Q + W\Delta t + \sigma_{A1} \sin\theta - b_{A1}}{\delta_{A1}} \tag{53}$$

The vertical coordinate of point A1 is

$$r_{A1} = r_Q - \sigma_{A1} \cos\theta \quad .$$

Because there is a one-to-one correspondence in the vertical direction, the transformed coordinate of point A1 is

$$\eta_{A1} = \eta_Q - \sigma_{A1} \cos\theta \tag{54}$$

The fluid properties at point A1 can now be obtained by a linear interpolation between the neighboring mesh points.

A characteristic with the slope

$$\frac{d\sigma}{dt} = \left[(U - a)_{Q1} + (U - a)_{A1}\right]/2 \tag{55}$$

is issued from point Q1 which causes point A1 to change locations. The fluid properties at the new point A1 are obtained by interpolation and are used in accordance with equation (55) to define the slope of a new characteristic which is issued from Q1. The process is repeated until the position of A1 stabilizes.

The right-hand side of equation (52), designated H, is now computed at points A1 and Q1 as follows:

$$H_{A1} = \left[- V \frac{\partial U}{\partial \nu} + \frac{aV}{\gamma} \frac{\partial P}{\partial \nu} + a \frac{\partial V}{\partial \nu} + \frac{a}{r} (V \sin\theta - U \cos\theta)\right]_{A1}$$

$$H_{Q1} = \left[- V \frac{\partial U}{\partial \nu} + \frac{aV}{\gamma} \frac{\partial P}{\partial \nu} + a \frac{\partial V}{\partial \nu} + \frac{a}{r} (V \sin\theta - U \cos\theta)\right]_{Q1}$$

The average of H_{A1} and H_{Q1}, which is considered constant with respect to time, is used in place of H in the subsequent integration. Equation (52) can be integrated with respect to time and a value of U_{Q1} can be obtained if the pressure at Q1 is assumed to be the value calculated by equation (41). Thus,

$$\int_{A1}^{Q1} dU - \frac{a_{A1} + a_{Q1}}{2\gamma} \int_{A1}^{Q1} dP = \int_{T_o}^{T_o + \Delta t} \frac{H_{A1} + H_{Q1}}{2} dt \quad ,$$

which yields

$$U_{Q1} - U_{A1} - \frac{a_{A1} + a_{Q1}}{2\gamma} (P_{Q1} - P_{A1}) = \frac{(H_{A1} + H_{Q1})}{2} \Delta t \tag{56}$$

If U_{Q1} does not agree with the value of U calculated by equation (40), the assumed shock velocity was incorrect. Thus, the shock velocity is changed and the entire shock point process is repeated (except the location and angle of the shock wave remain fixed) as many times as necessary to obtain the correct shock velocity at the new time. This shock velocity is used in the interior point calculations for the current time increment and is used to establish the shock location at the next time increment. The above procedure is valid for any and all points along the shock.

2.2.3.2 <u>Body Points</u> - The boundary conditions of the body points are treated in a manner similar to the shock point boundary conditions. However, there are no straightforward equations such as the Rankine-Hugoniot shock relations which can be used to calculate the fluid properties along the body at time $T_o + \Delta t$. Therefore, additional information must be obtained from an auxiliary set of equations that are valid specifically along the body. A body-fixed Cartesian coordinate system as shown in Figure 2-7 is used to develop the necessary equations.

The equations of motion for the flow field written in terms of the body-fixed coordinate system are

$$\frac{\partial R}{\partial t} + U \frac{\partial R}{\partial \sigma} + \frac{\partial U}{\partial \sigma} = - \frac{\partial V}{\partial \nu} - V \frac{\partial R}{\partial \nu} - (V \sin \phi - U \cos \phi) \frac{1}{r} \tag{57}$$

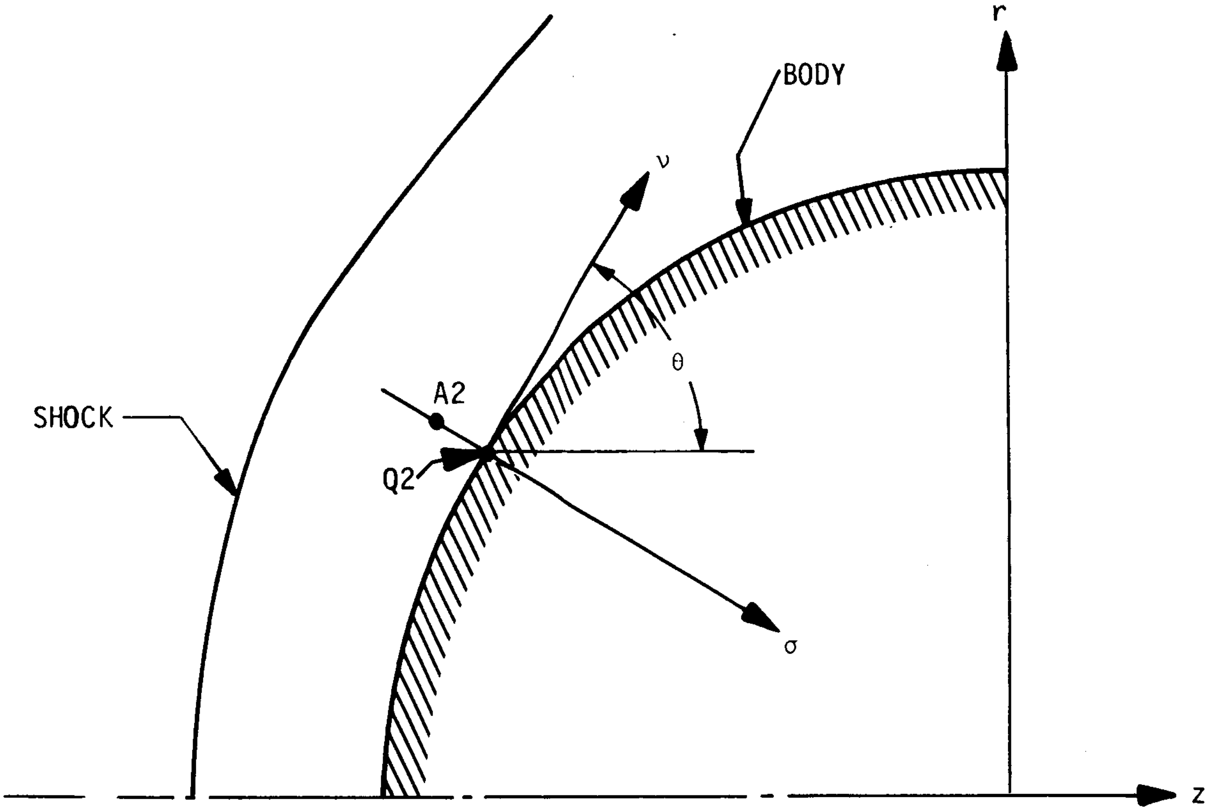

Figure 2-7. BODY-FIXED COORDINATE SYSTEM

$$\frac{\partial U}{\partial t} + U \frac{\partial U}{\partial \sigma} + \frac{p}{\rho} \frac{\partial P}{\partial \sigma} = - V \frac{\partial U}{\partial \nu} \tag{58}$$

$$\frac{\partial V}{\partial t} + U \frac{\partial V}{\partial \sigma} = - V \frac{\partial V}{\partial \nu} - \frac{p}{\rho} \frac{\partial P}{\partial \nu} \tag{59}$$

$$\frac{\partial P}{\partial t} - \gamma \frac{\partial R}{\partial t} + U \frac{\partial P}{\partial \sigma} - \gamma U \frac{\partial R}{\partial \sigma} = \gamma V \frac{\partial R}{\partial \nu} - V \frac{\partial P}{\partial \nu} \tag{60}$$

Since the primary concern at this time is to develop the fluid properties along the body, the condition of no flow through the body can be applied to reduce the complexity of these equations. The resulting equations are

$$\frac{\partial R}{\partial t} + \frac{\partial U}{\partial \sigma} = - \frac{\partial V}{\partial \nu} - V \frac{\partial R}{\partial \nu} - \frac{V}{r} \sin \phi \tag{61}$$

$$\frac{\partial P}{\partial \sigma} = 0 \tag{62}$$

$$\frac{\partial V}{\partial t} = - V \frac{\partial V}{\partial \nu} - \frac{p}{\rho} \frac{\partial P}{\partial \nu} \tag{63}$$

$$\frac{\partial P}{\partial t} - \gamma \frac{\partial R}{\partial t} = \gamma V \frac{\partial R}{\partial \nu} - V \frac{\partial P}{\partial \nu} \tag{64}$$

This set of equations completely defines the first time derivative of R, P, and V in terms of available space derivatives and the variables R, P, and V at time T_o. A first-order Taylor series for these variables with respect to time will yield good approximations of the flow along the body at time $T_o + \Delta t$. For example,

$$P(T_o + \Delta t) = P(T_o) + \frac{\partial P}{\partial t} \Delta t \tag{65}$$

Coupled with such first-order Taylor series approximations, a quasi-one-dimensional method of characteristics is used similar to the technique used for shock points. Equations (48), (49), (50), (57), (58) and (60) will yield the three characteristics of equation (51). The second characteristic $\frac{d\sigma}{dt} = U + a$ is applicable for the body because of its leftward direction as shown in Figure 2-8. The compatibility equation for this characteristic is

$$\frac{dU}{dt} + \frac{a}{\gamma}\frac{dP}{dt} = - V \frac{\partial U}{\partial \nu} - \frac{aV}{\gamma}\frac{\partial P}{\partial \nu} - a \frac{\partial V}{\partial \nu} - \frac{a}{r}(V \sin \phi - U \cos \phi) \quad (66)$$

The pressure is considered as the significant parameter used to determine the accuracy of the first-order Taylor expansions because the σ-component of velocity vanishes on the body. The characteristic is issued from any body point Q2 and intersects the physical plane along the σ-axis at time T_o as shown in Figure 2-8.

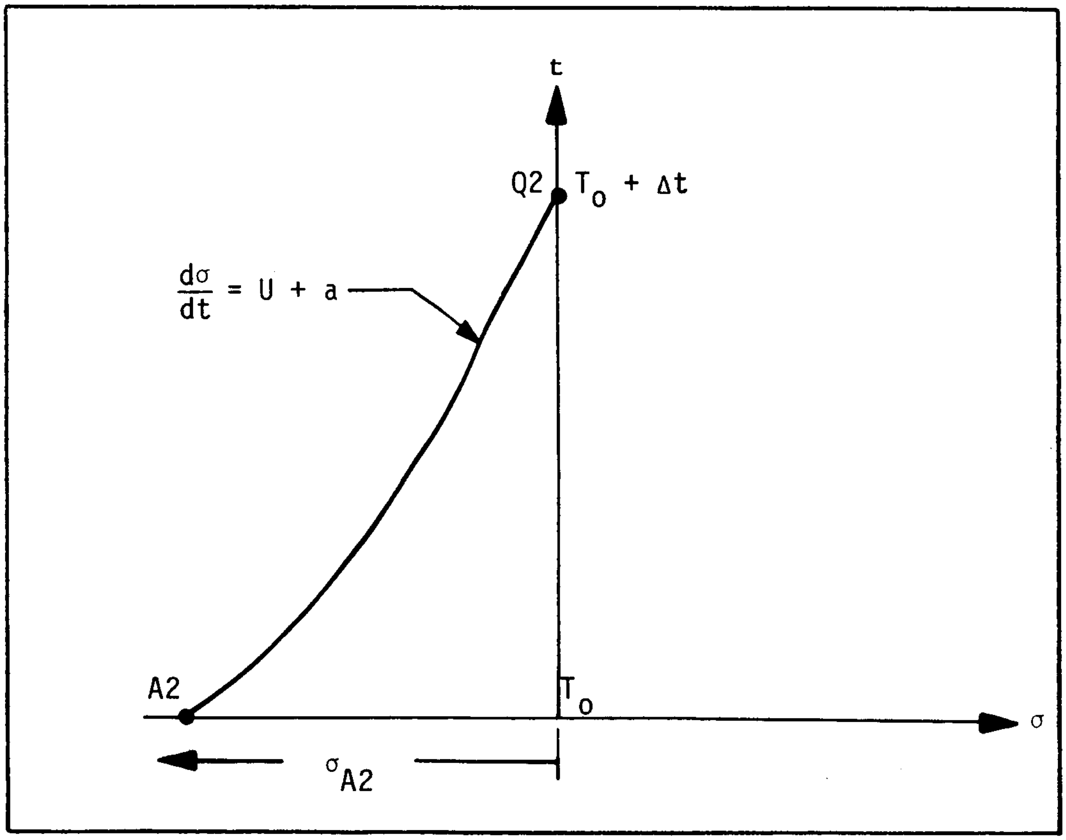

Figure 2-8. BODY-POINT CHARACTERISTIC

Point A2 is located in a manner similar to the shock point location procedure. The length of the characteristic equation, σ_{A2}, is

$$\sigma_{A2} = -\ (U + a)\ \Delta t.$$

The z coordinate of point A2 is written mathematically as

$$z_{A2} = z_{Q2} - \sigma_{A2} \sin\ \phi,$$

where ϕ is the body angle at point Q2. The transformed coordinate, ξ_{A2}, written with z_{Q2} replaced by b_{Q2} is

$$\xi_{A2} = \frac{b_{Q2} - \sigma_{A2} \sin \phi - b_{A2}}{\delta_{A2}} \tag{67}$$

The transformed vertical coordinate

$$\eta_{A2} = \eta_{Q2} + \sigma_{A2} \cos \phi \tag{68}$$

Equations (67) and (68) establish the location of point A2. The fluid properties at this point may be found by interpolation.

A procedure similar to that of the shock points is used to stabilize point A2. Since the second characteristic is used for the body, the right-hand side of equation (66), designated K, is computed at points A2 and Q2.

$$K_{A2} = \left[- V \frac{\partial U}{\partial \nu} - \frac{aV}{\gamma} \frac{\partial P}{\partial \nu} - a \frac{\partial V}{\partial \nu} - \frac{a}{r} (V \sin \phi - U \cos \phi) \right]_{A2}$$

$$K_{Q2} = \left[- \frac{aV}{\gamma} \frac{\partial P}{\partial \nu} - a \frac{\partial V}{\partial \nu} - \frac{a}{r} V \sin \phi \right]_{Q2}$$

As before, K_{A2} and K_{Q2} are arranged and used in place of K in the subsequent integration. Equation (66) is integrated so that the pressure at point Q2 can be calculated. Thus,

$$\int_{A2}^{Q2} dU + \frac{a_{Q2} + a_{A2}}{2\gamma} \int_{A2}^{Q2} dP = \int_{T_o}^{T_o+\Delta t} \frac{K_{A2} + K_{Q2}}{2} dt \quad ,$$

which yields

$$U_{Q2} - U_{A2} + \frac{a_{Q2} + a_{A2}}{2\gamma} (P_{Q2} - P_{A2}) = \frac{(K_{A2} + K_{Q2})}{2} \Delta t \quad .$$

Use of the condition that $U_{Q2} = 0$ and rearrangement of the remaining terms produce an expression for P_{Q2} which is

$$P_{Q2} = P_{A2} + \frac{2\gamma}{a_{Q2} + a_{A2}} \left[U_{A2} + \frac{(K_{A2} + K_{Q2})}{2} \Delta t \right] \tag{69}$$

The pressure calculated in equation (65) is compared to P_{Q2}. If the agreement is outside of the accepted tolerance, a correction that is proportional to the difference between P_{Q2} and $P(T_o+\Delta t)$ of equation (65) is made to $\frac{\partial P}{\partial t}$. The corresponding change in density is calculated by equation (64). The procedure for determining the fluid variables on the body at time $T_o + \Delta t$ is repeated until the agreement is within tolerance. After the agreement is within the accepted tolerance, the remaining properties are computed from the first-order Taylor expansions.

2.2.3.3 Upper and Lower Points - Symmetry conditions are applied to the centerline of the flow field between points A and B of Figure 2-2. Calculations of the fluid properties along this line are included in the interior point solution as a special case.

The values of P, R, v_z, and v_r at points on the upper boundary, CD of Figure 2-2, are extrapolated linearly from the values computed in the interior point region. Such a shortcut is justified provided the upper region is supersonic for the steady-state condition. Since the location of this boundary is left to the discretion of the investigator, a workable knowledge of blunt-body flow fields is necessary to insure that the flow downstream of line CD does not affect the subsonic-transonic region ABCE. Line CE of Figure 2-2 represents the down-running characteristic issued from point C. No perturbations can be sent downward from the points above line CE. For this reason, the region ABCE is insensitive to the technique by which the properties along line CD are computed. The only requirement is to use values which do not generate local instabilities along this line. However, the location of point C is directly related to the free-stream Mach number. The vertical height of point C is higher than the adjoining cylindrical section of the vehicle body for Mach numbers below a value of approximately 2. Therefore, the present interior point flow field must be modified to extend above the body as shown in Figure 2-9. When this modification is made, the definition of δ, the distance between the shock and the body, has little or no meaning. This results in a fictitious body downstream of the limiting characteristic, but such a fictitious body will not affect the location of the sonic line or the subsonic flow field. Another interesting problem area is obtained for a Mach number between 2.0 and 3.0 for air. For this flow condition, the location of the knee of the sonic line is higher than the sonic point on the shock wave. The limiting characteristic issued at the shock will also be higher than point C which means that the interior grid must be large enough to include all of the region beneath the characteristic line. The easiest way to handle both problem areas (Mach numbers less than approximately 3.0 for air) is to concentrate on the lowest Mach number range. If the grid can handle the flow for Mach numbers below 2.0, then it will automatically be capable of treating the flow for Mach numbers between 2.0 and 3.0. The technique used in this investigation is to locate point D of Figure 2-9 on the body such that a defined δ still exists. The location of point D in this manner is sufficiently far downstream so that the limiting characteristic will terminate upstream of point D. Thus, the values of P, R, v_r, and v_z along lines CF and FD are extrapolated linearly from the interior region without introducing perturbations inside the transonic region.

2.3 SHARP-NOSE BODY

If the shock wave is attached, Northrop-Norair's existing Taylor-Maccoll method of numerical integration (ref. 14) for flow past a cone can be used to calculate the flow field downstream of the shock.

The blunt-body technique can be used to compute the flow behind the detached shock wave of a sharp-nose body. Essentially the only modification necessary is

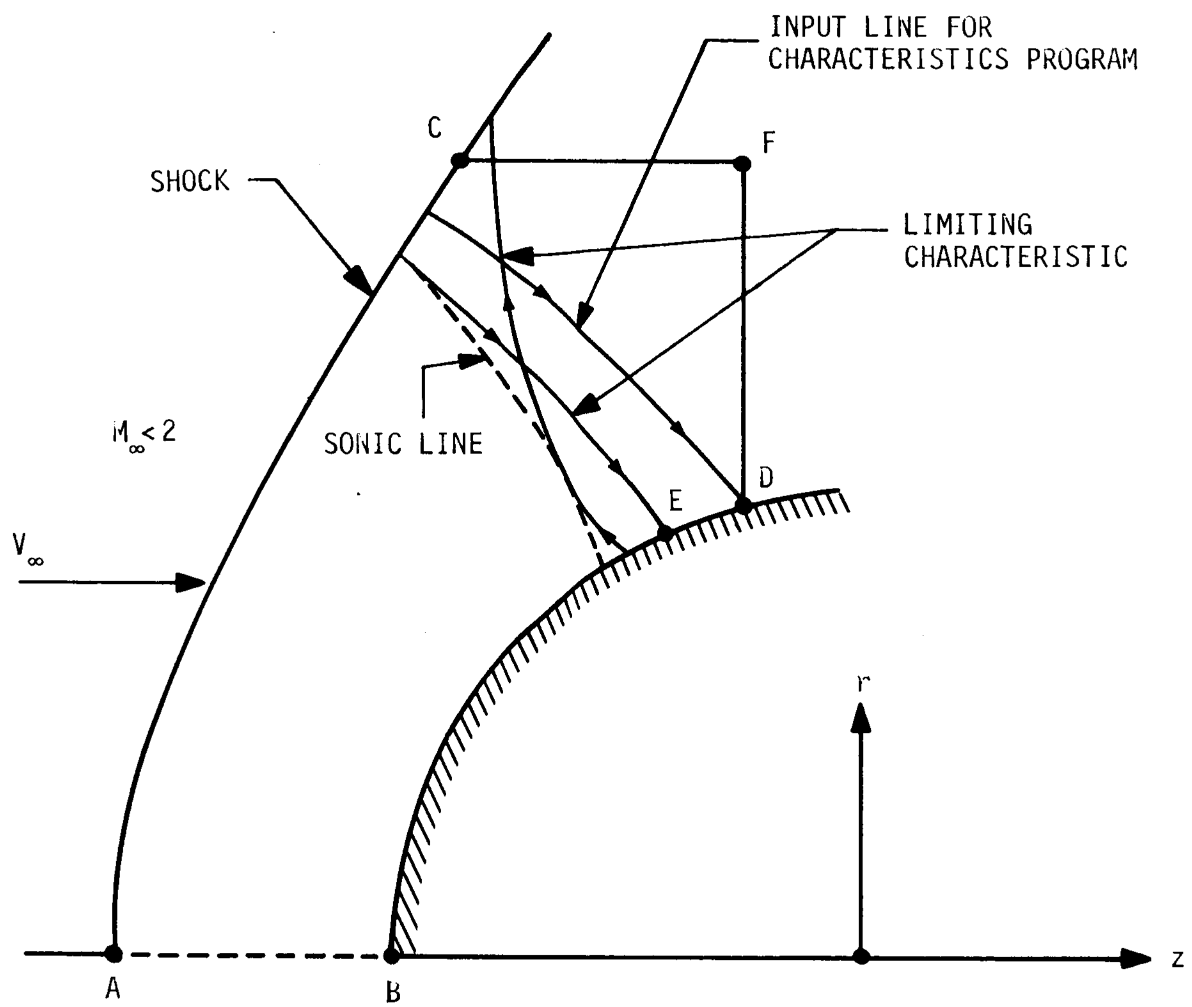

Figure 2-9. LOW MACH FLOW REGIONS

to specify a different body. There is one difficulty associated with a body of this type since the upper corner represents a discontinuous derivative of the body shape. This discontinuous point cannot be represented by any realistic boundary condition. To avoid this difficulty, the corner is rounded so that the body derivatives are continuous and the boundary conditions can be specified. A fix of this type is justified because most machined corners are rounded. More details concerning this corner are given in the frustum discussion.

2.4 CYLINDRICAL SECTION SUPERSONIC FLOW

The supersonic flow region around the conical sections of the axisymmetric body can be treated with a two-dimensional method of characteristics (ref. 14) developed by Northrop. The blunt-body technique computes the fluid properties along an initial line which is used to start the method of characteristics computation.

2.5 FRUSTUM

2.5.1 Selection of Technique

Subsonic flow behind a detached shock on a frustum, as shown in Figure 2-10, can be treated in a manner very similar to blunt-body flow. The primary difference is that the center streamline of the blunt-body flow field is replaced by a solid boundary, a cylindrical section of the vehicle. Another difference is the fact that the frustum has a non-uniform free-stream velocity. The previously developed blunt-body technique can compute the flow field around a frustum by applying different boundary conditions. Due to the fact that only minor modifications were necessary, this technique was selected to compute the frustum flow field.

2.5.2 Interior Points

If the coordinate system of the blunt-body technique is used on the frustum, the governing differential equations and the manner in which their numerical solution is found will be the same as those of the blunt body. However, the area of the interior points must include the region of ABDFC of Figure 2-10 regardless of the Mach number range. The reason for this condition is that all pertinent investigations locate the sonic point on the body at the expansion corner. The interior point calculations do not include line AB since the symmetry conditions do not apply along the body. This line is treated separately in the boundary conditions section.

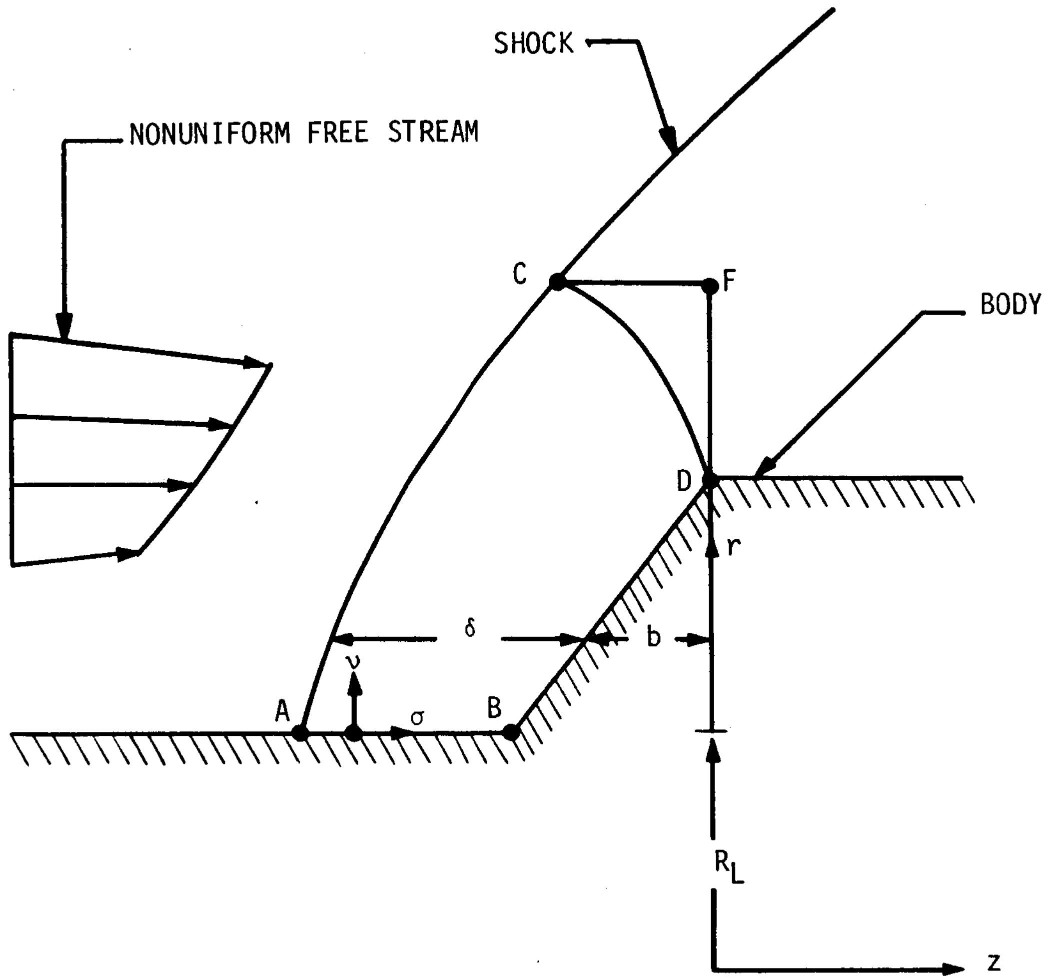

Figure 2-10. FRUSTUM FLOW

2.5.3 Boundary Conditions

2.5.3.1 Shock Points - The nonuniform free-stream flow is handled by the Rankine-Hugoniot shock relations without any difficulties since such relations apply to each shock point independently. The free-stream velocity and other fluid properties which are substituted into these relations are those values in the nonuniform supersonic flow field generated by the two-dimensional method of characteristics which correspond in space to a particular shock point. The remaining shock point procedures are exactly the same as those discussed in subsection 2.2.3.1 for the blunt body.

2.5.3.2 Body Points - The fluid properties between points B and D of Figure 2-10 are computed in exactly the same manner as the body points were for the blunt body. According to the available literature, the sonic point is located at point D, the extremity of the sharp corner. This implies that the limiting characteristic as discussed in subsection 2.2.3.3 also terminates at point D. However, at this point the body surface has discontinuous derivatives which cannot be treated with the computer program. To avoid this discontinuous point, the sharp corner is rounded as shown in Figure 2-11. The body shape at point D is assumed to be approximately the average of the slopes on both sides of it. Based on this assumption the direction and derivative of the velocity have realistic meanings. The sonic point, D', for the rounded corner is located upstream of point D, while the termination point, E, of the limiting characteristic is located downstream of point D'. Because of the limiting characteristic, the grid used for this flow case must include all points upstream of point D''. In reality, this report assumes that the body downstream of point D'' does not affect the location of the sonic line.

Because axisymmetry conditions do not apply to the solid boundary from points A to B of Figure 2-10, the properties along this boundary are developed by a finite, time-dependent, quasi-one-dimensional method of characteristics. Once again an auxiliary set of cartesian coordinates is applied to the flow along the body as shown in Figure 2-10.

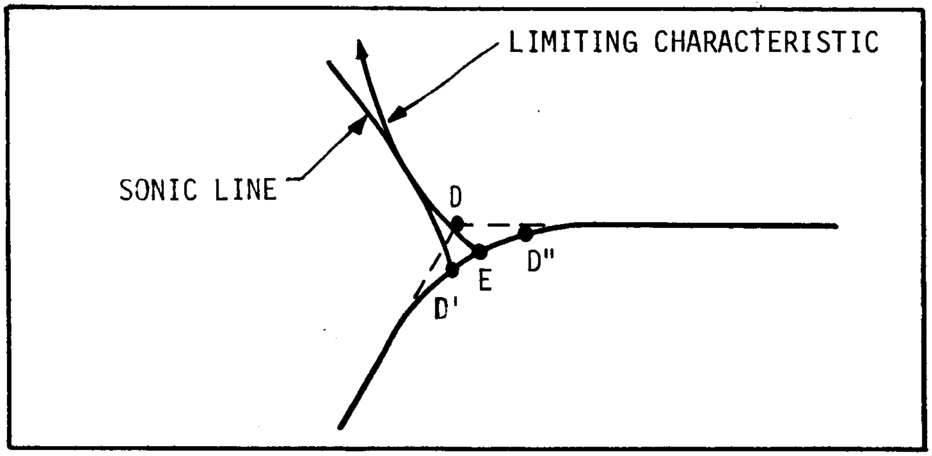

Figure 2-11. ENLARGED VIEW OF POINT D

Substitution of the boundary conditions for line AB ($V = 0$, $\frac{\partial V}{\partial t} = 0$, and $\frac{\partial V}{\partial \sigma} = 0$) into the equations of motion results in a reduced form for these equations which can be written as

$$\frac{\partial R}{\partial t} + \frac{\partial U}{\partial \sigma} + U \frac{\partial R}{\partial \sigma} = - \frac{\partial V}{\partial \nu} \tag{70}$$

$$\frac{\partial U}{\partial t} + U \frac{\partial U}{\partial \sigma} + \frac{p}{\rho} \frac{\partial P}{\partial \sigma} = 0 \tag{71}$$

$$\frac{\partial P}{\partial \nu} = 0 \tag{72}$$

$$\frac{\partial P}{\partial t} - \gamma \frac{\partial R}{\partial t} + U \left(\frac{\partial P}{\partial \sigma} - \gamma \frac{\partial R}{\partial \sigma}\right) = 0 \tag{73}$$

Equations (70), (71), (73), (48), (49), and (50) are used to obtain equations of characteristic curves such as those obtained in subsection 2.2.3.1. The compatibility equation along the characteristic $\frac{d\sigma}{dt} = U - a$ is

$$\frac{dU}{dt} - \frac{a}{\gamma} \frac{dP}{dt} = a \frac{\partial V}{\partial \nu} \tag{74}$$

The compatibility equation corresponding to the characteristic curve $\frac{d\sigma}{dt} = U + a$ is

$$\frac{dU}{dt} + \frac{a}{\gamma} \frac{dP}{dt} = - a \frac{\partial V}{\partial \nu} \tag{75}$$

Equations (74) and (75) are used to calculate the correct U and P at point Q3 for time $T_o+\Delta t$. Figure 2-12 shows the characteristic curves that are issued from point Q3 and terminate at points A3 and B3 at time T_o.

The procedure used to locate and stabilize points A3 and B3 for the cylindrical section in the transformed plane is similar to that used in locating point A1 for the shock and point A2 for the body in Subsection 2.2.3. The primary difference is that for the cylindrical section two compatibility equations must be solved simultaneously for two unknowns, U and P. Equations (70), (71), and (73) are used to calculate $\frac{\partial R}{\partial t}$, $\frac{\partial U}{\partial t}$, and $\frac{\partial P}{\partial t}$, respectively, from the known fluid properties at time T_o. A first-order Taylor expansion in time yields a good first approximation of the properties at point Q3 for time $T_o+\Delta t$.

$$U(T_o+\Delta t) = U(T_o) + \frac{\partial U}{\partial t}\Delta t \tag{76}$$

$$P(T_o+\Delta t) = P(T_o) + \frac{\partial P}{\partial t}\Delta t \tag{77}$$

$$R(T_o+\Delta t) = R(T_o) + \frac{\partial R}{\partial t}\Delta t \tag{78}$$

These properties at point Q3 are necessary so that the initial characteristic curves can be issued. The subscripts below refer to points shown in Figure 2-12. The length of the characteristic curve, σ_{A3}, for point A3 is

$$\sigma_{A3} = - \frac{d\sigma}{dt} dt = - (U - a) \Delta t \ .$$

The z coordinate of point Q3 is

$$z_{Q3} = z_Q + W\Delta t\xi_Q \quad ,$$

where $W\xi_Q\Delta t$ represents the physical distance moved by point Q in the time increment Δt. The z coordinate of point A3 is given by

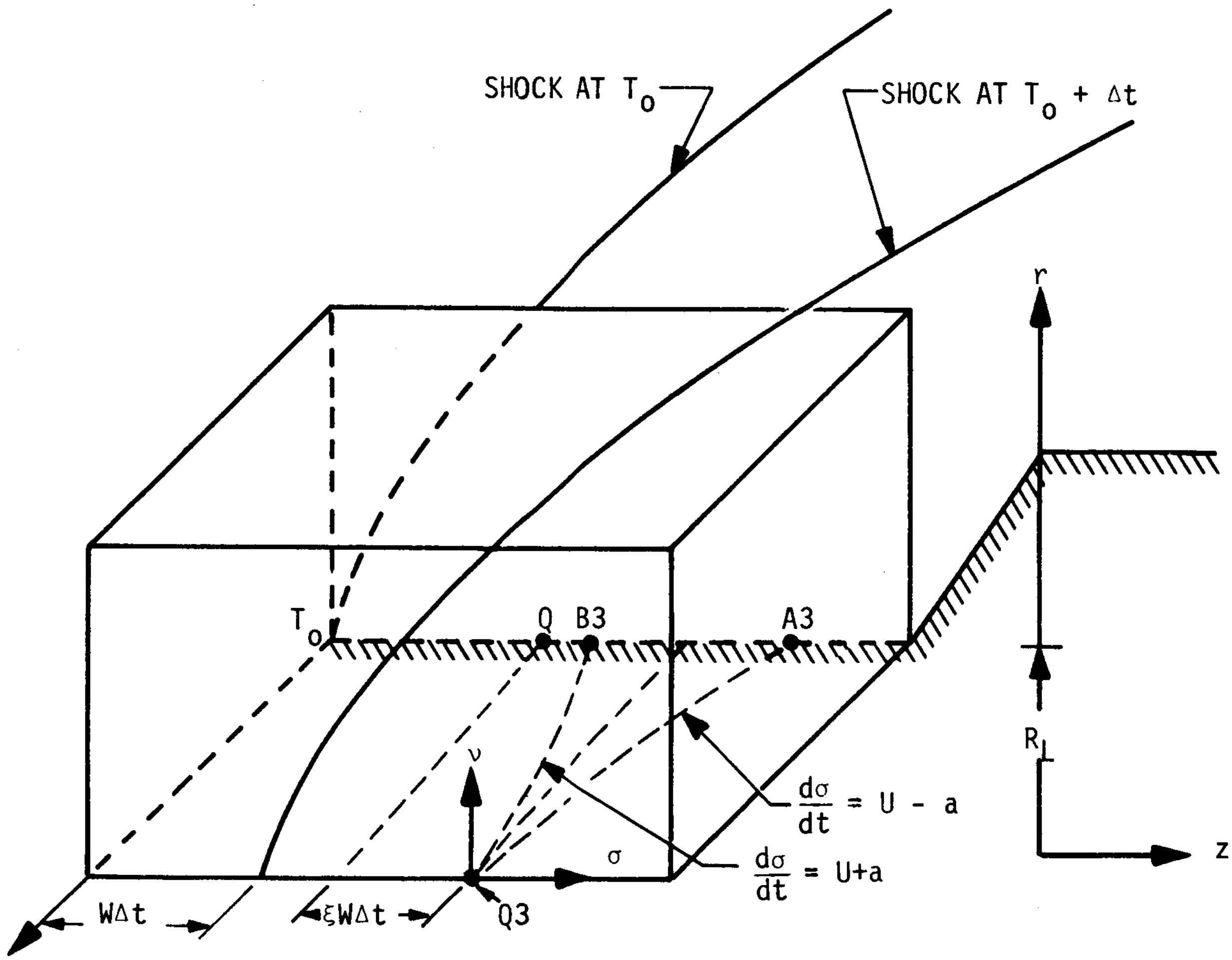

Figure 2-12. LOCATIONS OF POINTS A3 AND B3 IN PHYSICAL PLANE AT TIME T_o

$$z_{A3} = z_{Q3} + \sigma_{A3} = z_Q + W\Delta t \xi_Q + \sigma_{A3} \quad .$$

The transformed ξ coordinate of point Q is

$$\xi_Q = \frac{z_Q - b_Q}{\delta_Q} \quad .$$

Rearrangement results in an equation for z_Q which is

$$z_Q = \delta_Q \xi_Q + b_Q \quad .$$

Substitution of z_Q into the expression for z_{A3} yields

$$z_{A3} = \delta_Q \xi_Q + b_Q + \xi_Q W\Delta t + \sigma_{A3} \quad .$$

The transformed coordinate of point A3, ξ_{A3}, is

$$\xi_{A3} = \frac{z_{A3} - b_{A3}}{\delta_{A3}} \quad .$$

Substitution of z_{A3} into ξ_{A3} results in

$$\xi_{A3} = \frac{(\delta_Q + W\Delta t)\xi_Q + \sigma_{A3} - b_{A3} + b_Q}{\delta_{A3}} \quad .$$

However,

$$\delta_Q = \delta_{A3} \quad \text{and} \quad b_{A3} = b_Q \quad ,$$

which result in the final expression for ξ_{A3}

$$\xi_{A3} = \frac{(\delta_{A3}+W\Delta t)\xi_Q + \sigma_{A3}}{\delta_{A3}} \tag{79}$$

A similar expression for ξ_{B3} can be written as

$$\xi_{B3} = \frac{(\delta_{B3}+W\Delta t)\xi_Q - \sigma_{B3}}{\delta_{B3}} \tag{80}$$

Because the location of both points A3 and B3 are on the body at time T_o, the r coordinates are

$$r_{A3} = r_{B3} = 0 \quad .$$

The transformed vertical coordinate η of each point is

$$\eta_{A3} = \eta_{B3} = 0 \tag{81}$$

The properties at points A3 and B3 are interpolated linearly between neighboring grid points at time T_o. New characteristics with average slopes are issued from point Q3 until the location of points A3 and B3 stabilize. This process was discussed in detail in subsection 2.2.3.1.

The right-hand side of equation (74), designated N, can now be computed for points Q3 and A3 as follows:

$$N_{Q3} = \left[a \frac{\partial V}{\partial \nu}\right]_{Q3}$$

$$N_{A3} = \left[a \frac{\partial V}{\partial \nu}\right]_{A3} \quad .$$

As before, the average of N_{Q3} and N_{A3} is used in place of N for subsequent integration along the characteristic curve with slope $\frac{d\sigma}{dt} = U - a$. Integration of equation (74) with respect to time from point A3 to point Q3 yields an expression with both U_{Q3} and P_{Q3} as unknowns. This expression is

$$U_{Q3} - U_{A3} - \frac{a_{Q3} + a_{A3}}{2\gamma} (P_{Q3} - P_{A3}) = \frac{(N_{Q3}+N_{A3})}{2} \Delta t \qquad (82)$$

A similar expression for the integrated compatibility equation corresponding to the characteristic curve with slope $\frac{d\sigma}{dt} = U + a$ is written as

$$U_{Q3} - U_{B3} + \frac{a_{Q3} + a_{B3}}{2\gamma} (P_{Q3} - P_{B3}) = - \frac{(N_{Q3}+N_{B3})}{2} \Delta t \qquad (83)$$

where

$$N_{B3} = \left[a \frac{\partial V}{\partial \nu}\right]_{B3} .$$

Equations (82) and (83) are used to calculate values of U_{Q3} and P_{Q3}. These values are compared to the values calculated by equations (76) and (77) as part of an iterative procedure. Since the density is related to the pressure through equation (73), the pressure term is used as the criteria for accuracy. If P_{Q3} is different from $P(T_o+\Delta t)$, which was obtained from equation (77), these two values are averaged and a new $\frac{\partial P}{\partial t}$ is computed with a Taylor expansion which is

$$\frac{1}{\Delta t} \left[\frac{P_{Q3} + P(T_o+\Delta t)}{2} - P(T_o)\right] = \frac{\partial P}{\partial t} \qquad (84)$$

A new $\frac{\partial R}{\partial t}$ is also computed and the properties are once again expanded in first-order Taylor series with respect to time. A new sonic velocity is computed so that new characteristics with slopes

$$\frac{d\sigma}{dt} = U_{Q3} - a_{new}$$

and

$$\frac{d\sigma}{dt} = U_{Q3} + a_{new}$$

are issued from point Q3. The above process is repeated until the pressure computed by equation (77) is within the allotted tolerance of that found through the compatibility equations. When this agreement has been obtained, the correct values of the other fluid properties have also been obtained for point Q3 at time $T_o+\Delta t$. This procedure is used for all points along line AB of Figure 2-10.

2.5.3.3 Upper Points - The upper boundary, line CFD in Figure 2-10, is treated exactly as the boundary of the blunt body for the low Mach number flow cases. That is, the properties at these points are extrapolated from the interior point region. The limiting characteristic is assumed to terminate at point D due to the expansion corner. The literature search has revealed no information that refutes this assumption. Extreme care was taken as discussed in subsection 2.5.3.2, to round the corner at point D to insure that realistic boundary conditions are applied.

2.6 INTERFACE BETWEEN FLOW REGIONS

The discussion above presents the technique of describing the subsonic flow field behind a detached shock wave in supersonic flow. It is necessary to couple the subsonic and supersonic flow fields to describe the entire flow field around Saturn type vehicles. Care must be taken that the process of coupling does not change already established flow field properties. The programs developed utilizing the above techniques and the details of coupling are presented in Section III.

Section III

COMPUTER PROGRAM

3.1 PROGRAM DEVELOPMENT

As the state-of-the-art of mathematics is not yet sufficiently advanced to allow the calculation of both subsonic and supersonic flows by the same analytical technique, it is necessary to develop a separate technique for each flow region as described in Section II. The techniques and the methods necessary to combine the separate solutions for the subsonic and supersonic regions have been programmed in FORTRAN IV for the IBM 7094 computer. These programs, along with a description of each subroutine, and program execution are described in the subsections which follow. Descriptions of the inputs and outputs are contained in Appendix A. Appendix B provides sample inputs and outputs. Source listings are contained in Appendix C.

3.1.1 Blunt Body Routine

Based on the techniques presented in Section II, a program has been developed that is capable of calculating the flow field behind a detached shock wave in supersonic flow. The vehicle shape behind the shock may be a cylinder or hemisphere, a wedge or cone, or a frustum in two-dimensional or axisymmetric flow. If a wedge, cone, or frustum flow field is to be calculated, the shoulder must be rounded to avoid singularities in the flow field. The vehicle shape immediately upstream and downstream of a frustum flow field is assumed to be parallel to the free stream flow direction.

3.1.2 Cone Routine

A program is provided to calculate the supersonic attached shock wave flow over a cone. The Taylor-Maccoll (ref. 14) technique is used. In the event that the Mach number is so low as to cause the shock wave to be completely detached, the Blunt Body program is automatically called to calculate the flow field.

3.1.3 Supersonic Flow Routine

The solutions to the supersonic flow regions downstream of the nose of the body are provided by the NORAIR Method of Characteristics Program (ref. 15). This program is capable of calculating the flow over a two-dimensional or axisymmetric vehicle of almost any shape. The program starts from an initial value or characteristic line along which the flow values are known, and continues the characteristics program downstream. If a frustum is encountered for which the frustum angle is too great to support supersonic flow, the program automatically terminates.

3.2 INTERFACE BETWEEN FLOW FIELDS

Because a numerical solution of the complete flow field surrounding a Saturn-type flow field (Figure 2-1) is the desired result, the solutions of the separate flow regions must be coupled together. This results in two types of flow field interfaces: the supersonic to subsonic interface and the subsonic to supersonic interface.

The supersonic to subsonic interface, a shock wave, occurs at any place where the Blunt Body Routine must be used. In the flow over a cylinder, hemisphere, wedge, or cone, the upstream supersonic flow may be assumed to be uniform, and the Rankine-Hugoniot equations for moving shocks represent the interface.

For subsonic flow over a frustum, the upstream conditions are non-uniform, with all flow variables being functions of both space variables. In this case, the supersonic flow field which would occur in the absence of the frustum must be defined by the Supersonic Flow Routine. The resulting characteristic lines, and associated property values are stored off-line on a tape. A second run is then made, with the tape as an input and the frustum included. The characteristics stored on the tape are used to define the local flow field upstream of the shock wave by a quasi-two-dimensional curve-fitting technique, as shown in Figure 3-1. In the quasi-two-dimensional curve fitting technique,

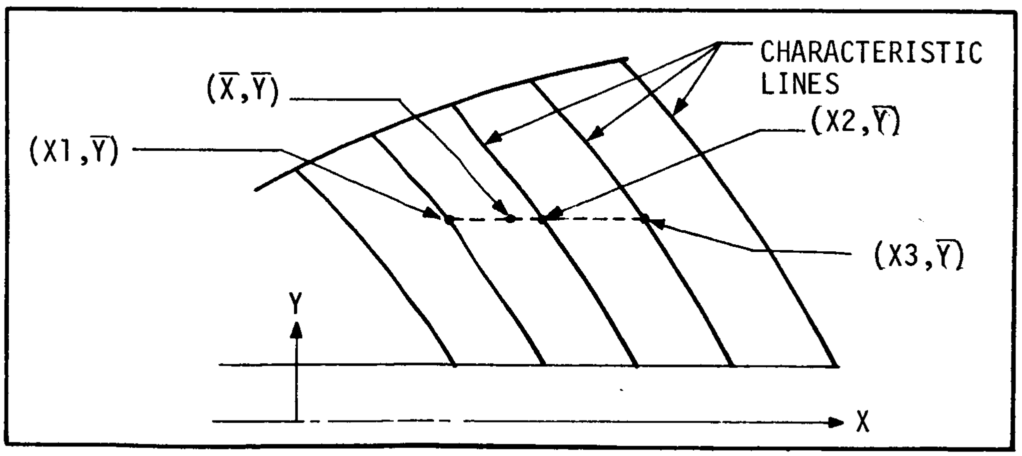

Figure 3-1. QUASI-TWO-DIMENSIONAL CURVE-FITTING TECHNIQUE

the flow variables and the axial distance X are curve-fitted by the least squares technique against the radial distance Y along each characteristic line in the vicinity of the shock. To establish the flow at some point $(\overline{X},\overline{Y})$ upstream of the shock, the flow variables and X coordinate at a height $\overline{Y}$ on the three characteristic lines nearest the point $(\overline{X},\overline{Y})$ are calculated by means of curve-fit polynomials evaluated at $\overline{Y}$. This procedure results in the flow variables being defined at points $(X1, \overline{Y})$, $(X2, \overline{Y})$, and $(X3, \overline{Y})$. A three-point Lagrangian interpolation formula is used for these three points to evaluate the flow variables at the point $(\overline{X}, \overline{Y})$. The Rankine-Hugoniot equations for moving shocks, with the local upstream conditions, then represent the interface. The source listings of these subroutines are included in Appendix C.

The subsonic to supersonic interface is encountered when going from the Blunt Body Routine or Cone Routine to the Supersonic Flow Routine. The interface is represented by a right-running characteristic between the shock and the body. This characteristic is normally constructed from the uppermost node point on the body (see Figure 2-9). This method of construction insures that the starting characteristic line for the Supersonic Flow Routine is beyond the limiting characteristic from the body to the sonic line (Figure 2-9). Thus the shock and body shape downstream of the starting characteristic do not affect the already calculated upstream flow field. The starting line for the Supersonic Flow Routine is thus established, regardless of the body shape downstream of the starting line. The establishment of the flow field beyond the starting line, as well as the shock shape, is left to the Supersonic Flow Routine.

3.3 PROGRAM EXECUTION

After the first two data cards have been input, the main executive program determines the sequence of routines to be used. If the input specifies that the forebody is a cone, the Cone Routine is called. The Cone Routine determines if the shock is attached or detached, by comparing the Mach number and cone angle to data from reference 16. If the shock is detached, control is given to the Blunt Body Routine; otherwise, the Cone Routine finds the solution to the conical flow field and sets up on tape the necessary variables to couple the solution to the method of characteristics. Control is then returned to the main executive program.

If the input specifies that the body shape is a cylinder, hemisphere, or frustum, control is passed to the Blunt Body Routine to find the flow values behind the detached shock. Variables are read in to define the body shape and grid shape, an initial flow field is defined, and the calculations are performed to change the flow field in time towards its asymptotic final value. After a set number of iterations, the flow field is assumed to be found and the variables necessary to couple the solution to the method of characteristics are written on tape.

After a solution is found by either the Cone or Blunt Body Routines, control is passed to the Supersonic Flow Routine. This routine generates the supersonic flow field over the remainder of the body beginning with the solution written on the tape. If a frustum is encountered such that the Supersonic Flow Routine cannot compute the flow field, the program terminates. This termination implies that the shock wave over the frustum is detached and the flow behind the shock is subsonic, and it is necessary once again to employ the Blunt Body Routine. Before the Blunt Body can be used, however, as described in subsection 3.2, the supersonic flow around the cylindrical body, which would occur in the absence of the frustum must be generated by means of the Supersonic Flow Routine. This is done by restarting the program at some characteristic line upstream of the frustum region, and calculating the supersonic flow field as it would occur if no frustum had been present. Calculation of this flow field extends downstream of the point where the frustum actually occurs, as shown in Figure 3-2. All of the data necessary for restarting the Supersonic Flow Routine can be found in the punched output from the previous run. The flow field data from the restarted run is stored on Output Tape B7, which must be saved.

A final run is made with Output Tape B7. This final run calculates the mixed flow field behind the shock with the Blunt Body Routine using the Frustum option and again proceeds with the Supersonic Flow Routine. The procedure must be repeated for each frustum. The first run, which determines if the shock is detached, may be left out if it is known in advance that the shock is detached.

3.4 SUBROUTINE DESCRIPTIONS

Descriptions of all of the subroutines necessary to calculate the mixed flow field are provided in this subsection. For convenience, the descriptions are arranged in alphabetical order. The source listing of these subroutines is provided in Appendix C. A flow chart of each subroutine is provided in Figure 3-3.

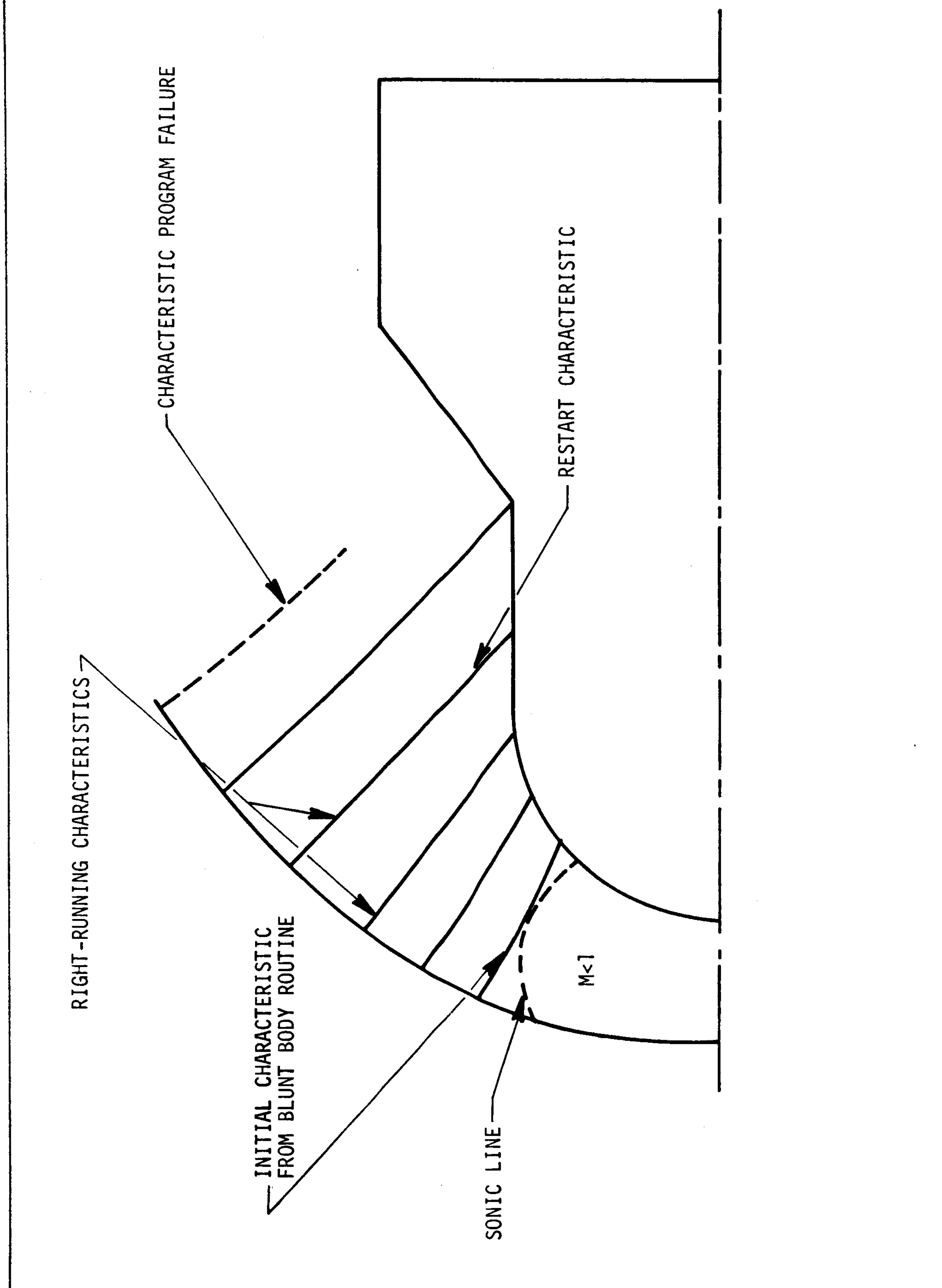

Figure 3-2a. RUN 1 INITIAL RUN WITH FAILURE AT FRUSTUM

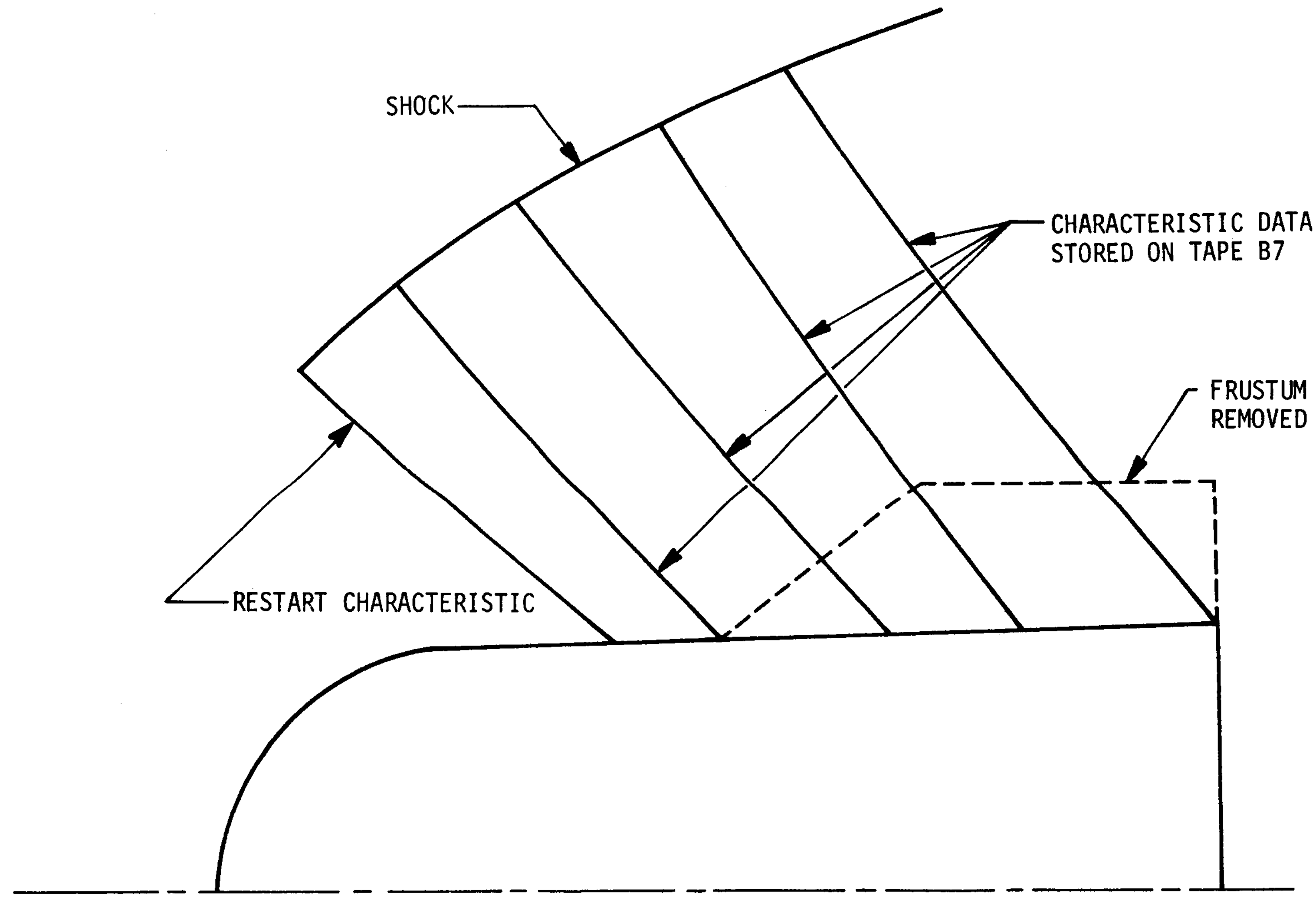

Figure 3-2b. RUN 2 DEFINITION OF UPSTREAM FLOW FIELD FOR FRUSTUM

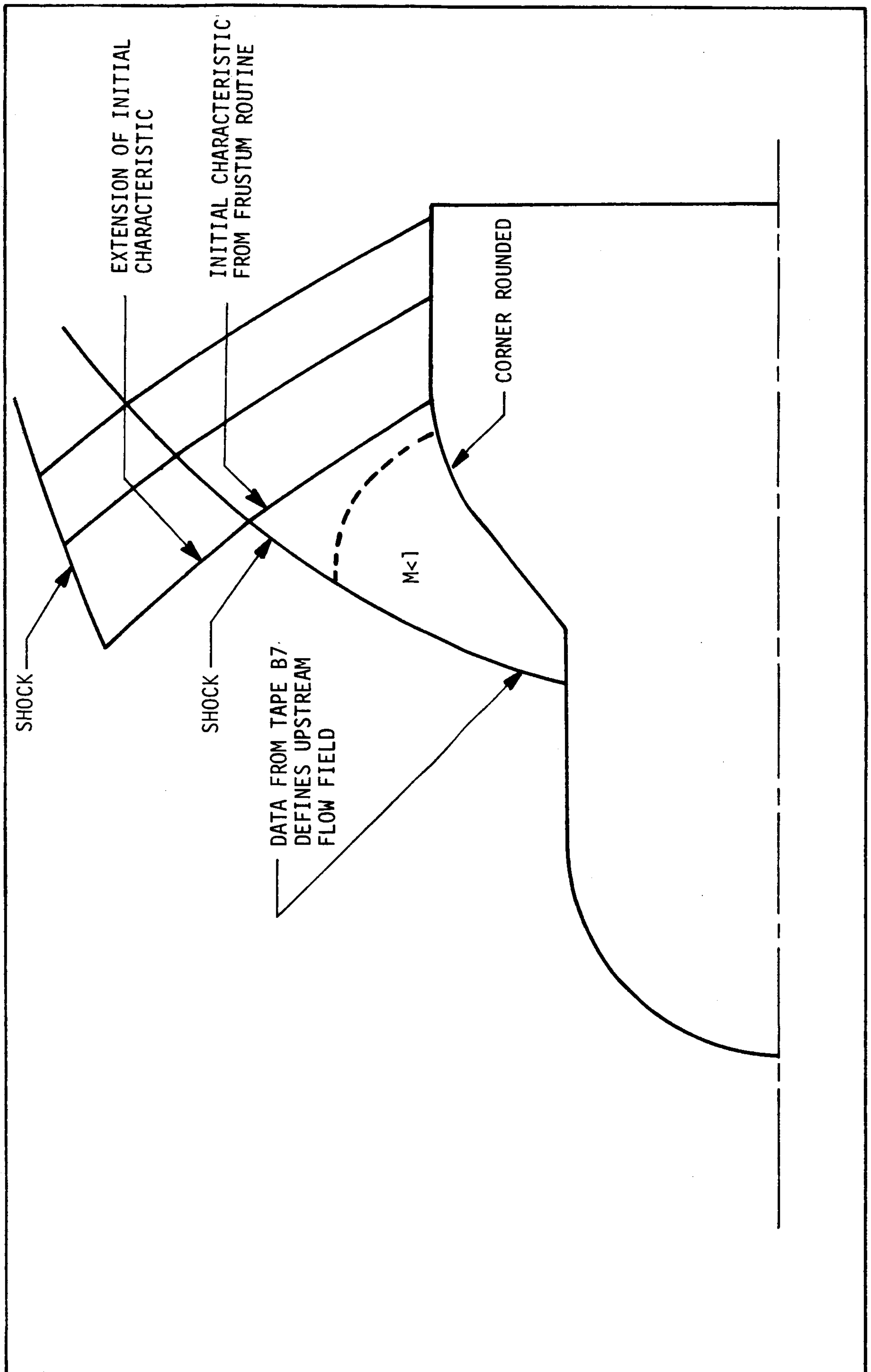

Figure 3-2c. RUN 3 FINAL RUN WITH FRUSTUM CALCULATIONS AND METHOD OF CHARACTERISTICS TO END OF BODY

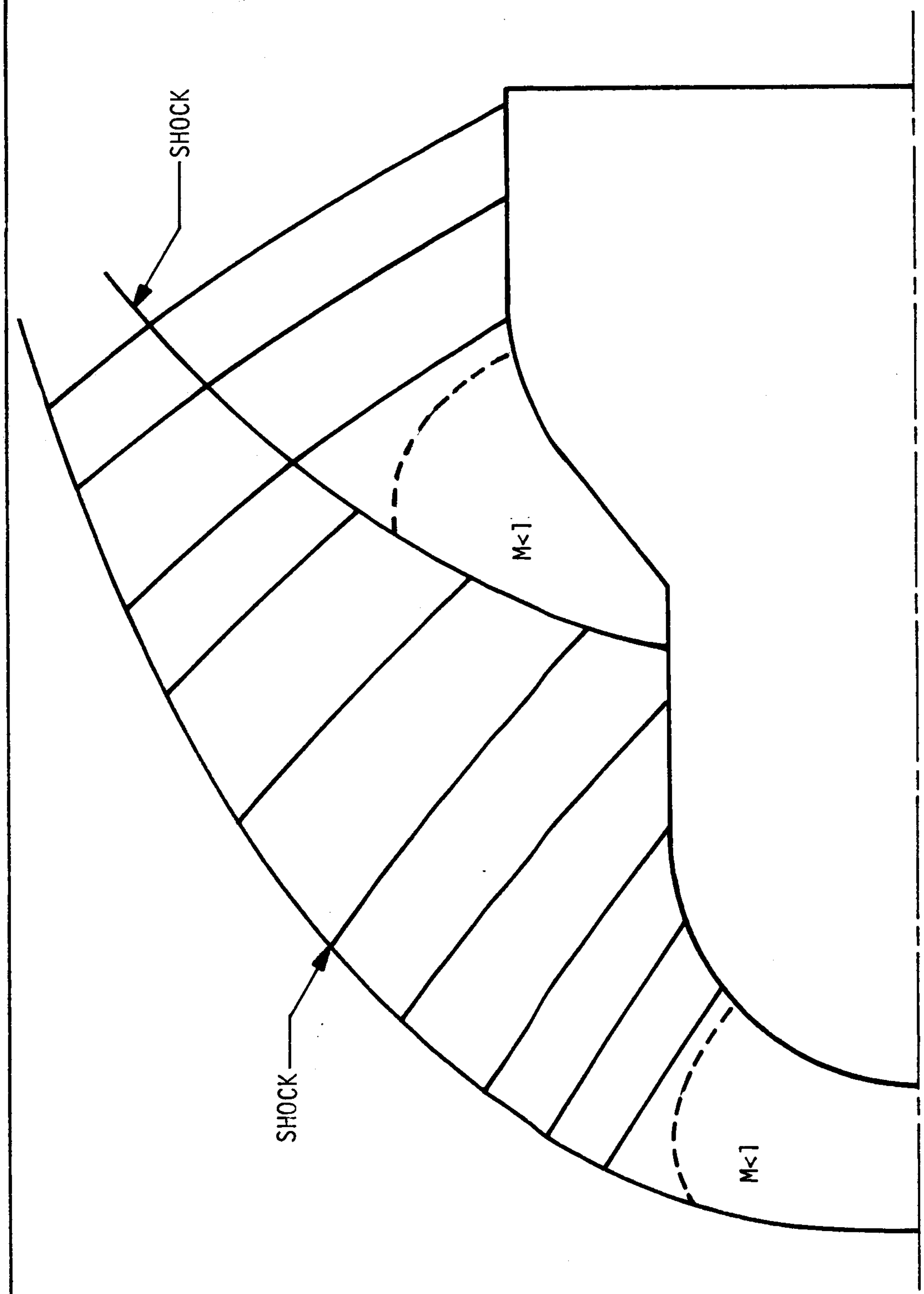

Figure 3-2d. FINAL FLOW FIELD CONFIGURATION

B

Function B provides a horizontal coordinate of the body as a function of the vertical coordinate. It has an option to provide this information for either a blunted (hemispherical or cylindrical nose) or a flat (wedge, cone, or frustum) vehicle shape. The corner of a flat type vehicle is automatically rounded.

BLUNT

Subroutine BLUNT is the main executive program for the mixed flow field program. After a solution to the flow field is found, the subroutine constructs a right running characteristic to provide coupling to the characteristics program.

BDYPTS

Subroutine BDYPTS is the subroutine that calculates the flow values at a new time step along the face of the vehicle. The quasi-one dimensional characteristics technique (Section 2.2.3.2) is used.

BP

Subroutine BP provides the first and second derivatives of the horizontal coordinate of the body with respect to the vertical coordinate. It will provide this information for the same shapes allowable in Function B.

CTL

Subroutine CTL uses the techniques described in Section 2.5.3.2 to calculate the flow variables on the cylindrical section of the body if a frustum is being calculated.

COFFER

Subroutine COFFER accepts characteristic data from a tape and, if the data is in the region around the frustum, curve-fits the flow variables and the horizontal coordinates along a characteristic line against the vertical coordinates. The coefficients of the curve-fit are stored.

DERIV

Subroutine DERIV provides first derivatives of flow variables with respect to the vertical coordinate.

ENTER

Subroutine ENTER is a two-dimensional interpolator.

EXTRA

Subroutine EXTRA extrapolates to the outer boundary those flow properties that are a function of the vertical coordinate only.

EXTRA1

Subroutine EXTRA1 extrapolates to the outer boundary those flow properties that are a function of both spacial coordinates.

INDR1

Subroutine INDR1 provides the necessary spacial derivatives for subroutines NTRNP and NTRNP2.

INITL

Subroutine INITL reads in the input pertaining to the program and sets up the initial values for the flow field.

INPRT

Subroutine INPRT prints out several initial calculations pertaining to the flow field.

NSMTH

Subroutine NSMTH provides a linear interpolation for the calculation of the points between the shock and the body to set up the initial flow field.

NTRNP

Subroutine NTRNP calculates the flow values at the next time step for all points internal to the boundaries using the techniques shown in Section 2.2.2.

NTRNP2

Subroutine NTRNP2 uses the same techniques as NTRNP to calculate the flow values at the next time step for the points above the body.

PRINT

Subroutine PRINT prints out the flow variables after the flow field solution has been found.

RANKH

Subroutine RANKH provides the shock jump equations for subroutine SHKPTS.

RES

Subroutine RES uses the curve-fitted characteristic data to provide the upstream flow conditions to subroutine RANKH as a function of both coordinates for a frustum type flow field.

SHKPTS

Subroutine SHKPTS calculates the flow variables behind the shock at a new time step. The quasi-one-dimensional characteristics technique of Section 2.2.3.1 is used.

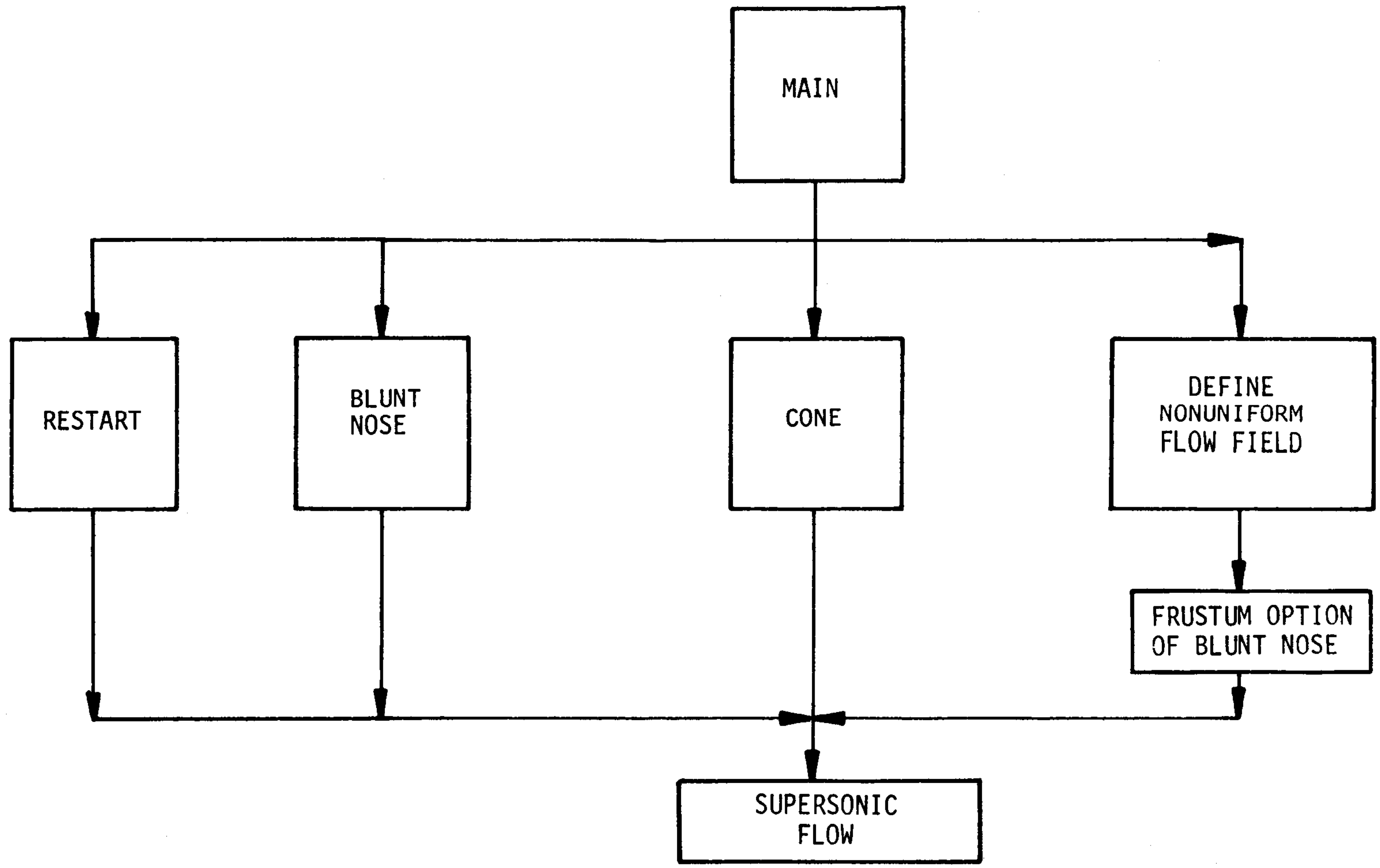

Figure 3-3a. OVERALL FLOW OF ENTIRE PROGRAM

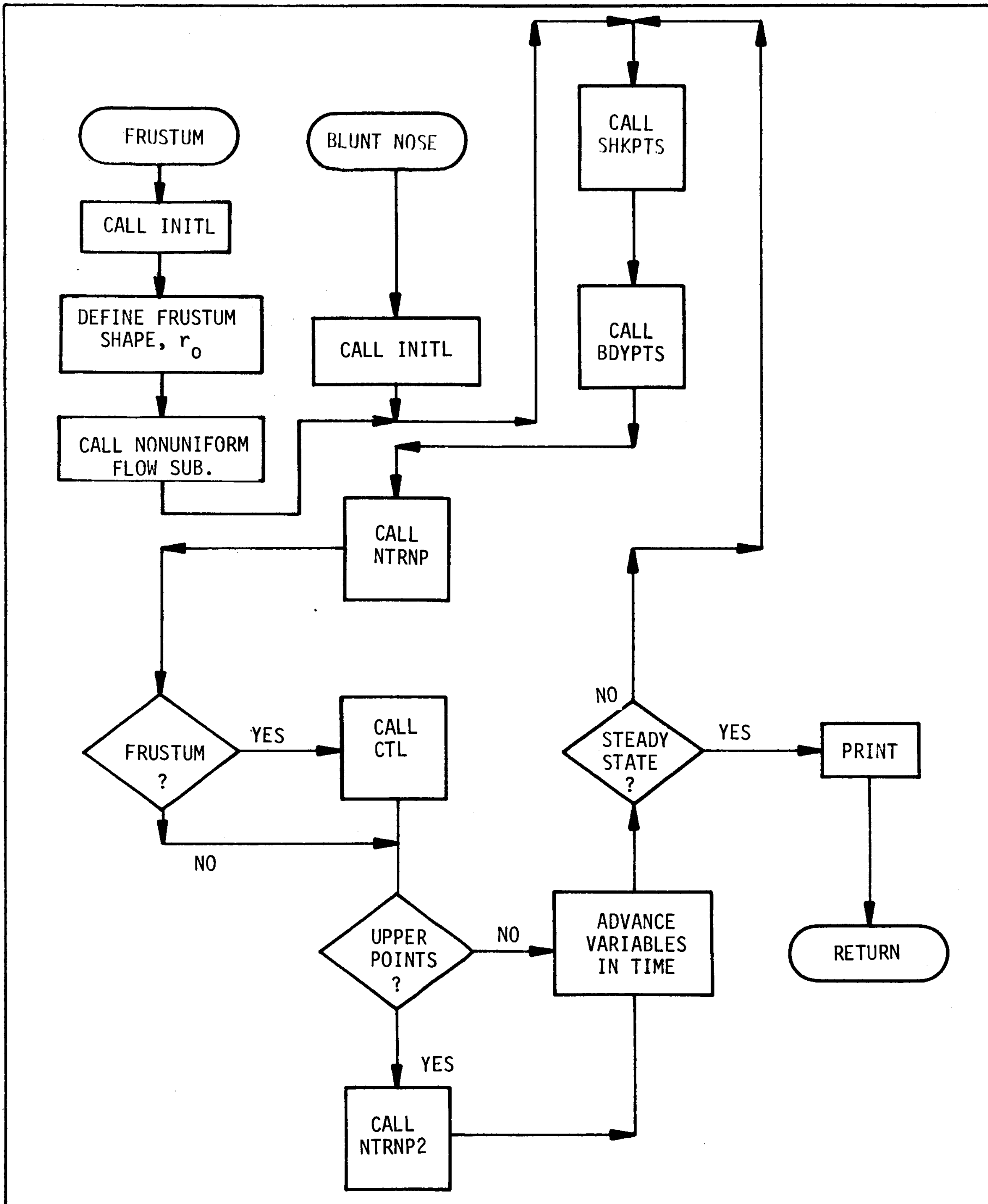

Figure 3-3b. MAIN BLUNT BODY PROGRAM

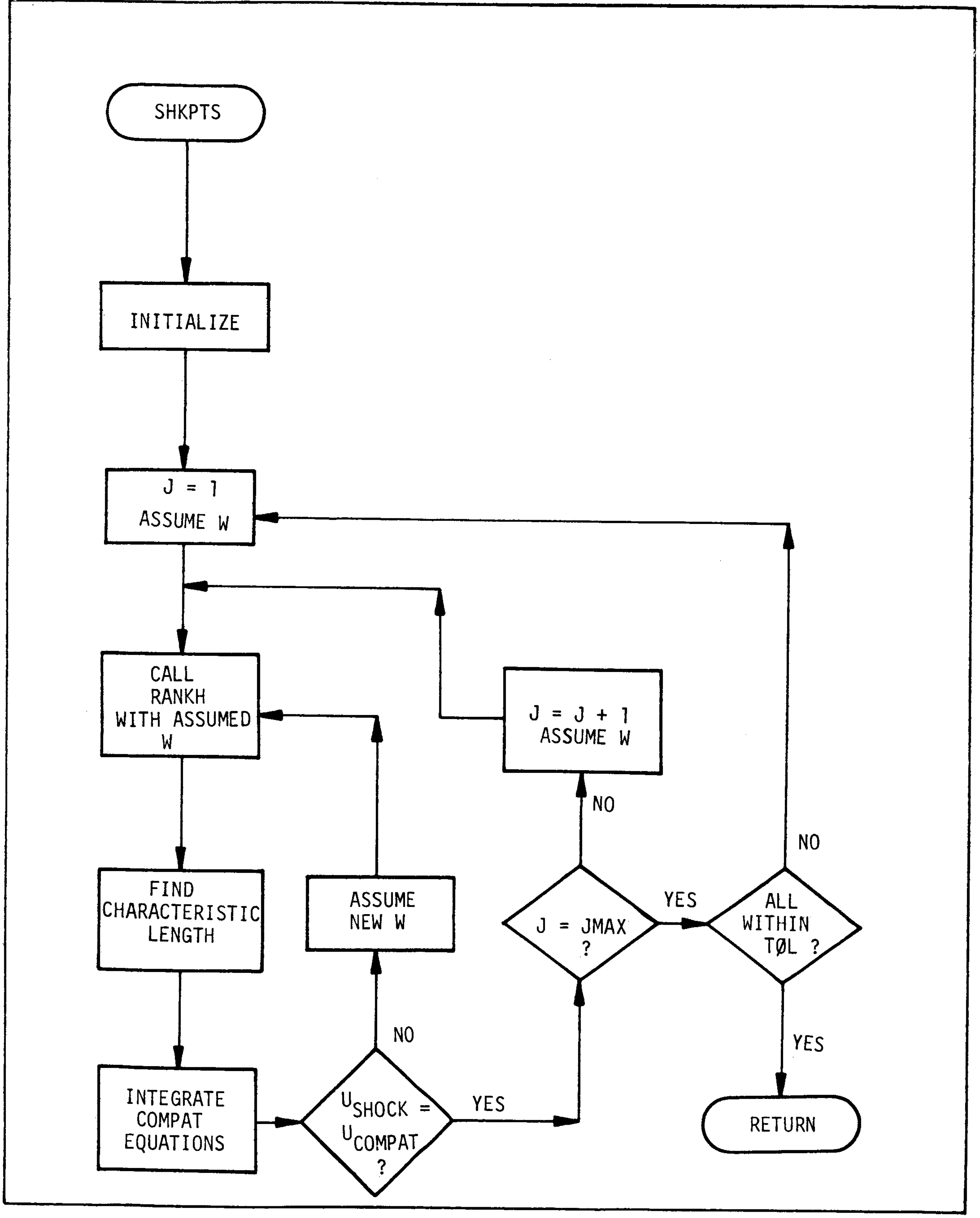

Figure 3-3c. SUBROUTINE FOR CALCULATION OF SHOCK POINTS

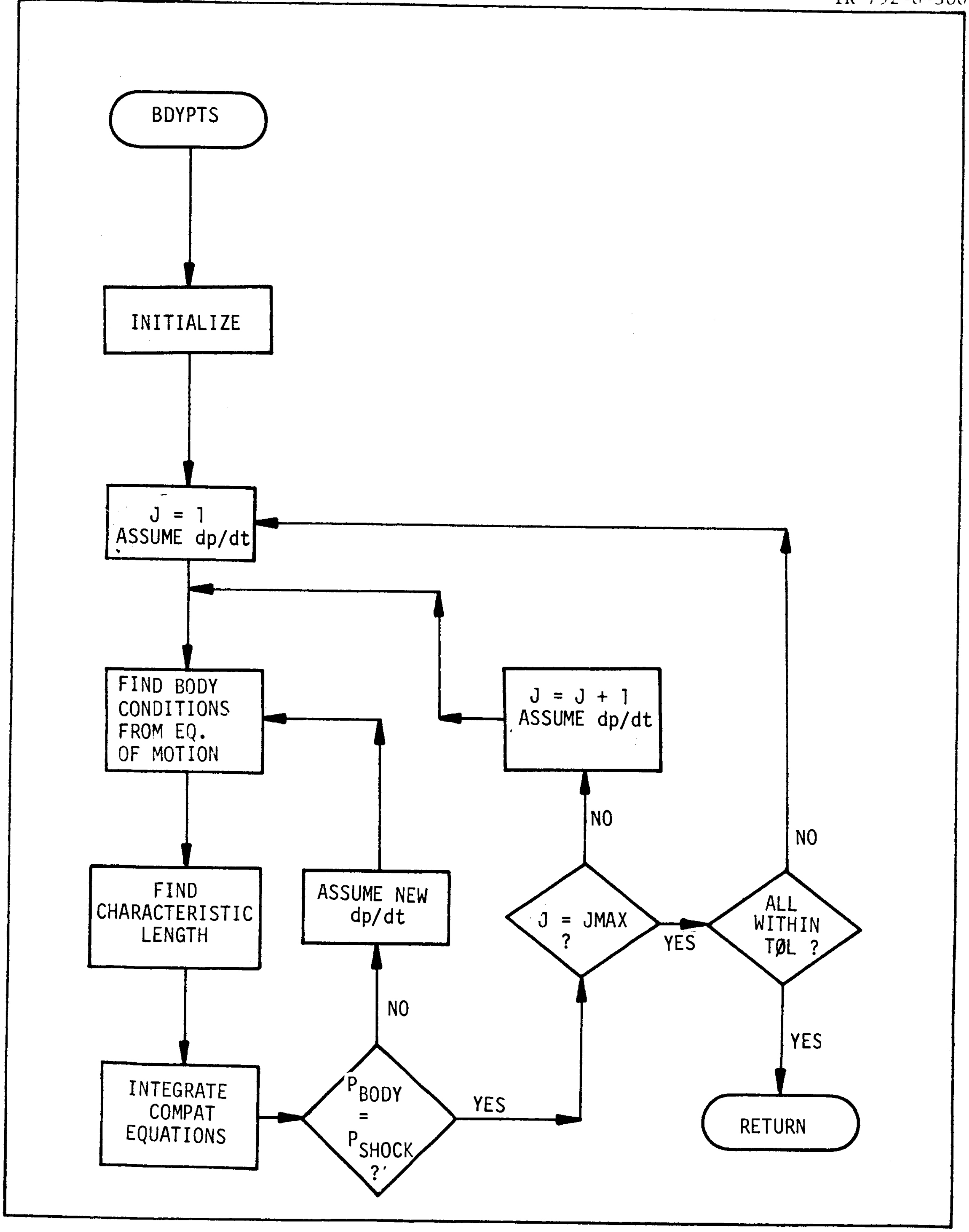

Figure 3-3d. SUBROUTINE FOR CALCULATION OF BODY POINTS

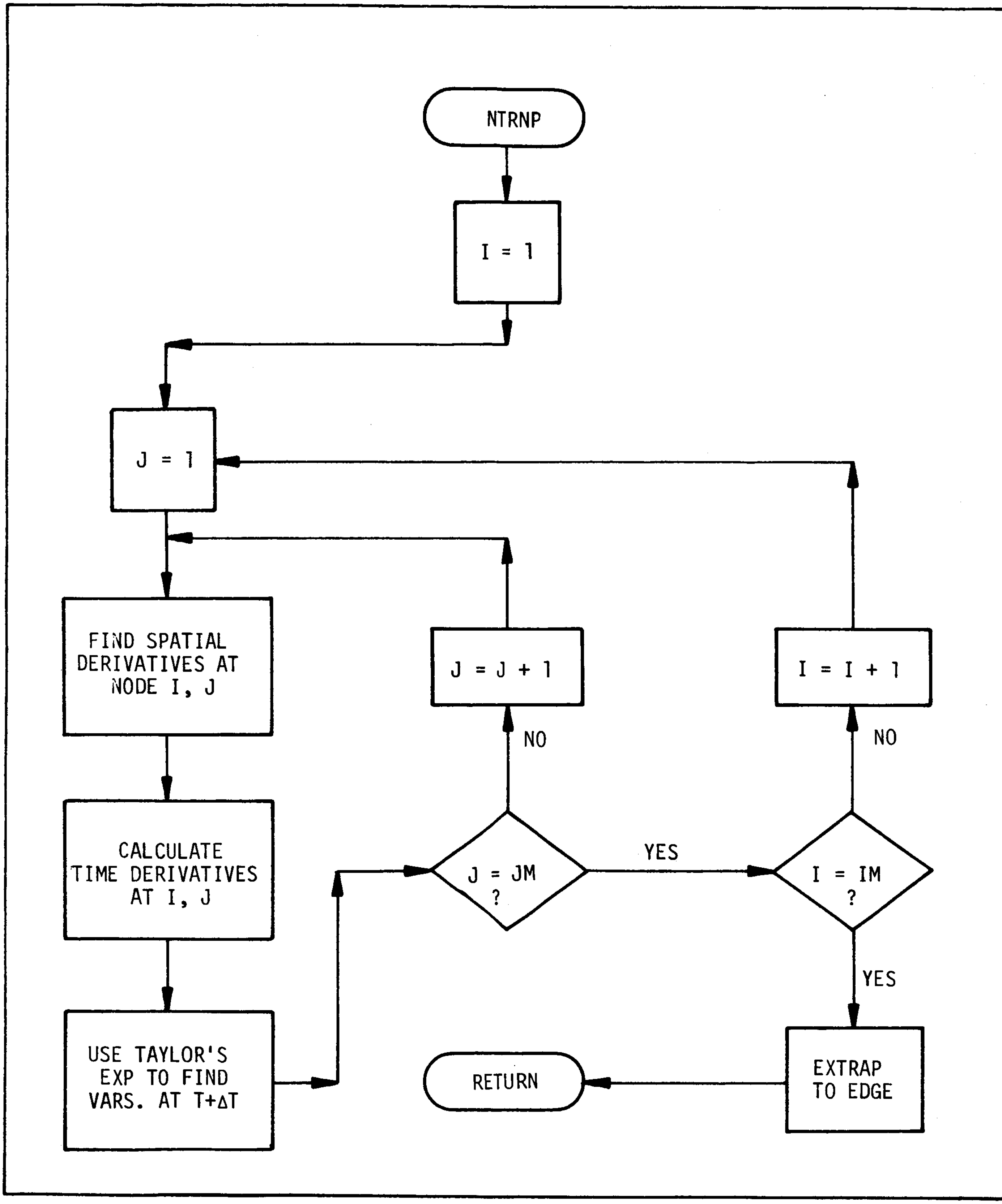

Figure 3-3e. SUBROUTINE FOR CALCULATION OF INTERNAL POINTS

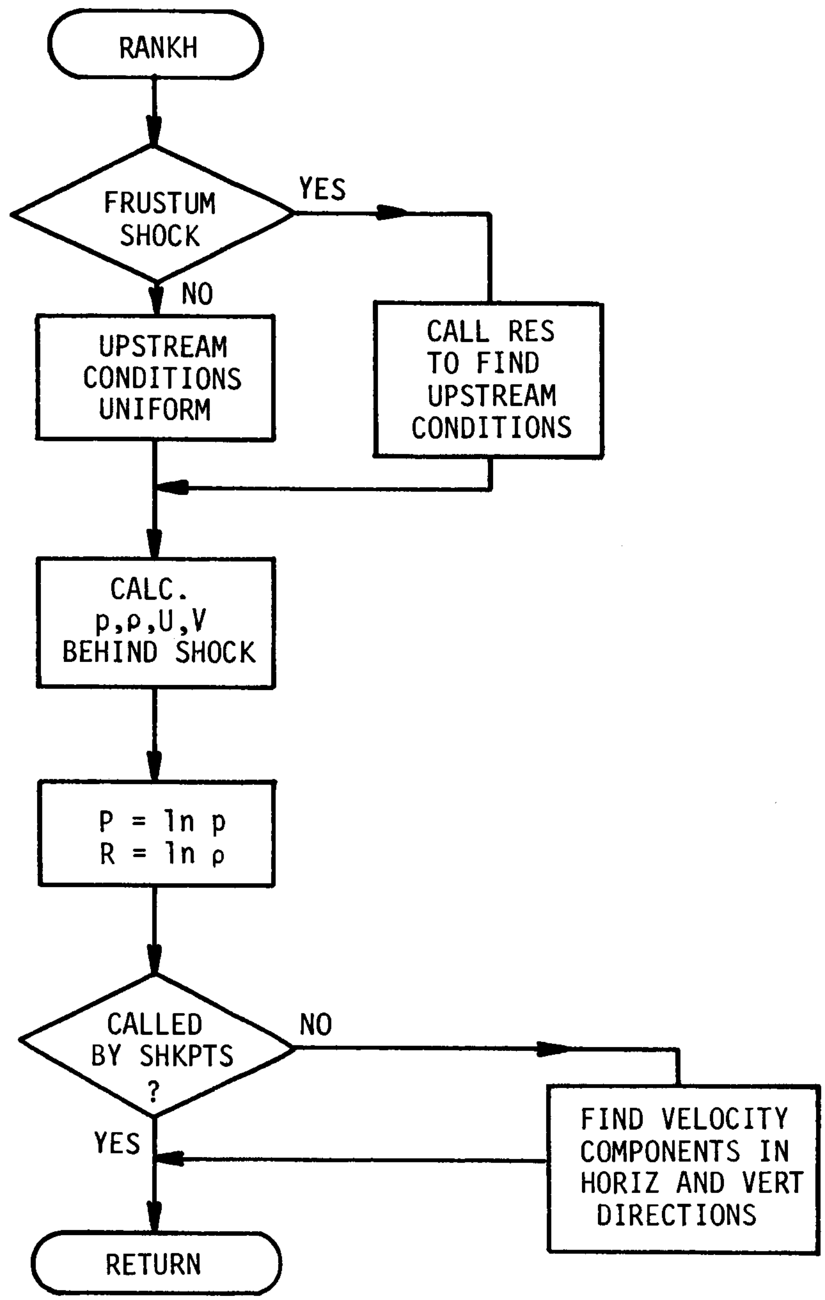

Figure 3-3f. SUBROUTINE FOR CALCULATION OF SHOCK JUMP CONDITIONS

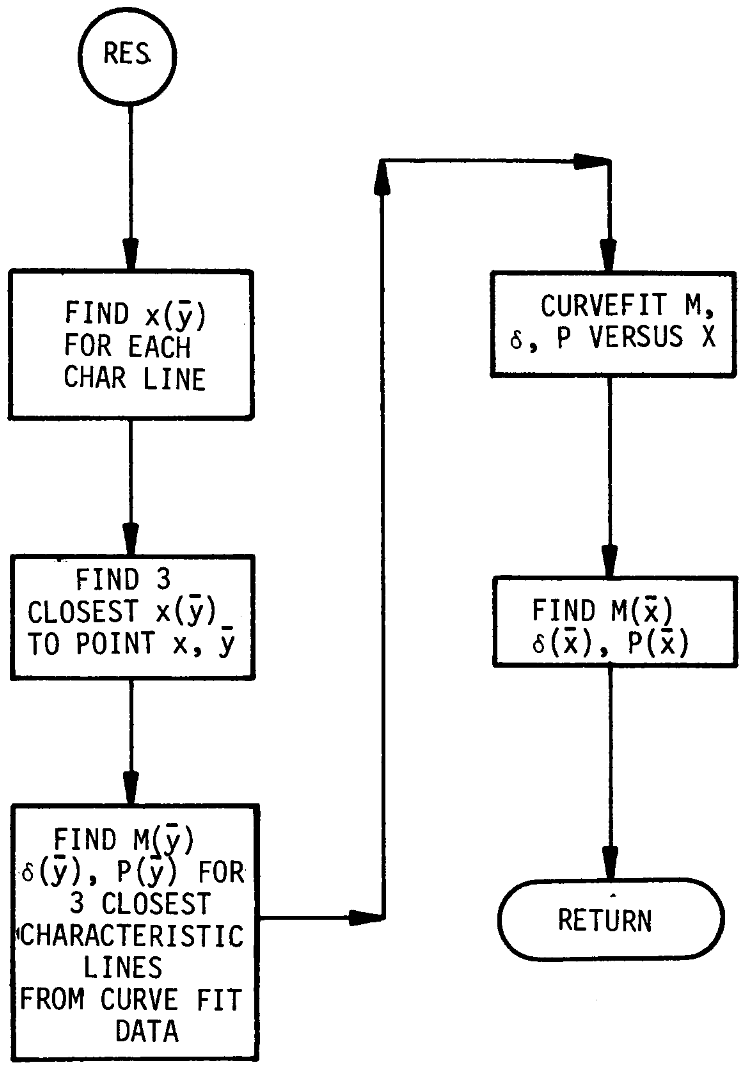

Figure 3-3g. SUBROUTINE FOR CALCULATION OF UPSTREAM CONDITIONS ON SHOCK OVER A FRUSTUM

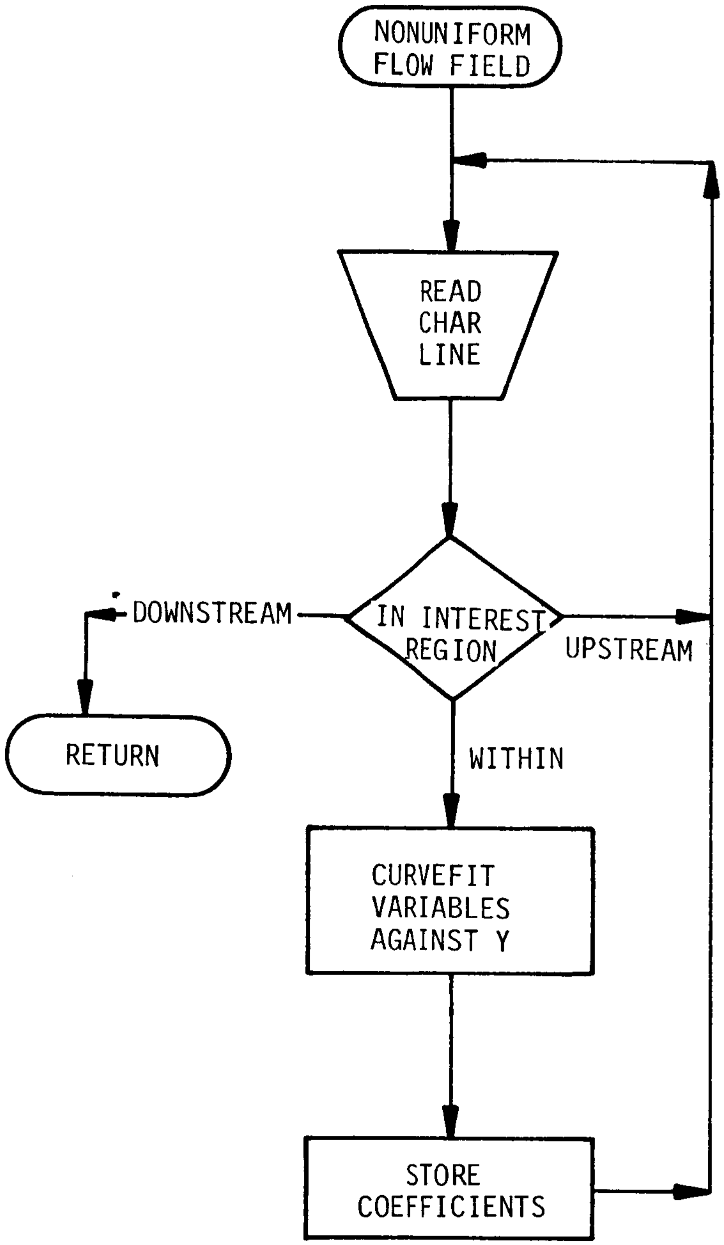

Figure 3-3h. SUBROUTINE FOR QUASI-TWO-DIMENSIONAL CURVE FIT OF UPSTREAM CONDITIONS OVER A FRUSTUM

Section IV

DISCUSSION OF RESULTS

The computer program described in Section III was used to compute a number of test cases, each designed to test various routines within the total program for extreme Mach number cases. The results from these test runs are presented in the subsections that follow. Pertinent input data for each case are presented in Table 4-1.

Table 4-1. INPUT FOR TEST CASES

Subsection	4.1	4.2	4.3	4.4
Body Shape	Hemisphere	Hemisphere	Cylinder	Frustum
Mach No.	4.0	1.62	4.0	1.9
Gamma	1.4	1.4	1.4	1.4
Free Stream Pressure (lbs/ft^2)	2116.2	2116.2	2116.2	2116.2
Free Stream Density ($slugs/ft^3$)	.002378	.002378	.002378	.002378
No. of Horiz. Grid Pts	5	8	5	6
No. of Vert. Grid Pts	8	20	11	19
Dimensional Time Step	$1. \times 10^{-5}$	$2. \times 10^{-6}$	$1. \times 10^{-5}$	$2. \times 10^{-6}$
Horizontal Step Size	.25	.143	.25	.2
Vertical Step Size	.14	.1	.14	.12

4.1 MACH 4.0 HEMISPHERE

The program was used to compute the flow field over a one-foot radius hemisphere at Mach 4.0. The coordinate system did not extend above the body. A graph showing the predicted lines of constant Mach number is presented in Figure 4-1. The sonic line and shock wave shape from a solution by Belotserkovskiy, as presented in reference 18, is also presented in Figure 4-1. As can be seen, the results agree quite well with Belotserkovskiy's solution.

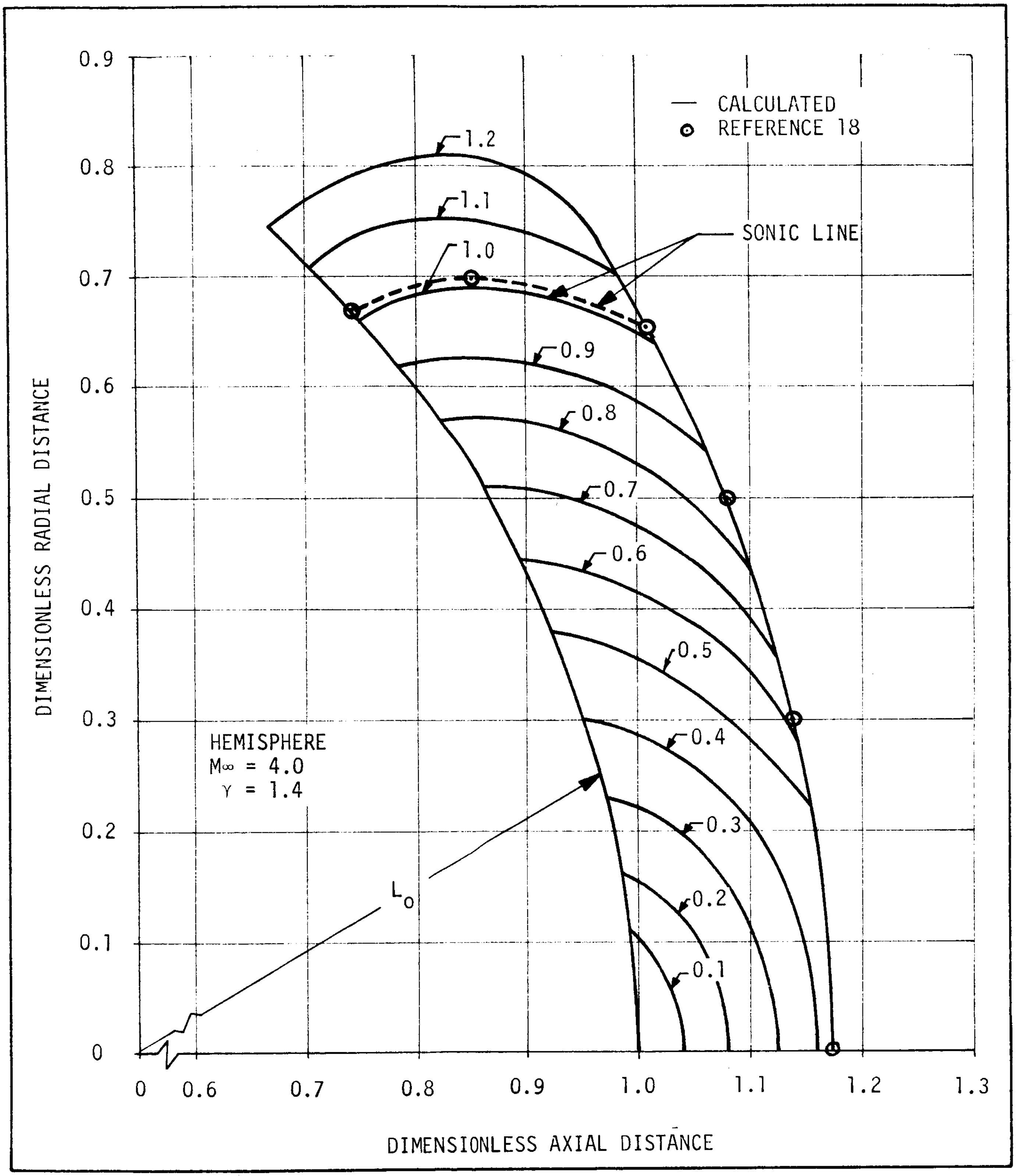

Figure 4-1. LINES OF CONSTANT MACH NUMBER OVER A MACH 4.0 HEMISPHERE

4.2 MACH 1.62 HEMISPHERE

The flow field over a one-foot radius hemisphere at Mach 1.62 was calculated by the program. For this case, it was necessary to extend the flow field grid above the body. A plot of the density distribution along the body surface, along with experimental data from reference 17, is presented in Figure 4-2. Figure 4-3 presents the shock and body configuration. The predicted body density agrees with the experimental data in reference 17, but the predicted shock standoff distance is about 10% smaller than the experimental data from the same reference.

This extreme Mach number case exposed an apparent weakness in the technique. As the Mach number decreases, the step size in time demanded by stability requirements also decreases, resulting in an extremely short characteristic for the boundary conditions. This short characteristic appears to provide information to the shock and body node points that is somewhat inaccurate. This results in a smaller shock standoff distance and a zigzag shock pattern near the axis of symmetry. If the zigzag shock is not too pronounced, a good approximation to the flow field may be made by fairing a curve through the points. The problem can be reduced by a judicious choice of input parameters.

4.3 MACH 4.0 TWO-DIMENSIONAL BLUNT-CYLINDER-FLARE

The flow field over a two-dimensional blunt-nose-cylinder-flare configuration was calculated to demonstrate the coupling between the Blunt Body Routine and the Supersonic Flow Routine. The configuration had a one foot radius cylindrical nose followed by a one foot long segment with a slope of 0° and a one foot long segment with a slope of 10°. The resulting shock wave configuration, along with some of the significant characteristic lines, is presented in Figure 4-4. To conserve computation time, the subsonic flow field in this run was not allowed to reach a steady-state condition, and thus the true flow field is not accurately represented.

4.4 MACH 1.9 FRUSTUM

The flow field over an axisymmetric frustum at Mach 1.9 was calculated to demonstrate the capability of the program. The configuration consisted of a frustum with a 45° slope, an upstream radius of one foot, a downstream

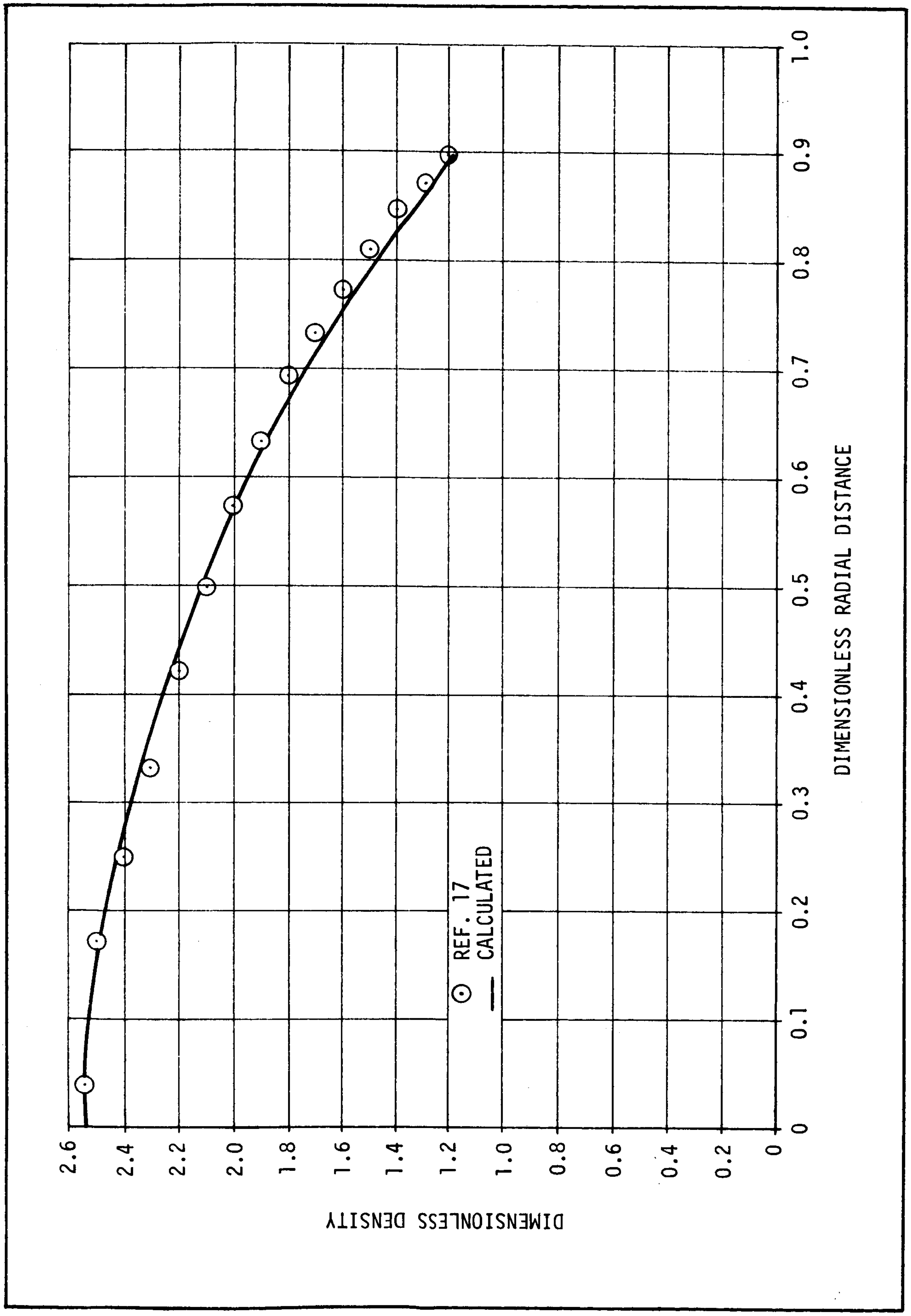

Figure 4-2. DENSITY OVER A MACH 1.62 HEMISPHERE

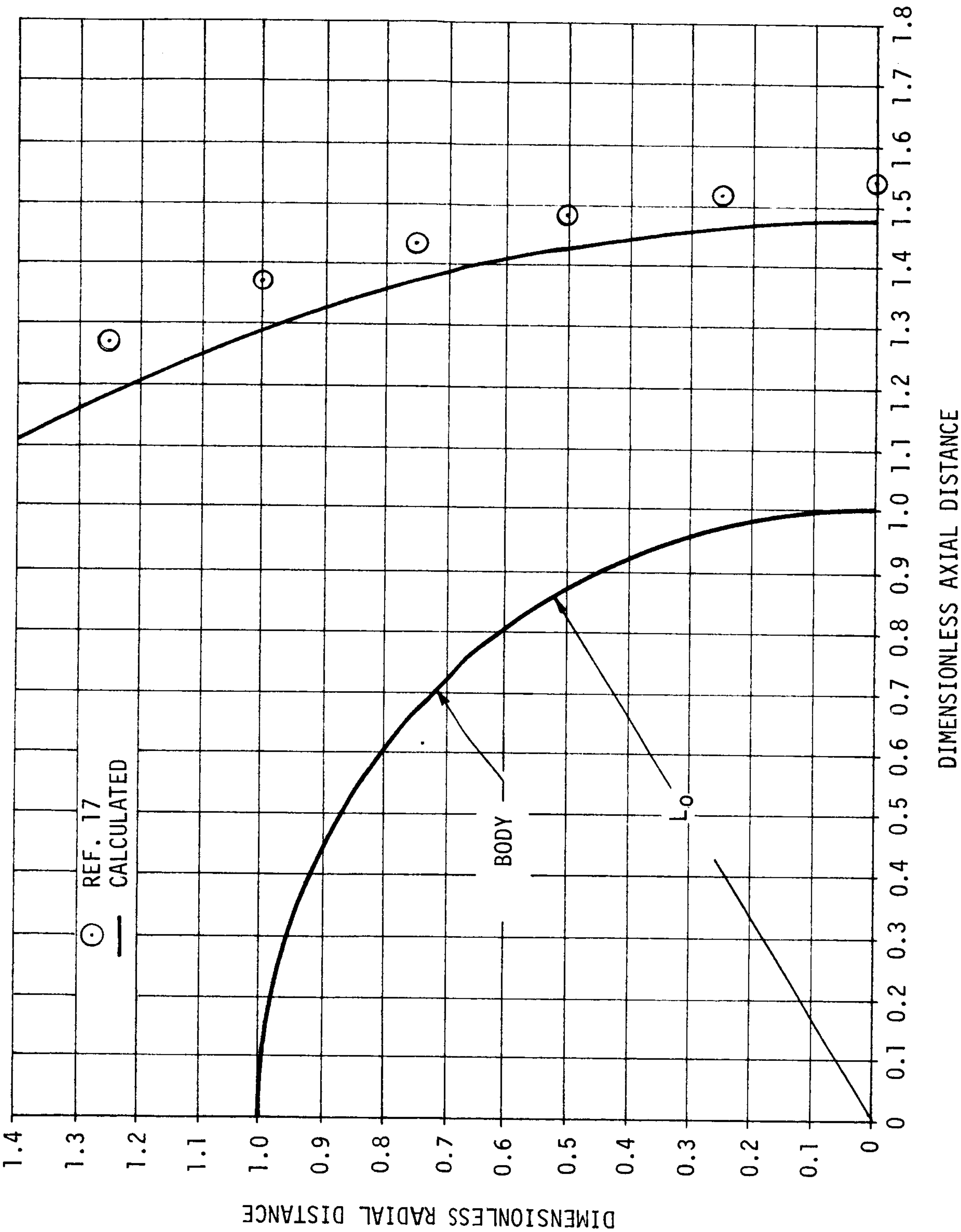

Figure 4-3. SHOCK SHAPE OVER A MACH 1.62 HEMISPHERE

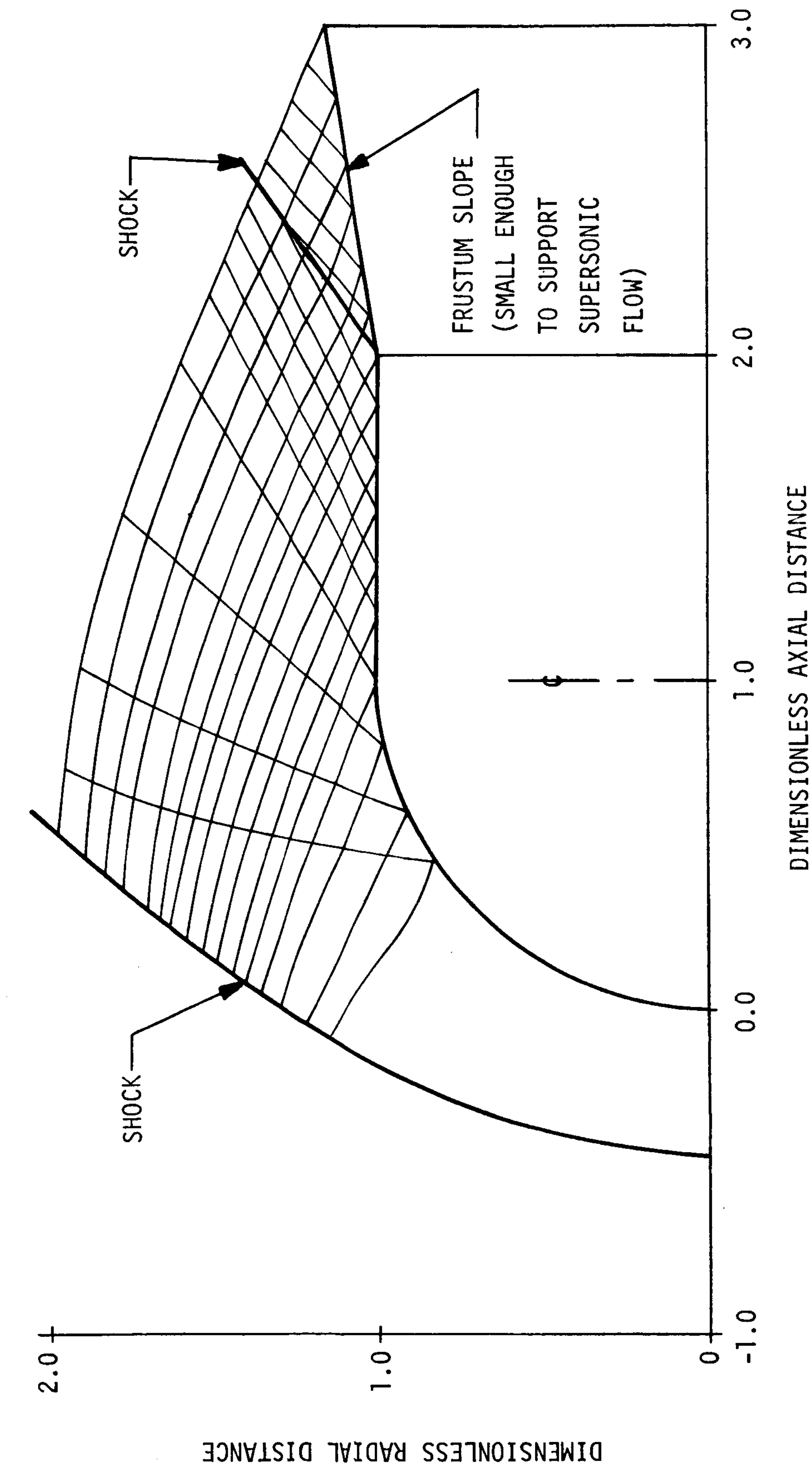

Figure 4-4. FLOW PATTERN OVER A MACH 4.0 TWO-DIMENSIONAL BLUNT-NOSE CYLINDER-FRUSTUM-CYLINDER

radius of two feet, and a uniform upstream Mach number of 1.9. A plot of the shock and body shapes and the resultant Mach lines is presented in Figure 4-5. A plot of the body pressure distribution is presented in Figure 4-6. Unfortunately, comparative experimental data is not available.

The general shape of the shock and of the Mach lines is seen to be similar to those observed over a hemisphere. As the upper corner of the frustum represents an unresolvable singularity in the flow field, the corner was replaced by a radial segment. An interesting result is the fact that the sonic line intersects the body almost exactly at the place on the body where the curvature begins, and the flow is supersonic over the entire curved region.

4.5 MACH 1.9 HEMISPHERE-CYLINDER-DETACHED FRUSTRUM-CYLINDER

Because of excessive computer turn-around time and contractual limitations, the results for flow at Mach 1.9 over a hemisphere-cylinder-detached-frustum-cylinder configuration were not available in time to include in this report. The results, which are presently being calculated, will be presented in a supplement to be published at a later date. The configuration consists of a hemisphere with a radius of one foot, a cylinder one foot long, a one-foot-long frustum with a slope of 45°, and another cylinder one foot long. The blunt nose solution can be compared to an inverse technique, but for the remainder of the flow field, little, if any, experimental data exists.

4.6 DISCUSSION OF TIME STEP SIZE

While working with a preliminary version of the flow field deck it was discovered that the use of the time step size decreed by the Courant-Friedrichs-Lewy criterion, as discussed in Subsection 2.2.2 and based on the free stream flow properties, led to instabilities and the degeneration of results. This problem was eliminated by decreasing the step size arbitrarily to the point where the instabilities disappeared. Later detailed analysis of flow fields have shown that the minimum time step size is decreed by the lowermost grid point on the shock (a point for which all the values necessary for the stability criterion can be found before the execution of the program). However, the use

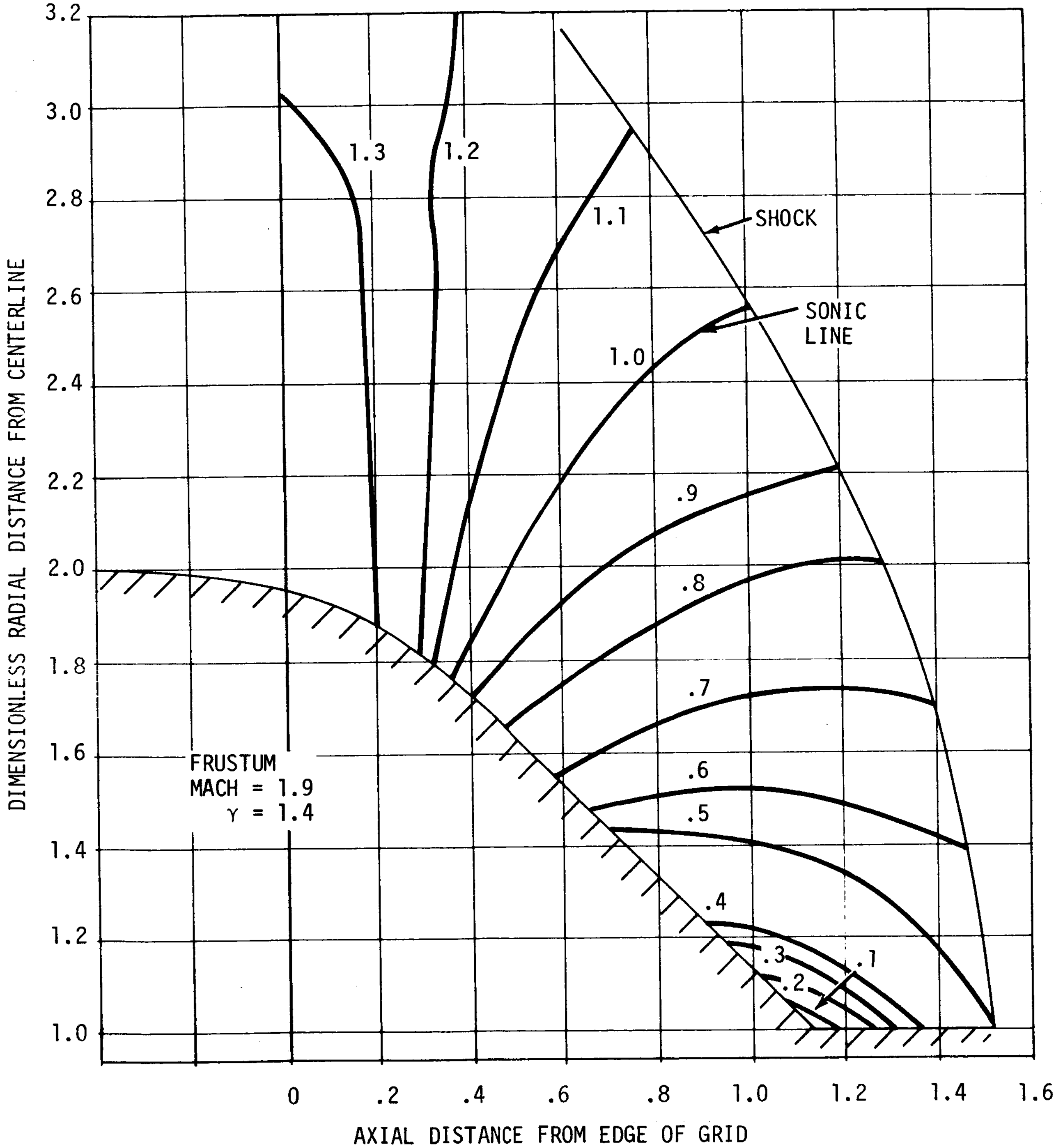

Figure 4-5. LINES OF CONSTANT MACH NUMBER OVER A MACH 1.9 FRUSTUM

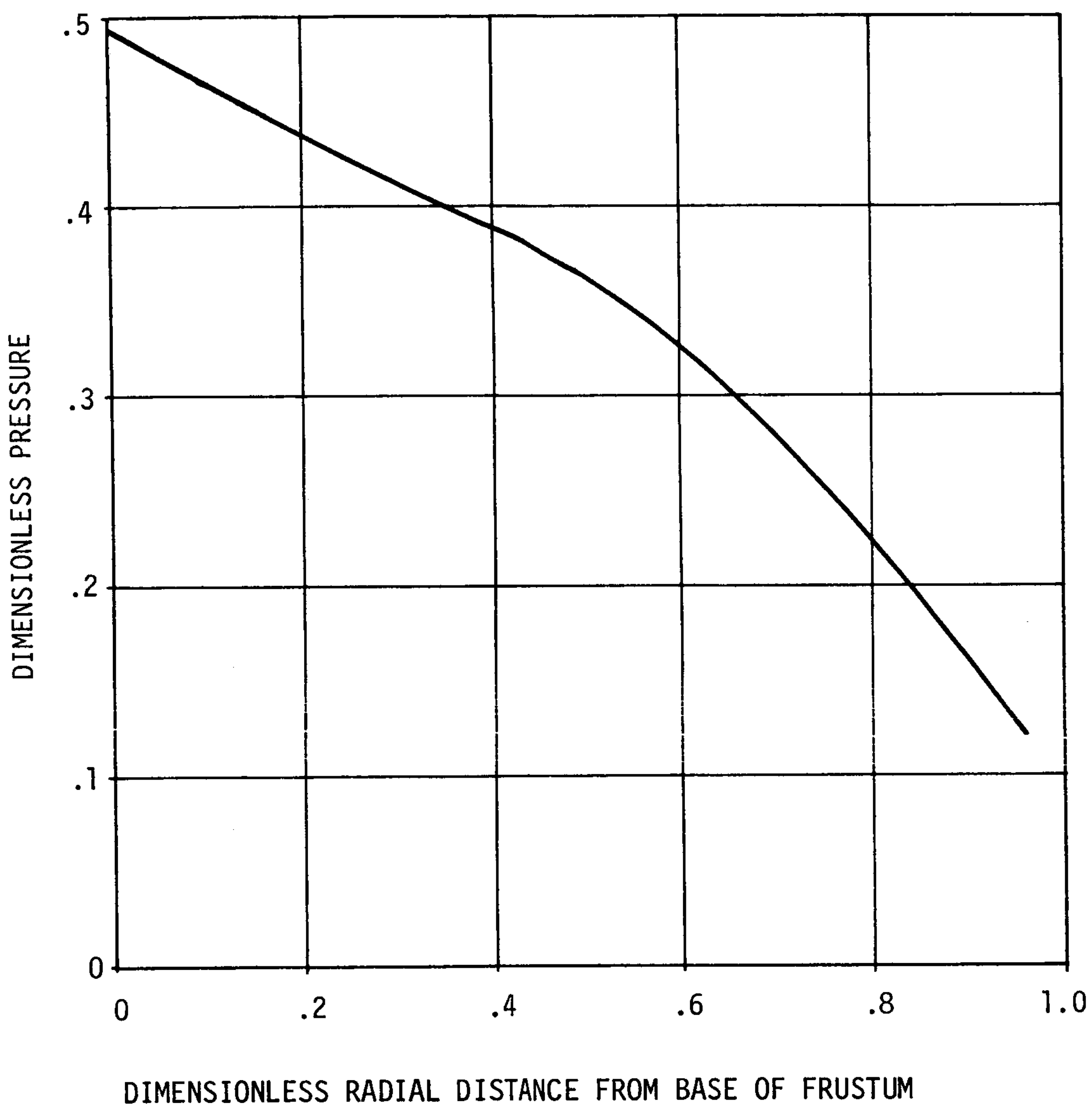

Figure 4-6. PRESSURE DISTRIBUTION ALONG FRUSTUM FACE

of these step sizes also proved to be unstable. The cause of these unsuspected unstabilities is thought to be in the characteristics used in the boundary conditions, rather than the interior points. A rule of thumb has been developed based on the step sizes used to generate stable flow fields:

> A stable step size is provided by dividing by 10 the step size predicted by the Courant-Freidrichs-Lewy criterion, based on the steady state flow field properties at the lowermost grid point on the shock (as found from normal shock relations).

Section V

CONCLUSIONS AND RECOMMENDATIONS

The program for an entire Saturn type flow field analysis is shown by the results to be a reasonable means to obtain Saturn type flow fields. The major disadvantages, i.e., the awkwardness in the necessity of multiple runs for analysis of detached frustum shocks and the amount of computer time necessary for each one, are more than compensated for by the unique capability of calculating supersonic flow fields with subsonic and mixed regions.

The accuracy of the Blunt Body Routine depended upon the time and step sizes and the free stream conditions. The program is seen to be an excellent means to obtain good results for the higher Mach numbers, and can provide reasonable results for the lower Mach numbers.

Although the Blunt Body Routine has been extended to allow the calculation of a detached shock over a frustum with a non-uniform free stream flow, little or no data exists to verify the results. However, as the technique is merely a minor extension of the proven Blunt Body technique, the results should be valid. If the results are valid, the technique represents a unique capability in the field of fluid dynamics.

Future work on the unsteady Blunt Body technique would need to establish the coordinate system of the body in spherical, rather than cylindrical, coordinates. A better method of matching the boundary point solutions to the interior point solutions should be found, particularly for the low Mach number cases. Finally, work should be done on the problem of singularities, such as corners, in the flow field.

Section VI

REFERENCES

1. Van Dyke, M.D., "The Supersonic Blunt-Body Problem-Review and Extension," Journal of Aerospace Sciences, August 1958.

2. Lomax, H. and Inouye, M., "Numerical Analysis of Flow Properties About Blunt Bodies Moving at Supersonic Speeds in an Equilibrium Gas," NASA TR-R-204, July 1964.

3. Lin, C. C. and Shen, S. F., "An Analytical Determination of the Flow Behind a Symmetrical Curved Shock in a Uniform Stream," MIT, NACA TN 2506, 1951.

4. Vaglio,Laurin, Roberts, "On the PLK Method and the Supersonic Blunt-Body Problem," Journal of Aerospace Sciences, February 1962.

5. Von Neumann, J. and Richtmyer, R. D., "A Method for the Numerical Calculation of Hydrodynamic Shocks," Journal of Applied Physics, 1949.

6. Belotserkovskiy, O. M., "On the calculation of Flow Past Axisymmetric Bodies with Detached Shock Waves Using an Electric Computing Machine," Appl. Math. Mech., Vol 24, 1960, pp. 511-517.

7. Bohachevsky, I. O. and Mates, R. E., "A Direct Method for Calculation ot the Flow about an Axisymmetric Blunt Body at Angle of Attack," AIAA Journal, Vol. 24, No. 5, May 1966, pp. 776-782.

8. Bohachevsky, I. O. and Rubin, E. L., "A Direct Method for Computation of Nonequilibrium Flows with Detached Shock Waves," AIAA Journal, Vol. 4, No. 4, April 1966, pp. 600-607.

9. Moretti, G. and Abbett, M., "A Fast, Direct, and Accurate Technique for the Blunt Body Problem," GASL TR-583, General Applied Science Laboratories, Inc., 1966.

10. Moretti, G. and Abbett, M., "A Time-Dependent Computational Method for Blunt Body Flows," AIAA Journal, Vol. 4, No. 12, December 1966, pp. 2136-2141.

11. Lox, P. D. and Wendroff, R., "Difference Schemes for Hyperbolic Equations with High Order of Accuracy," Comm. Pure Appl. Math., Vol. 17, 1964, p. 381.

12. Courant, R., Friedrichs, K. O., and Lewy, H., "Ueber die Partiellen Differenzengleichungen der Mathematischen Physik," Math. Ann., Vol. 100, 1928, p. 32.

13. Shapiro, Ascher H., The Dynamics and Thermodynamics of Compressible Fluid Flow, Vol. I, The Ronald Press Company, New York, N. Y., 1953.

14. Shapiro, Ascher H., The Dynamics and Thermodynamics of Compressible Fluid Flow, Vol. II, The Ronald Press Company, New York, N. Y., 1953.

15. Powers, S. A., "A Two-Dimensional and Axisymmetric Method of Characteristics Program," NORAIR Technical Note (to be published).

16. Ames Research Staff, "Equations, Tables, and Charts for Compressible Flow," NACA TR-1135, 1953.

17. Gooderum, P. B., and Wood, G. P., "Density Fields around a Sphere at Mach Numbers 1.30 and 1.62," NACA TN-2173, 1950.

18. Hayes, W. D., and Probstein, R. F., Hypersonic Flow Theory, 2nd ed. Vol. 1 Academic Press, New York, 1966.

Appendix A

INPUTS AND OUTPUTS

As the combined flow field program is divided into essentially three main routines (the Cone Routine, the Blunt Body Routine, and the Supersonic Flow Routine), it is considered expedient to break down the inputs and outputs of the combined program into these three areas.

A.1 INPUTS

In accordance with the above considerations, the inputs for the Cone Routine, Blunt Body Routine, and Supersonic Flow Routine are presented as separate blocks. Inputs for the special cases of a frustum and restarting input are also presented. Table A-1 contains a list of all input symbols and their definition.

A.1.1 Cone Input

Inputs to the Cone Routine consist of the free stream conditions, the conical half angle, the number of ray-lines in the Taylor-Maccoll solution, the number of points to be located on the initial right-running characteristic, and a parameter STEP. If the parameter STEP is zero, the shock is considered to be attached and certain cards as indicated in Figure A-1 are not included in the input. If the parameter STEP is not zero, a test is made to determine whether the cone shock is attached or detached. If the shock is detached, control is passed to the Blunt Body Routine and the last four cards in Figure A-1 are used as input to this routine. If the shock is attached, the Cone Routine is used in the same manner as with STEP equal to zero, and the last four cards are skipped.

5	10	15	20	25	30	35	40	45	50	55	60	65	70	75	80
ITYPE	IRAY	IVL	STEP												
	FORMAT(3I5,E10.0)														
DELTA		GAMMA			MACH										
	FORMAT(3E12.0)														
IM	JM	JT	EPS	IND	NSTOP										
	FORMAT(6I5)														
RMAX			DLT												
	FORMAT(2E15.0)														
PIN			RIN												
	FORMAT(2E15.0)														
XF			YLF			YF									
	FORMAT(3E15.0)														

NOTE: IF STEP IS ZERO, THE FOLLOWING CARDS ARE NOT TO BE INCLUDED

Figure A-1. CONE INPUT

A.1.2 Blunt Body Input

Input for the Blunt Body Routine consists of data necessary to describe the grid mesh, data to describe the free stream conditions, and data to describe the body. After the program calculates a set number of time steps (input), it is assumed that the solution has been found. A right-running characteristic is generated by the body to the shock to couple the solution to the supersonic flow.

5	10	15	20	25	30	35	40	45	50	55	60	65	70	75	80
ITYPE			STEP												
	FORMAT(I5,10XE10.0)														
MACH		GAMMA													
	FORMAT(2E12.0)														
IM	JM	JT	EPS	IND	NSTOP										
	FORMAT(6I5)														
RMAX			DLT			RSPHER									
	FORMAT(3E15.0)														
PIN			RIN												
	FORMAT(2E15.0)														

Figure A-2. BLUNT BODY INPUT

A.1.3 Supersonic Flow Input

Input to the Supersonic Flow program consists of control options and a complete description of the body. The control options specify the types of output desired, while the body is described in terms of segments. The program assumes there is a blunt nose on every body, but this nose can be of zero size. The program can handle attached shock frusta and expansion corners, but is limited to an ideal gas. If the program fails at a frustum, the program terminates. The frustum may then be treated with the Blunt Body program to continue the solution downstream.

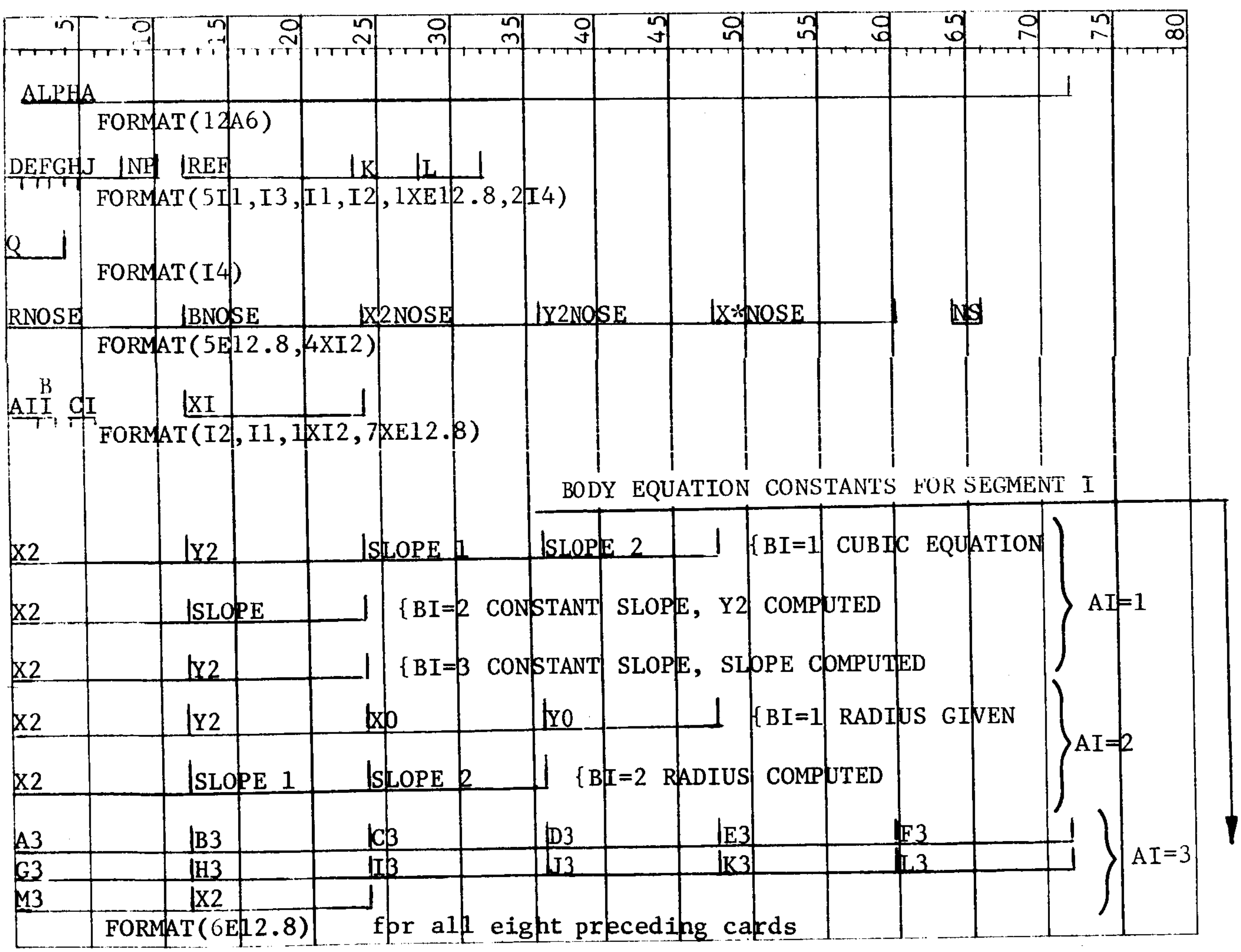

Figure A-3. SUPERSONIC FLOW INPUT

Notice should be taken that for each body segment, except the blunt nose, there must be a set of cards consisting of the fifth card and the corresponding body equation constants cards shown in Figure A-3. For AI = 3, the body equation constants are used in an equation of the form

$$Y = A3\ (X-F3)^{4} + B3(X-F3)^{3} + C3(X-F3)^{2} + D3(X-F3) + E3$$
$$+ G3(H3(X-L3)^{3} + I3(X-L3)^{2} + J3(X-L3) + K3)^{M3}$$

A.1.4 Restarting Input

The restarting mode enables the Supersonic Flow Routine to continue a solution downstream from any previously calculated right-running characteristic. This shortens the computation time necessary to calculate the flow over a given nose configuration with several possible tail configurations. The data necessary for the restart mode includes a pointwise description of the right-running characteristic line (or a left-running characteristic or any specified line), and a pointwise description of the total pressure ratio versus height of the low shock. The solution will continue downstream from the specified line.

Card fields (columns 1–80)	Format	
ITYPE	FORMAT(I5)	
MACH, GAMMA	FORMAT(2E12.8)	
CD	FORMAT(24XE12.8)	
ICHAR	FORMAT(I5)	
NG	FORMAT(I3)	
YSHOCK, PTPTS	FORMAT(2E12.8)	NG NUMBER OF DATA CARDS
MG	FORMAT(I5)	
X, Y, DEL, MACH, PTPTM	FORMAT(5E12.8)	MG NUMBER OF CARDS

Figure A-4. RESTARTING INPUT

A.1.5 Frustum Input

The input necessary to calculate the flow over a frustum is essentially the same as the input for a blunt body. Tape B7 from a previous run must be used to specify the non-uniform flow field upstream of the frustum. Additional input is necessary to define a region of interest around frustum, so as to minimize the amount of curve fitting necessary to define the upstream flow field. After a solution has been found, a right-running characteristic is generated from the body through the frustum shock to the bow shock to couple the solution to the Supersonic Flow Routine.

5	10	15	20	25	30	35	40	45	50	55	60	65	70	75	80
ITYPE			STEP												
	FORMAT(I5,10X,E10.0)														
MACH		GAMMA													
	FORMAT(2E12.0)														
IM	JM	JT	EPS	IND	NSTOP										
	FORMAT(6I5)														
RMAX			DLT			RL									
	FORMAT(2E15.8)														
PIN			RHOIN												
	FORMAT(2E15.0)														
XF			YLF			YF									
	FORMAT(3E15.8)														
XMIN			XMAX			DELTA									
	FORMAT(3E15.8)														

Figure A-5. FRUSTUM INPUT

Table A-1. LIST OF INPUT SYMBOLS

The following list of symbols defines every symbol used for inputs. The words Supersonic Flow Routine have been shortened to S.F.R. for brevity:

AI	Indicator for body segment type in S.F.R. AI=1 Cubic segment AI=2 Radial segment AI=3 General type body
ALPHA	72 character alphameric title for S.F.R.
A3	Constant in general type body segment in S.F.R.
BI	An indicator for body segment type in S.F.R. defines which segment end conditions are input.
BNOSE	Used in S.F.R. Has value of 1.0 if blunt nose, zero if cone.
B3	Constant in general type body segment in S.F.R.
CI	Specifies type corner of downstream corner of segment in S.F.R. CI-1 Compression corner CI=-1 Expansion corner
CD	Drag coefficient based on area REF for S.F.R.
C3	Constant in general type body segment in S.F.R.
D	Option for S.F.R. D=0 Print only body points D=1 Print only shock points D=2 Print all points
DEL	Local flow deflection angle for S.F.R. (degrees).
DELTA	Conical or frustum half angle for Cone or Blunt Body (degrees).
DLT	Time step (seconds) for Blunt Body Routine. Must satisfy Courant-Friedrich-Lewy criterion.
D3	Constant in general type body segment in S.F.R.
E	Indicator for S.F.R. E=0 Print CP E=1 Print P/PT_∞ E=2 Print P/PT E=3 Print P/P_∞

EPS	Indicator for Blunt Body Routine. EPS=0 Two-dimensional flow EPS=1 Rotationally symmetric flow
E3	Constant in general type body segment in S.F.R.
F	Indicator for S.F.R. program. F=0 Two dimensional flow F=1 Rotationally symmetric flow
F3	Constant in general type body segment in S.F.R.
G	Indicator for S.F.R. program. For use with frustum routine, must be set equal to 3.
GAMMA	Specific heat ratio for S.F.R., Blunt Body, and Cone.
G3	Constant in general type body segment in S.F.R.
H	Indicator for S.F.R. program. H=0 No action H=1 Punch C_p, X on body H=2 Punch P,X on body
H3	Constant in general type body segment in S.F.R.
ICHAR	Indicator for restart data for S.F.R. ICHAR=1 Initial value starting line ICHAR=2 Left-running characteristic starting line ICHAR=3 Right-running characteristic starting line
IM	The number of grid points between the shock and the body in the Blunt Body Routine.
IND	An indicator to the Blunt Body Routine. IND=0 Blunt body with hemispherical nose IND=1 Cone with detached shock IND=2 Frustum with detached shock
IRAY	The number of ray lines to be used in the Taylor Maccoll solution to the Cone.
ITYPE	Indicator for entire flow field. ITYPE=1 Conical nose ITYPE=2 Blunt nose or frustum ITYPE=3 Restarting input
IVL	The number of points to be found on the right running characteristic starting line on a conical nose, if shock attached.
I3	Constant in general type body segment in S.F.R.

J	Indicator for S.F.R. Number of first right-running characteristic summary. Normally equal to unity.
JM	Number of vertical node points between centerline and uppermost body point in Blunt Body Routine.
JT	Total number of vertical node points in Blunt Body Routine.
J3	Constant in general type body segment in S.F.R.
K	Indicator in S.F.R. Normally equal to unity.
K3	Constant in general type body segment in S.F.R.
L	Indicator in S.F.R. Normally equal to unity.
L3	Constant in general type body segment in S.F.R.
MACH	Free stream Mach number (Mach>1.0) for all Routines.
MG	Number of points on starting line for restart for S.F.R.
M3	Constant in general type body segment in S.F.R.
N	Indicator in S.F.R. N=0 Normal exit N=1 Build complete left-running characteristic from end of body to shock
NG	Number of points in shock wave table for restart for S.F.R.
NS	Total number of segments of body. Since the S.F.R. assumes all bodys have blunt nose segment, even if of zero size, include blunt nose in total number of segments NS.
NSTOP	The number of time steps to be taken by the Blunt Body Routine.
P	Indicator for S.F.R. Normally equal to unity.
PIN	Free stream pressure (lbs/ft^2).
PTPTM	The ratio of $P_T/P_{T\infty}$ along the starting line for S.F.R. restart option.
PTPTS	The ratio of $P_T/P_{T\infty}$ on the shock for the shock wave table for S.F.R. restart option.
Q	The maximum number of points on a characteristic line (Q<100) in S.F.R.

velocity, and cotangent of the shock angle are also printed out. After the completion of an input number of time steps, the program prints out the pressure and density ratios, the Mach number, and the flow deflection angle at each node point. The final shock standoff distance, velocity, and cotangent of the shock angle are also printed out. The coupling characteristic is formed and the position, Mach number, flow deflection angle, and total pressure ratio are printed out for each point on the characteristics. Control is then passed to the Supersonic Flow Routine.

A.2.3 Supersonic Flow Routine

The Supersonic Flow Routine prints out the body shape of each frustum, the free stream conditions, and the flow properties along the initial characteristic lines. A summary of the total pressure ratio behind the shock versus shock radius is also printed out. As the solution continues downstream, the flow properties at points along complete characteristics and the coordinates of these points are printed out. At the completion of the run, a body pressure summary is printed. Execution of the program is then complete.

REF	The reference area for the S.F.R. program. If zero, the reference area is the base area ($feet^2$).
RIN	The free stream density for Blunt Body ($slugs/ft^2$).
RL	The height of the base of the frustum from the centerline for Blunt Body. If body is blunt body and not frustum, must be zero (feet).
RMAX	The height above the centerline for the uppermost grid points in the Blunt Body Routine (feet).
RNOSE	If vehicle has blunt nose, the radius of the nose. If vehicle has sharp nose, zero (feet). For S.F.R.
RSPHER	The radius of the blunt nose for the Blunt Body Routine (feet).
SLOPE	The conical half angle of a segment at the upstream or downstream edge of the segment for S.F.R. (degrees).
STEP	The distance between points generated on the starting characteristic by the Blunt Body Routine (feet).
X	An axial distance for S.F.R. (feet).
XF	Used in automatically rounding a corner for the Blunt Body Routine. This is the axial distance to the downstream end of the rounded corner (feet).
XI	The percentage step size for the S.F.R. over the body segment.
XMAX	The axial distance to the downstream edge of the region of interest around a detached frustum shock for Blunt Body (feet).
XMIN	Used in defining a region of interest for the routine that provides the non-uniform upstream flow field to the detached frustum shock. This is the axial distance to the upstream edge of the region of interest for Blunt Body (feet).
XO	The axial distance to the center of a radial body segment in S.F.R. (ft.).
X2	The axial distance to the downstream edge of a body segment in S.F.R.(ft.).
X2NOSE	The axial distance to the downstream edge of the hemispherical nose segment in S.F.R. (ft.).
X*NOSE	The percentage step size for the S.F.R. over the nose segment.
Y	A radial distance from the centerline in S.F.R. (ft.).
YF	The radial distance at which the automatic rounding is to cease. The rounding will end tangential to a cylinder at the point XF,YF (feet). For Blunt Body Routine.

YLF	The radial distance at which the automatic corner rounding is to take place in the Blunt Body Routine (feet).
YO	The height above the centerline of the center of a radial body segment in S.F.R. (ft.).
YSHOCK	The height of the shock above the axis for the shock table in the restart option in S.F.R. (ft.).
Y2	The height of the downstream edge of a body segment in S.F.R. (ft.).
Y2NOSE	The height at the downstream edge of the first (blunt) segment for the S.F.R. (feet).

A.2 OUTPUT

In accordance with Section A.1, the outputs of the Cone Routine, Blunt Body Routine, and the Supersonic Flow Routine are presented as separate blocks. Table A-2 contains a list of the output symbols and their definitions.

A.2.1 Cone Output

The Cone Routine initially prints out the cone semi-vertex angle, the Mach number, and the ratio of specific heats. After the Taylor-Maccoll solution has been found, the routine prints out the ray angles and the pressure ratio, Mach number, flow deflection angle, and characteristic directions for each ray. A coupling characteristic is then formed, and the location of points on the characteristic and the values of the Mach number, flow deflection angle, and total pressure ratio, at each point are printed out. Control is then passed to the Supersonic Flow Routine.

A.2.2 Blunt Body Output

The Blunt Body Routine initially prints out pertinent information concerning the free stream conditions, the space and time steps, and the body shape. The initial flow field is calculated and the log of the pressure ratio, the log of the density ratio, and the nondimensionalized velocity components are printed out at each of the node points. The shock standoff distance, shock

Table A-2. LIST OF OUTPUT SYMBOLS

The following table is the list of output symbols used in the printout and their definitions.

CD	Drag coefficient, based on R-REF.
C+	Local characteristic direction in Cone Routine.
C-	Local characteristic direction in Cone Routine.
DE	Local flow deflection angle in the Blunt Body Routine.
DELTA	Local flow deflection angle in the Cone and Supersonic Flow Routines.
DELTA	The local shock stand-off distance in the Blunt Body Routine.
ETA	The vertical coordinate in the Blunt Body Routine.
GAMMA	The specific heat ratio.
I	The horizontal node point indicator in the Blunt Body Routine. (Unity on shock)
J	The vertical node point indicator in the Blunt Body Routine. (Unity on the centerline).
M	Mach number.
MACH NO	Mach number.
P	In Blunt Body Routine, log of the local to free stream pressure ratio during initial printout, and pressure ratio during final printout.
PHI	Local flow deflection angle.
P/PO	Local static to free stream static pressure ratio.
P/PT	Local static to local total pressure ratio.
P/PTO	Local static to free stream total pressure ratio.
PT/PTO	Local total to free stream total pressure ratio.
PT2/PT1	The same as PT/PTO.
R	In Blunt Body Routine, log of the local to free stream density ratio during initial printout, and density ratio during final printout.

Ray	A ray line in the Cone Routine.
R-REF	Reference Area.
SLOPE	Local body slope.
VR	Nondimensionalized vertical velocity in Blunt Body Routine.
VZ	Nondimensionalized horizontal velocity in Blunt Body Routine.
X	Horizontal coordinate from nose.
XI	Nondimensional horizontal coordinate in Blunt Body Routine.
X2	The X coordinate at the downstream edge of a segment.
X*	The percentage step size over a segment in the Supersonic Flow Routine.
Y2	The Y coordinate at the downstream edge of a segment.

Appendix B

SAMPLE INPUTS AND OUTPUTS

As an aid to the user of the program this appendix contains sample input and outputs data for the Blunt Body Routine corresponding to the flow over a hemisphere at Mach 4.0.

B.1 SAMPLE INPUT DATA

```
        2              .025
   4.0            1.4
        5      8      0      1      0   500
   .98                 .00001               1.0
   2116.2              .002378
```

B.2 SAMPLE OUTPUT DATA

Sample output data is shown on the following printouts.

```
                                         BLUNT NØSED BØDY
                                         AXISYMMETRIC CASE

NUMBER ØF  ZETA  PØINTS   5
NUMBER ØF RADIAL PØINTS   8
FREE STREAM MACH          0.40000000E 01
FREE STREAM DENSITY       0.23780000E-02
FREE STREAM PRESSURE      0.21162000E 04
FREE STREAM VELØCITY      0.44647427E 04
DELTA ZETA    0.25000000E 00
DELTA ETA     0.14000000E 00
DELTA T(ND)   0.94334907E-02

                                      INVERSE ØF BØDY SLØPE
0.00000000E-38  0.14139250E 00  0.29166666E 00  0.46279762E 00  0.67592635E 00  0.98019601E 00  0.15491405E 01  0.49246848E 01

                                  SECØND DERIVATIVE ØF BØDY SHAPE
0.10000000E 01  0.10301371E 01  0.11302807E 01  0.13379056E 01  0.17584664E 01  0.27456470E 01  0.62602727E 01  0.12689868E 03

                                     XI CØØRDINATES ØF PØINTS
0.10000000E 01  0.75000000E 00  0.50000000E 00  0.25000000E 00 -0.00000000E-38

                                    ETA CØØRDINATES ØF PØINTS
0.00000000E-38  0.14000000E 00  0.27999999E 00  0.41999999E 00  0.55999999E 00  0.69999999E 00  0.83999999E 00  0.98000000E 00


                                          INITIAL VALUES

I= 1 J= 1                          I= 1 J= 2                          I= 1 J= 3
P  0.29177707E 01  R  0.15198257E 01  P  0.29165108E 01  R  0.15195283E 01  P  0.29124201E 01  R  0.15185606E 01
VZ 0.10353140E 01  VR-0.00000000E-38  VZ 0.10402358E 01  VR 0.13052730E 00  VZ 0.10561730E 01  VR 0.26809219E 00

I= 1 J= 4                          I= 1 J= 5                          I= 1 J= 6
P  0.29043526E 01  R  0.15166436E 01  P  0.28893588E 01  R  0.15130500E 01  P  0.28589144E 01  R  0.15056296E 01
VZ 0.10874130E 01  VR 0.42177632E 00  VZ 0.11448089E 01  VR 0.60631522E 00  VZ 0.12587343E 01  VR 0.85133196E 00

I= 1 J= 7                          I= 1 J= 8
P  0.27768356E 01  R  0.14847813E 01  P  0.19814370E 01  R  0.12116790E 01
VZ 0.15491477E 01  VR 0.12322099E 01  VZ 0.34116429E 01  VR 0.16266491E 01

I= 2 J= 1                          I= 2 J= 2                          I= 2 J= 3
P  0.29502678E 01  R  0.15430379E 01  P  0.29418189E 01  R  0.15374549E 01  P  0.29157772E 01  R  0.15203194E 01
VZ 0.77648547E 00  VR 0.00000000E-38  VZ 0.79771375E 00  VR 0.22192531E 00  VZ 0.86235398E 00  VR 0.44183800E 00

I= 2 J= 4                          I= 2 J= 5                          I= 2 J= 6
P  0.28697431E 01  R  0.14903220E 01  P  0.27982805E 01  R  0.14446145E 01  P  0.26883197E 01  R  0.13768152E 01
VZ 0.97392103E 00  VR 0.65851490E 00  VZ 0.11413459E 01  VR 0.87303528E 00  VZ 0.13894778E 01  VR 0.10929255E 01

I= 2 J= 7                          I= 2 J= 8
P  0.24960448E 01  R  0.12678106E 01  P  0.16377019E 01  R  0.87598817E 00
VZ 0.18145273E 01  VR 0.13457384E 01  VZ 0.35001158E 01  VR 0.14111429E 01

I= 3 J= 1                          I= 3 J= 2                          I= 3 J= 3
P  0.29827649E 01  R  0.15662501E 01  P  0.29671270E 01  R  0.15553815E 01  P  0.29191344E 01  R  0.15220782E 01
VZ 0.51765698E 00  VR 0.00000000E-38  VZ 0.55519168E 00  VR 0.31332331E 00  VZ 0.66853498E 00  VR 0.61558380E 00

I= 3 J= 4                          I= 3 J= 5                          I= 3 J= 6
P  0.28351337E 01  R  0.14640004E 01  P  0.27072023E 01  R  0.13761790E 01  P  0.25177249E 01  R  0.12480008E 01
VZ 0.86042912E 00  VR 0.89525349E 00  VZ 0.11378829E 01  VR 0.11397553E 01  VZ 0.15202213E 01  VR 0.13345190E 01

I= 3 J= 7                          I= 3 J= 8
P  0.22152541E 01  R  0.10508399E 01  P  0.12939667E 01  R  0.54029730E 00
VZ 0.20799069E 01  VR 0.14592668E 01  VZ 0.35885887E 01  VR 0.11956367E 01

I= 4 J= 1                          I= 4 J= 2                          I= 4 J= 3
P  0.33152620E 01  R  0.15894624E 01  P  0.29924351E 01  R  0.15733081E 01  P  0.29224916E 01  R  0.15238370E 01
VZ 0.25882849E 00  VR 0.00000000E-38  VZ 0.31266962E 00  VR 0.40472130E 00  VZ 0.47471599E 00  VR 0.78932960E 00

I= 4 J= 4                          I= 4 J= 5                          I= 4 J= 6
P  0.28005243E 01  R  0.14376788E 01  P  0.26161241E 01  R  0.13077435E 01  P  0.23471301E 01  R  0.11191863E 01
VZ 0.74693720E 00  VR 0.11319921E 01  VZ 0.11344199E 01  VR 0.14064754E 01  VZ 0.16509648E 01  VR 0.15761126E 01

I= 4 J= 7                          I= 4 J= 8
P  0.19344634E 01  R  0.83386926E 00  P  0.95023160E 00  R  0.20460643E 00
VZ 0.23452865E 01  VR 0.15727953E 01  VZ 0.36770616E 01  VR 0.98013061E 00

I= 5 J= 1                          I= 5 J= 2                          I= 5 J= 3
P  0.33477591E 01  R  0.16126746E 01  P  0.30177433E 01  R  0.15912347E 01  P  0.29258488E 01  R  0.15255957E 01
VZ-0.00000000E-19  VR 0.00000000E-38  VZ 0.70147545E-01  VR 0.49611931E 00  VZ 0.28089698E 00  VR 0.96307541E 00

I= 5 J= 4                          I= 5 J= 5                          I= 5 J= 6
P  0.27659149E 01  R  0.14113573E 01  P  0.25250459E 01  R  0.12393080E 01  P  0.21765354E 01  R  0.99037194E 00
VZ 0.63344529E 00  VR 0.13687306E 01  VZ 0.11309569E 01  VR 0.16731955E 01  VZ 0.17817083E 01  VR 0.18177061E 01

I= 5 J= 7                          I= 5 J= 8
P  0.16536727E 01  R  0.61689858E 00  P  0.60649645E 00  R -0.13108444E 00
VZ 0.26106661E 01  VR 0.16863238E 01  VZ 0.37655345E 01  VR 0.76462445E 00

                                            DELTA
0.25030095E 00  0.25738732E 00  0.28000095E 00  0.31935787E 00  0.37863149E 00  0.46439381E 00  0.59306113E 00  0.85075282E 00
                                         SHØCK VELØCITY
0.00000000E-38  0.00000000E-38  0.00000000E-38  0.00000000E-38  0.00000000E-38  0.00000000E-38  0.00000000E-38  0.00000000E-38
                                         SHØCK CØTANGENT
0.00000000E-38  0.35348125E-01  0.72916664E-01  0.11569940E 00  0.16898159E 00  0.24504900E 00  0.38703512E 00  0.12311712E 01
```

```
                                          STEP 500
I= 1 J= 1                            I= 1 J= 2                            I= 1 J= 3
P  0.18499897E 02  R  0.45714225E 01  P  0.18295940E 02  R  0.45594301E 01  P  0.17758689E 02  R  0.45268545E 01
M  0.43496424E 00  DE 0.00000000E 00  M  0.48297441E 00  DE 0.19601226E 02  M  0.59417915E 00  DE 0.31133186E 02

I= 1 J= 4                            I= 1 J= 5                            I= 1 J= 6
P  0.16868179E 02  R  0.44694891E 01  P  0.15557091E 02  R  0.43764038E 01  P  0.14453659E 02  R  0.42888145E 01
M  0.75115299E 00  DE 0.36937751E 02  M  0.95263965E 00  DE 0.38762336E 02  M  0.11096160E 01  DE 0.38348053E 02

I= 1 J= 7                            I= 1 J= 8
P  0.12357011E 02  R  0.40933723E 01  P  0.10056718E 02  R  0.38202271E 01
M  0.13986997E 01  DE 0.35764091E 02  M  0.17254376E 01  DE 0.31667350E 02

I= 2 J= 1                            I= 2 J= 2                            I= 2 J= 3
P  0.19805393E 02  R  0.49027486E 01  P  0.19709210E 02  R  0.48018179E 01  P  0.19012371E 02  R  0.47310495E 01
M  0.31185305E 00  DE 0.00000000E 00  M  0.36285054E 00  DE 0.26165161E 02  M  0.49293097E 00  DE 0.39105140E 02

I= 2 J= 4                            I= 2 J= 5                            I= 2 J= 6
P  0.17972351E 02  R  0.46286649E 01  P  0.16373222E 02  P  0.44697542E 01  P  0.14964630E 02  R  0.42726888E 01
M  0.65227389E 00  DE 0.44035888E 02  M  0.85304308E 00  DE 0.44193054E 02  M  0.10146389E 01  DE 0.43146789E 02

I= 2 J= 7                            I= 2 J= 8
P  0.12084917E 02  R  0.37719693E 01  P  0.97593555E 01  R  0.33299293E 01
M  0.12493698E 01  DE 0.28736534E 02  M  0.15090761E 01  DE 0.35496444E 02

I= 3 J= 1                            I= 3 J= 2                            I= 3 J= 3
P  0.20428611E 02  R  0.49063215E 01  P  0.20174892E 02  R  0.48791523E 01  P  0.19259540E 02  R  0.47518825E 01
M  0.20989373E 00  DE 0.00000000E 00  M  0.28260797E 00  DE 0.35244773E 02  M  0.43169132E 00  DE 0.47058075E 02

I= 3 J= 4                            I= 3 J= 5                            I= 3 J= 6
P  0.17775913E 02  R  0.45213174E 01  P  0.15752388E 02  R  0.42434435E 01  P  0.13446298E 02  R  0.38616013E 01
M  0.60711908E 00  DE 0.49565742E 02  M  0.80685758E 00  DE 0.47344238E 02  M  0.10243506E 01  DE 0.43831726E 02

I= 3 J= 7                            I= 3 J= 8
P  0.99223938E 01  R  0.31503963E 01  P  0.73220043E 01  R  0.25701761E 01
M  0.12759091E 01  DE 0.36979950E 02  M  0.15645771E 01  DE 0.32026069E 02

I= 4 J= 1                            I= 4 J= 2                            I= 4 J= 3
P  0.21004756E 02  R  0.50105238E 01  P  0.20672126E 02  R  0.49570417E 01  P  0.19552715E 02  R  0.47956104E 01
M  0.10641065E 00  DE 0.00000000E 00  M  0.20899677E 00  DE 0.52583107E 02  M  0.48993692E 00  DE 0.59195246E 02

I= 4 J= 4                            I= 4 J= 5                            I= 4 J= 6
P  0.17739707E 02  R  0.44877500E 01  P  0.15209445E 02  R  0.40522756E 01  P  0.12223926E 02  R  0.35005166E 01
M  0.57239210E 00  DE 0.57166816E 02  M  0.78217685E 00  DE 0.51761726E 02  M  0.10352621E 01  DE 0.45435318E 02

I= 4 J= 7                            I= 4 J= 8
P  0.83434009E 01  R  0.26758728E 01  P  0.56947660E 01  R  0.20454964E 01
M  0.13203330E 01  DE 0.35823539E 02  M  0.16626997E 01  DE 0.29137210E 02

I= 5 J= 1                            I= 5 J= 2                            I= 5 J= 3
P  0.21020435E 02  R  0.50081091E 01  P  0.20653999E 02  R  0.49455909E 01  P  0.19285472E 02  R  0.47062437E 01
M  0.00000000E 00  DE 0.00000000E 00  M  0.17753854E 00  DE 0.81952224E 02  M  0.34998856E 00  DE 0.73739668E 02

I= 5 J= 4                            I= 5 J= 5                            I= 5 J= 6
P  0.17077308E 02  R  0.43174677E 01  P  0.13992683E 02  R  0.37448129E 01  P  0.10447021E 02  R  0.30393519E 01
M  0.57731902E 00  DE 0.65165466E 02  M  0.77479064E 00  DE 0.55944252E 02  M  0.10916762E 01  DE 0.45579036E 02

I= 5 J= 7                            I= 5 J= 8
P  0.63543205E 01  R  0.21308364E 01  P  0.38649668E 01  R  0.14936919E 01
M  0.14218068E 01  DE 0.32859909E 02  M  0.17946236E 01  DE 0.11478349E 02

                                          DELTA
 0.17117939E 00  0.17224552E 00  0.18175106E 00  0.19794074E 00  0.22659670E 00  0.27019901E 00  0.36520881E 00  0.58924195E 00
                                          SHØCK VELØCITY
-0.12168166E-04 -0.21592291E-04 -0.35276143E-04 -0.37887204E-04 -0.80533990E-04 -0.44506472E-04 -0.68708992E-04 -0.92911512E-04
                                          SHØCK CØTANGENT
 0.30791853E-07  0.10510120E 00  0.20333275E 00  0.30950625E 00  0.43258208E 00  0.52605031E 00  0.70036574E 00  0.90883105E 00
 0.00000000E-38  0.00000000E-38
```

Appendix C

SOURCE LISTING OF COMPUTER PROGRAM

A source listing of each subprogram or subroutine used in the detached shock calculations (Blunt Body and Frustum) is included in this appendix. The location of each portion of the program is indicated below.

```
$ORIGIN         ALPHA
$IBFTC NSL01    DECK
      SUBROUTINE BLUNT
      REAL MIN
      INTEGER EPS
      DIMENSION DELF(1),AMF(1),PF(1),X(1),Y(1)
      COMMON /FRUS/ DELT,X2,X1,Y2,RSPHER,XMIN,XMAX,Y1,IFR,RC,STEP
      COMMON DLY,DLZ,DLT,
     X        IM,JM,RMAT(25,25),RNEW(25,25),PMAT(25,25),PNEW(25,25),
     1      VRMAT(25,25),VRNEW(25,25),VZMAT(25,25),VZNEW(25,25),
     2      XI(25),ETA(25),W(25),WNEW(25),DELTA(25),DBDY(25),COT(25),G,
     3       D2BDY(25),D2ADY(25),EPS,THETA(25),DELNEW(25)
      COMMON /FRESTM/ VIN,RHOIN,PIN,VIN1,MIN,RL
      COMMON /CORNER/ JT,BPPP
      COMMON /BLNT/ STPP,NSTOP
      EQUIVALENCE (DELF,PNEW),(AMF,PNEW(1,12)),(PF,RNEW),(X,VZNEW),
     1(Y,VRNEW)
      SF(X)=SQRT(1./(1.+X*X))
      REWIND 4
      K=0
      CALL INITL(JT,RFIT,CDD)
      CALL INPRT(JT)
      CALL PRINT(JT)
   10 CALL SHKPTS(JT)
      CALL NTRNP
      IF(JT-JM .GT. 0) CALL NTRNP2(JT)
       IF(RL .GT. .0001) CALL CTL
      CALL BDYPTS
      K=K+1
      DO 50 J=1,JT
      W(J)=WNEW(J)
      COT(J)=COS(THETA(J))/SIN(THETA(J))
      DELTA(J)=DELNEW(J)
      DO 50 I=1,IM
      RMAT(I,J)=RNEW(I,J)
      PMAT(I,J)=PNEW(I,J)
      VRMAT(I,J)=VRNEW(I,J)
      VZMAT(I,J)=VZNEW(I,J)
   50 CONTINUE
      IF(MOD(K,10) .EQ. 0) CALL SMOO
      IF(MOD(K,10) .NE. 0) GO TO 10
      WRITE(6,900)K
      CALL PRINT(JT)
      IF(K .LT. NSTOP )GO TO 10
  200 DUM=0.
      WRITE(3)DUM,DUM
      WRITE(6,903)DUM,DUM
      DO 100 I=1,IM
      DO 100 J=1,JT
      DUM=ATAN(VRMAT(I,J)/VZMAT(I,J))
      VZMAT(I,J)=SQRT((VRMAT(I,J)**2+VZMAT(I,J)**2)/(G*EXP(PMAT(I,J)
     1-RMAT(I,J))))
      PMAT(I,J)=EXP(PMAT(I,J))
```

```
      RMAT(I,J)=EXP(RMAT(I,J))
100   VRMAT(I,J)=DUM
      WRITE(6,900)K
900   FORMAT(1H155X5HSTEP I3)
      CALL PRINT(JT)
      CDE=0.
      DA=ETA(2)
      DO 300 J=1,JM
      CD=(PMAT(IM,J)*SF(COT(J))+PMAT(IM,J-1)*SF(COT(J-1)))*DA/
     . (SF(COT(J))+SF(COT(J-1)))
      IF(EPS .NE. 0) CD=CD*3.1415926*(ETA(J)+ETA(J-1))
      CDE=CDE+CD
300   CONTINUE
      AR=1.
      IF(EPS .NE. 0) AR=3.1415926*RFIT
      CD=CD+CDE/(RFIT*AR*.5*G*PIN*MIN*MIN)
      IPE=3
      AM=MIN
      AM=AM**2
      DO 400 J=1,JT
      SN=(SIN(THETA(J)))**2
400   RMAT(1,J)=(((G+1.)*AM*SN)/((G-1.)
     X*AM*SN+2.))**(G/(G-1.))*((G+1.)/
     X(2.*G*AM*SN-(G-1.)))**(1./(G-1.))
      K=0
      I=1
      JJ=JM
420   ETAA=ETA(JJ)
      X(1)=B(0.)-B(ETAA)
      Y(1)=ETAA
      XIA=0.
450   CALL ENTER(XIA,ETAA,VRMAT,DEL,DUM)
      CALL ENTER(XIA,ETAA,VZMAT,AM,DUM)
      CALL ENTER(XIA,ETAA,PMAT,P,DUM)
      ANGLE=ARSIN(1./AM)-DEL
      X(I+1)=X(I)-STEP*COS(ANGLE)
      Y(I+1)=Y(I)+STEP*SIN(ANGLE)
      DEL=DEL*180./3.1415926
      DELF(I)=DEL
      AMF(I)=AM
      PTOPT=P*(((1.+(G-1.)*.5*AM*AM)/(1.+(G-1.)*.5*MIN*MIN      ))**(G/(
     1 G-1.)))
      PF(I)=PTOPT
      I=I+1
      J=IFIX(ETAA/ETA(2)+1.5)
      ETAA=Y(I)
      IF(ETAA .GT. ETA(JT) .OR. ETAA .LT. 0. .OR. XIA .LT. 0.) GO TO 600
      DEL=DELTA(J)+(DELTA(J+1)-DELTA(J))*(ETAA-ETA(J))/(ETA(J+1)-ETA(J))
      XIA=(B(0.)-X(I)-B(ETAA))/DEL
      IF(XIA.LT.(1.-STEP*.5)) GO TO 450
      IF(K.EQ.1) GO TO 500
      K=1
      XIA=1.0
      XO=1000.
460   X(I)=B(0.)-B(Y(I))-DEL
```

```
      IF(ABS(X(I)-XO).LT.STEP*.001) GO TO 450
      Y(I)=(X(I-1)-X(I))*SIN(ANGLE)/COS(ANGLE)+Y(I-1)
      ETAA=Y(I)
      XO=X(I)
      DEL=DELTA(J)+(DELTA(J+1)-DELTA(J))*(ETAA-ETA(J))/(ETA(J+1)-ETA(J))
      GO TO 460
  600 WRITE(6,905) ETAA,X(I),XIA,JJ
  905 FORMAT(12H ERROR EXIT 3E16.8,I6)
      JJ=JJ-1
      IF(JJ .LT. 1) CALL EXIT
      GO TO 420
  500 K=0
      DO 5005 IJ=1,I
 5005 Y(IJ)=Y(IJ)+RL
      IF(RL.LT..0001) GO TO 510
      X(I)=X(I-1)
      Y(I)=Y(I-1)
  501 CALL RES(X(I),Y(I),DEL,AMF(I),PF(I))
      DELF(I)=180./3.1415926*DEL
      I=I+1
      DEL=ARSIN(1./AMF(I-1))-DEL
      X(I)=X(I-1)-STEP*COS(DEL)
      Y(I)=Y(I-1)+STEP*SIN(DEL)
      CALL SHSHP(X(I),Y(I),YSK)
      IF(Y-YSK)501,503,503
  503 K=K+1
      IF(K.EQ.2) GO TO 510
  504 Y(I)=(Y(I)+YSK)*.5
      X(I)=X(I-1)-(Y(I)-Y(I-1))*COS(DEL)/SIN(DEL)
      CALL SHSHP(X(I),Y(I),YSK)
      IF(ABS(YSK-Y(I))-STEP*.001)501,501,504
  510 CONTINUE
      NIV=I-1
      WRITE(3)NIV,JT,CD,IPE
      WRITE(6,904)NIV,JT,CD,IPE
      WRITE(3) ETA(1),RFIT
      WRITE(6,903) ETA(1),RFIT
      WRITE(3) MIN,G
      WRITE(6,903) MIN,G
      WRITE(3)(ETA(J),RMAT(1,J),J=1,JT)
      WRITE(6,903)(ETA(J),RMAT(1,J),J=1,JT)
      DO 700 J=1,NIV
      I=NIV+1-J
      WRITE(6,903)X(I),Y(I),DELF(I),AMF(I),PF(I)
  700 WRITE(3)     X(I),Y(I),DELF(I),AMF(I),PF(I)
      REWIND 3
      RETURN
  903 FORMAT(4X6E16.8/(10X6E16.8))
  904 FORMAT(4XI2,14XI2,14X2E16.8)
      END
$IBFTC NSL02   DECK
      SUBROUTINE ENTER(X,Y,Z,ANS,DANS)
      DIMENSION Z(25,25)
      COMMON DLY,DLZ,DLT,
     X        IM,JD,RMAT(25,25),RNEW(25,25),PMAT(25,25),PNEW(25,25),
```

```
     1      VRMAT(25,25),VRNEW(25,25),VZMAT(25,25),VZNEW(25,25),
     2      XI(25),ETA(25),W(25),WNEW(25),DELTA(25),DBDY(25),COT(25),G
      COMMON /CORNER/JM
      JMAX=JM-1
      IMAX=IM-1
      IF(X-XI(1)) 1,1,100
  100 WRITE(6,900) X,Y
      X=XI(1)
    1 IF(X-XI(IM)) 200,2,2
  200 WRITE(6,900) X,Y
      X=XI(IM)
    2 IF(Y-ETA(1)) 300,3,3
  300 WRITE(6,900) X,Y
      Y=ETA(1)
    3 IF(Y-ETA(JM)) 4,4,400
  400 WRITE(6,900) X,Y
      Y=ETA(JM)
  900 FORMAT(14X2E16.8)
    4 DO 10 I=2,IMAX
      IF(X-XI(I)) 10,20,20
   10 CONTINUE
      I=IM
   20 I=I-1
      DO 30 J=2,JMAX
      IF(Y-ETA(J)) 40,40,30
   30 CONTINUE
      J=JM
   40 J=J-1
      F1=(X-XI(I))/(XI(I+1)-XI(I))
      F2=ETA(J+1)-ETA(J)
      G1=Z(I,J)+(Z(I+1,J)-Z(I,J))*F1
      G2=Z(I,J+1)+(Z(I+1,J+1)-Z(I,J+1))*F1
      ANS=G1+(G2-G1)*(Y-ETA(J))/F2
      DANS=(G2-G1)/F2
      RETURN
      END
$IBFTC NSL03   DECK
      FUNCTION B(YM)
      COMMON DLY,DLZ,DLT,
     X       IM,JM,RMAT(25,25),RNEW(25,25),PMAT(25,25),PNEW(25,25),
     1      VRMAT(25,25),VRNEW(25,25),VZMAT(25,25),VZNEW(25,25),
     2      XI(25),ETA(25),W(25),WNEW(25),DELTA(25),DBDY(25),COT(25),G,
     3       D2BDY(25),D2ADY(25),EPS,THETA(25),DELNEW(25)
      COMMON /FRESTM/ VIN,RHOIN,PIN,VIN1,MIN,RL
      COMMON /FRUS/ DELT,X2,X1,Y2,RSPHER,XMIN,XMAX,Y1,    IFR,RC,   STEP
      COMMON /CORNER/ JT,BPPP
      Y=YM
      IF(YM .GT. ETA(JM)) Y=ETA(JM)
      IF(IFR.GT.0) GO TO 10
      B=SQRT(RSPHER**2-Y**2)
      GO TO 20
   10 IF((Y2-Y) .GT. RC) GO TO 15
      B=SQRT(2.*RC*(Y2-Y)-(Y2-Y)**2)
     . -BPPP
      IF(B.LT.(X2-X1-BPPP)) GO TO 20
   15 CONTINUE
      B=X2-X1+(Y1-Y)*COS(DELT)/SIN(DELT)
     . -BPPP
   20 RETURN
      END
```

```
$IBFTC NSL04   DECK
      SUBROUTINE SHKPTS(JM)
      INTEGER EPS
      COMMON DLY,DLZ,DLT,
     X       IM,JD,RMAT(25,25),RNEW(25,25),PMAT(25,25),PNEW(25,25),
     1      VRMAT(25,25),VRNEW(25,25),VZMAT(25,25),VZNEW(25,25),
     2      XI(25),ETA(25),W(25),WNEW(25),DELTA(25),DBDY(25),COT(25),G,
     3       D2BDY(25),D2ADY(25),EPS,THETA(25),DELNEW(25)
      COMMON /FRESTM/ VIN,RHOIN,PIN,VIN1,MIN,RL
      EPX=EPS
      TL=.0001
      KL=0
      I=1
      DO 10 J=1,JM
      DELNEW(J)=DELTA(J)+W(J)*DLT
   10 WNEW(J)=W(J)
      DELNEW(1)=(4.*(DELNEW(2)+B(ETA(2)))-(DELNEW(3)
     . +B(ETA(3))))/3.-B(0.)
      JMA=JM-1
      DO 20 J=2,JMA
   20 THETA(J)=1.5707963-ATAN((B(ETA(J-1))-B(ETA(J))+DELNEW(J-1)
     . -DELNEW(J)) /(ETA(J)-ETA(J-1)))
      THETA(1)=1.5707963
      CALL EXTRA(THETA)
      KSUM=0
   22 DO 23 J=1,JM
      SN=SIN(THETA(J))
      CALL RANKH(1,J,WNEW,SN,2)
   23 CONTINUE
      KL=KL+1
      IF(MOD(KL,10) .EQ.0) TL=TL*10.
      DO 100 J=1,JMA
      SN=SIN(THETA(J))
      CS=COS(THETA(J))
      SNA=SQRT(1./(1.+COT(J)**2))
      CSA=SQRT(1.-SNA**2)
      AQ1=SQRT(G*EXP(PNEW(1,J)-RNEW(1,J)))
      DSDTQ=VZNEW(1,J)-AQ1
      DSDT=DSDTQ
   25 SIGA=-DSDT*DLT
      IF(J-1) 30,40,30
   30 ETAA=ETA(J)-SIGA*CS
      ANUM=DELTA(J)-SIGA*SN+W(J)*DLT
      IF(J .LE. JD) ANUM=ANUM+B(ETA(J))-B(ETAA)
      XIA=ANUM/(DELTA(J-1)+(DELTA(J)-DELTA(J-1))
     X      *(ETAA-ETA(J-1))/(ETA(J)-ETA(J-1)))
      GO TO 50
   40 XIA=1.-(SIGA-W(J)*DLT)/DELTA(J)
      ETAA=0.
   50 CALL ENTER(XIA,ETAA,PMAT,P,DP)
      CALL ENTER(XIA,ETAA,RMAT,R,DR)
      CALL ENTER(XIA,ETAA,VZMAT,U,DU)
      CALL ENTER(XIA,ETAA,VRMAT,V,DV)
   55 UA=U*SNA-V*SQRT(1.-SNA**2)
      AA=SQRT(G*EXP(P-R))
```

```
      DSDTN=.5*(DSDTQ+UA-AA)
      IF(ABS(DSDT-DSDTN) .LT. .0001) GO TO 60
      DSDT=DSDTN
      GO TO 25
   60 IF(J .EQ. 1) GO TO 65
      CALL DERIV(VRNEW,I,J,DVDN)
      CALL DERIV(PNEW,I,J,DPDN)
      CALL DERIV(VZNEW,I,J,DUDN)
      DUM=DVDN*SN+DUDN*CS
      DUDN=DUDN*SN-DVDN*CS
      DVDN=DUM
      HQ1=              -SN*(AQ1*VRNEW(1,J)*DPDN/G+AQ1*DVDN-VRNEW(1,J)
     X     *DUDN)-EPX*(VRNEW(1,J)*SN-VZNEW(1,J)*CS)/(ETA(J)+RL)*AQ1
      VA=U*SQRT(1.-SNA**2)+V*SNA
      DVT=DU*CSA+DV*SNA
      DUN=DU*SNA-DV*CSA
      HA=-SNA*(AA*VA*DP/G+AA*DVT-VA*DUN)-EPX*V/(ETAA+RL)*AA
      GO TO 70
   65 HQ1=-AQ1*(EPX+1.)*(VRNEW(1,2)*SIN(THETA(2))-VZNEW(1,2)*COS(
     .     THETA(2)))/DLY
      HA=-AA*DV*(EPX+1.)
      IF(RL .LT. .0001) GO TO 70
      HQ1=HQ1/(EPX+1.)
      HA=HA/(EPX+1.)
   70 CONTINUE
      HAV=(HA+HQ1)*.5
      AAV=(AQ1+AA)*.5
      UQ1=AAV*(PNEW(1,J)-P)/G+UA-HAV*DLT
      IF(ABS(UQ1-VZNEW(1,J)) .LT. ABS(VZNEW(1,J)*TL)) GO TO 90
      DUDW=2.*SN*(1.+   G/(((VIN1+WNEW(J))*SN)**2))/(G+1.)*2.
      WNEW(J)=WNEW(J)-(UQ1-VZNEW(1,J))/DUDW
      GO TO 100
   90 KSUM=KSUM+1
      IF(KSUM .EQ. JMA) GO TO 105
  100 CONTINUE
      KSUM=0
      CALL EXTRA(WNEW)
      GO TO 22
  105 DO 110 J=2,JM
      U=+VZNEW(1,J)*SIN(THETA(J))+VRNEW(1,J)*COS(THETA(J))
      V=-VZNEW(1,J)*COS(THETA(J))+VRNEW(1,J)*SIN(THETA(J))
      VZNEW(1,J)=U
  110 VRNEW(1,J)=V
      VRNEW(1,1)=0.
      JMA=JD-1
      DO 120 J=2,JMA
      D2ADY(J)=(DELTA(J+1)+DELTA(J-1)-2.*DELTA(J)+B(ETA(J+1))+B(ETA(J-1)
     X     )-2.*B(ETA(J)))/(DLY**2)
      D2ADY(J)=-D2ADY(J)
  120 CONTINUE
      IF(JD.EQ.JM) GO TO 140
      JMA=JD+1
      D2ADY(JD)=-(DELTA(JD+1)+DELTA(JD-1)-2.*DELTA(JD)
     X     -B(ETA(JD))+B(ETA(JD-1)))/(DLY**2)
      DO 130 J=JMA,JM
```

```
130 D2ADY(J)=-(DELTA(J+1)+DELTA(J-1)-2.*DELTA(J))/(DLY**2)
140 CONTINUE
    D2ADY(1)=-2.*(DELTA(2)-DELTA(1)+B(ETA(2))-B(ETA(1)))/
   X      (DLY**2)
    RETURN
    END
```

```
*IBFTC NSL05    DECK
      SUBROUTINE BDYPTS
      INTEGER EPS
      DIMENSION DPAT(25),DRAT(25),DVAT(25), STO(25),VAT(25),DVMAT(25)
      EQUIVALENCE(DVAT(25),DVMAT(25))
      COMMON DLY,DLZ,DLT,
     X        IM,JM,RMAT(25,25),RNEW(25,25),PMAT(25,25),PNEW(25,25),
     1      VRMAT(25,25),VRNEW(25,25),VZMAT(25,25),VZNEW(25,25),
     2      XI(25),ETA(25),W(25),WNEW(25),DELTA(25),DBDY(25),COT(25),G,
     3        D2BDY(25),D2ADY(25),EPS,THETA(25),DELNEW(25)
      COMMON /FRESTM/ VIN,RHOIN,PIN,VIN1,MIN,RL
      COMMON /CORNER/ JT
      TOLER=1000.
      KT=0
      JMA=JM-1
      IF(JT .NE. JM) JMA=JM
      KSUM=0
      STO(1)=0.
      DPAT(1)=0.
      DRAT(1)=0.
      IB=IM-1
      JMM=JM+2
      DO 155 J=2,JMM
      IF(J .GT. JM) GO TO 2
      SN=SQRT(1./(1.+DBDY(J)**2))
      CS=SQRT(1.-SN**2)
    2 CONTINUE
      DO 155 I=IB,IM
      VAT1=VRMAT(I,J)*SN+VZMAT(I,J)*CS
      VZMAT(I,J)=VZMAT(I,J)*SN-VRMAT(I,J)*CS
  155 VRMAT(I,J)=VAT1
      DO 6 J=2,JMA
      SN=SQRT(1./(1.+DBDY(J)**2))
      CS=SQRT(1.-SN**2)
      VZMAT(IM,J)=0.
      IF(J .EQ. JM) GO TO  3
      CALL DERIV(PMAT,IM,J,DPAT(J))
      CALL DERIV(RMAT,IM,J,DRAT(J))
      CALL DERIV(VRMAT,IM,J,DVMAT(J))
      GO TO 4
```

```
3 DPAT(J)=( PMAT(IM,J-2)-4.* PMAT(IM,J-1)+3.* PMAT(IM,J))/(2.*DLY)
  DRAT(J)=( RMAT(IM,J-2)-4.* RMAT(IM,J-1)+3.* RMAT(IM,J))/(2.*DLY)
  DVMAT(J)=(VRMAT(IM,J-2)-4.*VRMAT(IM,J-1)+3.*VRMAT(IM,J))/(2.*DLY)
4 CONTINUE
5 STO(J)=0.
  DPAT(J)=DPAT(J)*SN
  DRAT(J)=DRAT(J)*SN
  DVMAT(J)=DVMAT(J)*SN
  VAT(J)=VRMAT(IM,J)
  DVDT=-VAT(J)*DVAT(J)-EXP(PMAT(IM,J)-RMAT(IM,J))*DPAT(J)
6 VRNEW(IM,J)=(VAT(J)+DVDT*DLT)
  VAT(1)=0.
  IF(JM .NE. JT) GO TO 7
  VZNEW(IM,JM)=2.*VZNEW(IM,JM-1)-VZNEW(IM,JM-2)
  VRNEW(IM,JM)=2.*VRNEW(IM,JM-1)-VRNEW(IM,JM-2)
7 DO 8 J=1,JMA
  PNEW(IM,J)=PMAT(IM,J)+STO(J)*DLT
8 RNEW(IM,J)=RMAT(IM,J)+DLT*(STO(J)/G+DPAT(J)*VAT(J)/G-VAT(J)
 X      *DRAT(J))
  KT=KT+1
  IF(MOD(KT,10) .EQ. 0) TOLER=TOLER*.1
  IF(JM .NE. JT) GO TO 9
  PNEW(IM,JM)=2.*PNEW(IM,JM-1)-PNEW(IM,JM-2)
  RNEW(IM,JM)=2.*RNEW(IM,JM-1)-RNEW(IM,JM-2)
9 CONTINUE
  DO 40 J=1,JMA
  AP=SQRT(G*EXP(PNEW(IM,J)-RNEW(IM,J)))
  SN=SQRT(1./(1.+DBDY(J)**2))
  CS=SQRT(1.-SN**2)
  IF(J .NE. 1) GO TO 10
  DPDN=0.
  DRDN=0.
  DVDN=VRMAT(IM,2)/DLY
  GO TO 15
10 IF(J .EQ. JM) GO TO 11
  CALL DERIV(RNEW,IM,J,DRDN)
  CALL DERIV(PNEW,IM,J,DPDN)
  CALL DERIV(VRNEW,IM,J,DVDN)
  GO TO 12
11 DRDN=( RNEW(IM,J-2)-4.*RNEW(IM,J-1)+3.*RNEW(IM,J))/(2.*DLY)
  DPDN=( PNEW(IM,J-2)-4.*PNEW(IM,J-1)+3.*PNEW(IM,J))/(2.*DLY)
  DVDN=(VRNEW(IM,J-2)-4.*VRNEW(IM,J-1)+3.*(VRNEW(IM,J)))/(2.*DLY)
12 CONTINUE
  DVDN=DVDN*SN
  DPDN=DPDN*SN
  DRDN=DRDN*SN
15 V=VRNEW(IM,J)
  DSDT=AP
20 SIGB=DSDT*DLT
  ETAB=ETA(J)+SIGB*CS
  DELB=DELTA(J)+(DELTA(J+1)-DELTA(J))*(ETAB-ETA(J))/(ETA(J+1)
 X      -ETA(J))
  XIB=   (B(ETA(J))+SIGB*SN-B(ETAB))/DELB
  CALL ENTER(XIB,ETAB,PMAT,PB,DP)
  CALL ENTER(XIB,ETAB,RMAT,RB,DR)
  CALL ENTER(XIB,ETAB,VZMAT,UBB,DU)
  CALL ENTER(XIB,ETAB,VRMAT,VBB,DV)
```

```
 23 VR=VPB*SN-URB*CS
    DSDTN=.5*(AP+UBB+SQRT(G*EXP(PB-RB)))
    IF(ABS(DSDT-DSDTN) .LT. ABS(DSDT/TOLER))  GO TO 25
    DSDT=DSDTN
    GO TO 20
 25 AB=SQRT(G*EXP(PB-RB))
    IF(J .EQ. 1) GO TO 26
    HP=-(V*DPDN+DVDN*G)-FLOAT(EPS)*V*G*SN/(ETA(J)+RL)
    HB=-(DP*VBB+G*DV+VBB*DU*G/AB)*SN-FLOAT(EPS)*VB*G/(ETAB+RL)
    GO TO 27
 26 HB=-G*DV*(FLOAT(EPS)+1.)
    HP=-G*DVDN*(FLOAT(EPS)+1.)
    IF(RL .LT. .0001) GO TO 27
    HB=HB/(FLOAT(EPS)+1.)
    HP=HP/(FLOAT(EPS)+1.)
 27 CONTINUE
    PP=PB+2.*G*UBB/(AP+AB)+(HP+HB)*DLT*.5
    IF(ABS(PP-PNEW(IM,J)) .LT. ABS(PNEW(IM,J))/TOLER) GO TO 30
    STO(J)=STO(J)+(PP-PNEW(IM,J))/(2.*DLT)
    GO TO 40
 30 KSUM=KSUM+1
    IF((KSUM+1).EQ.JMA)GO TO 60
 40 CONTINUE
    KSUM=0
    GO TO 7
 60 DO 70 J=2,JM
    VAT1=VRNEW(IM,J)
    SN=SQRT(1./(1.+DBDY(J)**2))
    CS=SQRT(1.-SN**2)
    VZNEW(IM,J)=VAT1*CS
 70 VRNEW(IM,J)=VAT1*SN
    RETURN
    END
$IBFTC NSL06    DECK
      SUBROUTINE NTRNP 2(JT)
      INTEGER EPS
      COMMON DLY,DLZ,DLT,
     X        IM,JM,RMAT(25,25),RNEW(25,25),PMAT(25,25),PNEW(25,25),
     1      VRMAT(25,25),VRNEW(25,25),VZMAT(25,25),VZNEW(25,25),
     2      XI(25),ETA(25),W(25),WNEW(25),DELTA(25),DBDY(25),COT(25),G,
     3        D2BDY(25),D2ADY(25),EPS
      COMMON /FRESTM/ DMY(5),RL
      IMAX=IM-1
      JMAX=JT-1
      DO 100 J=JM,JMAX
      Y=ETA(J)+RL
      WT=-(WNEW(J)-W(J))/DLT
      WY=-(W(J+1)-W(J-1))/(2.*DLY)
      DEL=-DELTA(J)
      DEL2=DEL**2
      DELT=-W(J)
      DELY=COT(J)
      DO 100 I=2,IMAX
      Z=XI(I)
      E=-Z*COT(J)
      ET=-Z*WY
```

```
      EY=-Z*D2ADY(J)
      IF(J-JM) 20,10,20
   10 DELY=DELY-DBDY(J)
      E=E+(Z-1.)*DBDY(J)
      EY=EY+(Z-1.)*D2BDY(J)
   20 CONTINUE
      EZ=-DELY
      R=RMAT(I,J)
      VZ=VZMAT(I,J)
      VR=VRMAT(I,J)
      P=PMAT(I,J)
      EP=EXP(P)
      ER=EXP(R)
      EPOER=EP/ER
      CALL INDR1(RMAT,RY,RZ,RYY,RZZ,RYZ,I,J)
      CALL INDR1(PMAT,PY,PZ,PYY,PZZ,PYZ,I,J)
      CALL INDR1(VZMAT,VZY,VZZ,VZYY,VZZZ,VZYZ,I,J)
      CALL INDR1(VRMAT,VRY,VRZ,VRYY,VRZZ,VRYZ,I,J)
      D=(+W(J)*Z+VR*E+VZ)/DEL
      DZ=(W(J)+E*VRZ+VR*EZ+VZZ)/DEL
      DY=(-D*DELY+E*VRY-WY*Z+VR*EY+VZY)/DEL
      RT=-(D*RZ+VR*RY+VRY+(E*VRZ+VZZ)/DEL)
      RT=RT-VR/Y*FLOAT(EPS)
      VRT=-(D*VRZ+VR*VRY+EP*E*PZ/(DEL*ER)+EP/ER*PY)
      VZT=-(D*VZZ+VR*VZY+EP/ER*PZ/DEL)
      PT=G*RT-(D*(PZ-G*RZ)+VR*(PY-G*RY))
      DT=-D*DELT/DEL+(-Z*WT+E*VRT+VR*ET+VZT)/DEL
      RTZ=-(DZ*RZ+D*RZZ+VRZ*RY+VR*RYZ+(EZ*VRZ+E*VRZZ)/DEL+VRYZ
     1      +VZZZ/DEL)
      RTY=-(DY*RZ+D*RYZ+VRY*RY+VR*RYY+(DEL*EY-E*DELY)*VRZ/DEL2+E*VRYZ
     1      /DEL+VRYY-DELY*VZZ/DEL2+VZYZ/DEL)
      RTY=RTY-(VRY/Y-VR/(Y**2))*FLOAT(EPS)
      RTZ=RTZ-VRZ/Y*FLOAT(EPS)
      VRTZ=-(DZ*VRZ+D*VRZZ+VRZ*VRY+VR*VRYZ+EPOER*((E*PZ+EZ-E*RZ)
     1      *PZ/DEL+E*PZZ/DEL+PY*(PZ-RZ)+PYZ))
      VRTY=-(DY*VRZ+D*VRYZ+VRY*VRY+VR*VRYY+EPOER*((E*PY+EY-E*RY
     1      -E*DELY/DEL)*PZ/DEL+E*PYZ/DEL+PY*(PY-RY)+PYY))
      VZTZ=-(DZ*VZZ+D*VZZZ+VRZ*VZY+VR*VZYZ+EPOER*(PZ/DEL*(PZ-RZ)
     1      +PZZ/DEL))
      VZTY=-(DY*VZZ+D*VZYZ+VRY*VZY+VR*VZYY+EPOER*(PZ*(PY-RY
     1      -DELY/DEL)+PYZ)/DEL)
      PTZ=G*RTZ-(DZ*(PZ-G*RZ)+D*(PZZ-G*RZZ)+VRZ*(PY-G*RY)
     1     +VR*(PYZ-G*RYZ))
      PTY=G*RTY-(DY*(PZ-G*RZ)+D*(PYZ-G*RYZ)+VRY*(PY-G*RY)
     1     +VR*(PYY-G*RYY))
      RTT=-(DT*RZ+D*RTZ+VRT*RY+VR*RTY+(DEL*ET-DELT*E)*VRZ/DEL2
     1      +(VRTZ*E+VZTZ)/DEL+VRTY-DELT*VZZ/DEL2)
      RTT=RTT-VRT/Y*FLOAT(EPS)
      VRTT=-(DT*VRZ+D*VRTZ+VRT*VRY+VR*VRTY+EPOER*((E*PT+ET-E*RT
     1      -E*DELT/DEL)*PZ/DEL+E*PTZ/DEL+PY*(PT-RT)+PTY))
      VZTT=-(DT*VZZ+D*VZTZ+VRT*VZY+VR*VZTY+EPOER*(PZ/DEL*(PT-RT
     1      -DELT/DEL)+PTZ/DEL))
      PTT=G*RTT-(DT*(PZ-G*RZ)+D*(PTZ-G*RTZ)+VRT*(PY-G*RY)
     1     +VR*(PTY-G*RTY))
```

```
      PNEW(I,J)=P+PT*DLT+PTT*DLT*DLT*.5
      RNEW(I,J)=R+RT*DLT+RTT*DLT*DLT*.5
      VRNEW(I,J)=VR+VRT*DLT+VRTT*DLT*DLT*.5
      VZNEW(I,J)=VZ+VZT*DLT+VZTT*DLT*DLT*.5
  100 CONTINUE
      DO 110 I=2,IMAX
      CALL EXTRA1(PNEW,I)
      CALL EXTRA1(RNEW,I)
      CALL EXTRA1(VZNEW,I)
      CALL EXTRA1(VRNEW,I)
  110 CONTINUE
      JMAX=JM
      DO 120 J=JMAX,JT
      PNEW(IM,J)=2.*PNEW(IMAX,J)-PNEW(IM-2,J)
      RNEW(IM,J)=2.*RNEW(IMAX,J)-RNEW(IM-2,J)
      VZNEW(IM,J)=VZNEW(IMAX,J)*2.-VZNEW(IM-2,J)
  120 VRNEW(IM,J)=VRNEW(IMAX,J)*2.-VRNEW(IM-2,J)
      RETURN
      END

$IBFTC NSL07   DECK
      SUBROUTINE NTRNP
      INTEGER EPS
      COMMON DLY,DLZ,DLT,
     X       IM,JM,RMAT(25,25),RNEW(25,25),PMAT(25,25),PNEW(25,25),
     1     VRMAT(25,25),VRNEW(25,25),VZMAT(25,25),VZNEW(25,25),
     2     XI(25),ETA(25),W(25),WNEW(25),DELTA(25),DBDY(25),COT(25),G,
     3      D2BDY(25),D2ADY(25),EPS
      COMMON/CORNER/JT
      COMMON /FRUS/ DUN(8),IFR
      COMMON /FRESTM/ DUNN(5),RL
C     DLY - ND DISTANCE BETWEEN PTS IN R DIRECTION
C     DLZ - ND DISTANCE BETWEEN PTS IN Z DIRECTION
C     DLT = DELTA T
C     I - Z AXIS COUNTER
C     J - R AXIS COUNTER
C     RMAT - RHO MATRIX AT TIME T
C     RNEW - RHO MATRIX AT TIME T + DLT
C     PMAT - PRESSURE MATRIX AT TIME T
C     PNEW - PRESSURE MATRIX AT TIME T +DLT
C     VRMAT - RADIAL VELOCITY AT TIME T
C     VRNEW - RADIAL VELOCITY AT TIME T + DLT
C     VZMAT - AXIAL VELOCITY AT TIME T
C     VZNEW - AXIAL VELOCITY AT TIME T + DLT
C     XI - ND AXIAL DISTANCE
C     ETA - ND RADIAL DISTANCE
C     W - ND SHOCK VELOCITY
C     WNEW - ND SHOCK VELOCITY AT TIME T + DLT
C     G - GAMMA
C     D2BDY - SECOND DERIVATIVE OF BODY SHAPE
C     D2ADY - SECOND DERIVATIVE OF SHOCK SHAPE
      IMAX=IM-1
      JMAX=JM-1
      JN=2
      IF(IFR .NE. 0) JN=2
      DO 100 J=1,JMAX
      NTEST=(J-1)*EPS
```

```
      IF(RL.GT..0001)NTEST=1
      Y=ETA(J)+RL
      WT=-(WNEW(J)-W(J))/DLT
      WY=-(W(J+1)-W(J-1))/(2.*DLY)
      IF(J .EQ. 1) WY=0.
      DEL=-DELTA(J)
      DEL2=DEL**2
      DELT=-W(J)
      DELY=COT(J)-DBDY(J)
      DO 100 I=2,IMAX
      Z=XI(I)
      E=DBDY(J)*(Z-1.)-Z*COT(J)
      ET=-Z*WY
      EY=(Z-1.)*D2BDY(J)-Z*D2ADY(J)
      EZ=-DELY
      R=RMAT(I,J)
      VZ=VZMAT(I,J)
      VR=VRMAT(I,J)
      P=PMAT(I,J)
      EP=EXP(P)
      ER=EXP(R)
      EPOER=EP/ER
      CALL INDR1(RMAT,RY,RZ,RYY,RZZ,RYZ,I,J)
      CALL INDR1(PMAT,PY,PZ,PYY,PZZ,PYZ,I,J)
      CALL INDR1(VZMAT,VZY,VZZ,VZYY,VZZZ,VZYZ,I,J)
      IF(J-1) 11,12,11
   11 CALL INDR1(VRMAT,VRY,VRZ,VRYY,VRZZ,VRYZ,I,J)
      GO TO 13
   12 VRZ=0.
      VRZZ=0.
      VRY=VRMAT(I,2)/DLY
      VRYY=0.
      VRYZ=-(VRMAT(I+1,2)-VRMAT(I-1,2))/(DLY*2.*DLZ)
   13 CONTINUE
      D=(+W(J)*Z+VR*E+VZ)/DEL
      DZ=(W(J)+E*VRZ+VR*EZ+VZZ)/DEL
      DY=(-D*DELY+E*VRY-WY*Z+VR*EY+VZY)/DEL
      RT=-(D*RZ+VR*RY+VRY+(E*VRZ+VZZ)/DEL)
      IF(NTEST) 135,140,135
  135 RT=RT-VR/Y
      GO TO 145
  140 RT=RT-VRY*FLOAT(EPS)
  145 CONTINUE
      VRT=-(D*VRZ+VR*VRY+EP*E*PZ/(DEL*ER)+EP/ER*PY)
      VZT=-(D*VZZ+VR*VZY+EP/ER*PZ/DEL)
      PT=G*RT-(D*(PZ-G*RZ)+VR*(PY-G*RY))
      DT=-D*DELT/DEL+(-Z*WT+E*VRT+VR*ET+VZT)/DEL
      RTZ=-(DZ*RZ+D*RZZ+VRZ*RY+VR*RYZ+(EZ*VRZ+E*VRZZ)/DEL+VRYZ
     1     +VZZZ/DEL)
      RTY=-(DY*RZ+D*RYZ+VRY*RY+VR*RYY+(DEL*EY-E*DELY)*VRZ/DEL2+E*VRYZ
     1     /DEL+VRYY-DELY*VZZ/DEL2+VZYZ/DEL)
      IF(NTEST) 16,16,15
   15 RTY=RTY-(VRY/Y-VR/(Y**2))
      RTZ=RTZ-VRZ/Y
      GO TO 20
```

```
   16 RTZ=RTZ-VRYZ*FLOAT(EPS)
   20 VRTZ=-(DZ*VRZ+D*VRZZ+VRZ*VRY+VR*VRYZ+EPOER*((E*PZ+EZ-E*RZ)
     1      *PZ/DEL+E*PZZ/DEL+PY*(PZ-RZ)+PYZ))
      VRTY=-(DY*VRZ+D*VRYZ+VRY*VRY+VR*VRYY+EPOER*((E*PY+EY-E*RY
     1      -E*DELY/DEL)*PZ/DEL+E*PYZ/DEL+PY*(PY-RY)+PYY))
      VZTZ=-(DZ*VZZ+D*VZZZ+VRZ*VZY+VR*VZYZ+EPOER*(PZ/DEL*(PZ-RZ)
     1      +PZZ/DEL))
      VZTY=-(DY*VZZ+D*VZYZ+VRY*VZY+VR*VZYY+EPOER*(PZ*(PY-RY
     1      -DELY/DEL)+PYZ)/DEL)
      PTZ=G*RTZ-(DZ*(PZ-G*RZ)+D*(PZZ-G*RZZ)+VRZ*(PY-G*RY)
     1     +VR*(PYZ-G*RYZ))
      PTY=G*RTY-(DY*(PZ-G*RZ)+D*(PYZ-G*RYZ)+VRY*(PY-G*RY)
     1     +VR*(PYY-G*RYY))
      RTT=-(DT*RZ+D*RTZ+VRT*RY+VR*RTY+(DEL*ET-DELT*E)*VRZ/DEL2
     1      +(VRTZ*E+VZTZ)/DEL+VRTY-DELT*VZZ/DEL2)
      IF(NTEST) 25,30,25
   25 RTT=RTT-VRT/Y
      GO TO 35
   30 RTT=RTT-VRTY*FLOAT(EPS)
   35 CONTINUE
      VRTT=-(DT*VRZ+D*VRTZ+VRT*VRY+VR*VRTY+EPOER*((E*PT+ET-E*RT
     1      -E*DELT/DEL)*PZ/DEL+E*PTZ/DEL+PY*(PT-RT)+PTY))
      VZTT=-(DT*VZZ+D*VZTZ+VRT*VZY+VR*VZTY+EPOER*(PZ/DEL*(PT-RT
     1      -DELT/DEL)+PTZ/DEL))
      PTT=G*RTT-(DT*(PZ-G*RZ)+D*(PTZ-G*RTZ)+VRT*(PY-G*RY)
     1     +VR*(PTY-G*RTY))
      PNEW(I,J)=P+PT*DLT+PTT*DLT*DLT*.5
      RNEW(I,J)=R+RT*DLT+RTT*DLT*DLT*.5
      VRNEW(I,J)=VR+VRT*DLT+VRTT*DLT*DLT*.5
      VZNEW(I,J)=VZ+VZT*DLT+VZTT*DLT*DLT*.5
  100 CONTINUE
      DO 105 I=1,IMAX
  105 VRNEW(I,1)=0.
      IF(JM.NE.JT)RETURN
      DO 110 I=2,IMAX
      CALL EXTRA1(PNEW,I)
      CALL EXTRA1(RNEW,I)
      CALL EXTRA1(VZNEW,I)
      CALL EXTRA1(VRNEW,I)
  110 CONTINUE
      RETURN
      END
$IBFTC NSL08    DECK
      SUBROUTINE CTL
      COMMON DLY,DLZ,DLT,
     X       IM,JD,RMAT(25,25),RNEW(25,25),PMAT(25,25),PNEW(25,25),
     1       VRMAT(25,25),VRNEW(25,25),VZMAT(25,25),VZNEW(25,25),
     2       XI(25),ETA(25),W(25),WNEW(25),DELTA(25),DBDY(25),COT(25),G,
     3       D2BDY(25),D2ADY(25),EPS,THETA(25),DELNEW(25)
      J=1
      IMA=IM-1
      TOLER=1000.
      DO 44 I=2,IMA
      DVZZ=(VZMAT(I+1,1)-VZMAT(I-1,1))/(2.*DLZ)
      DPZ=(PMAT(I+1,1)-PMAT(I-1,1))/(2.*DLZ)
      DRZ=(RMAT(I+1,1)-RMAT(I-1,1))/(2.*DLZ)
```

```
      DVZT=-(VZMAT(I,1)*DVZZ+DPZ*EXP(PMAT(I,1)-RMAT(I,1)))
      DVRY=(4.*VRMAT(I,2)-VRMAT(I,3))/(2.*DLY)
      DRT=-(DVRY+DVZZ+VZMAT(I,1)*DRZ)
      DPT=-VZMAT(I,1)*DPZ+G*DRT+G*VZMAT(I,1)*DRZ
      VZNEW(I,1)=VZMAT(I,1)+DVZT*DLT
      PNEW(I,1)=PMAT(I,1)+DPT*DLT
   13 RNEW(I,1)=RMAT(I,1)+DRT*DLT
      A=SQRT(G*EXP(PNEW(I,1)-RNEW(I,1)))
      DSDTA=VZNEW(I,1)-A
   15 XIA=(XI(I)*DELNEW(1)+DSDTA*DLT)/DELTA(1)
      ETAA=0.
      CALL ENTER(XIA,ETAA,PMAT,PA,DPA)
      CALL ENTER(XIA,ETAA,RMAT,RA,DRA)
      CALL ENTER(XIA,ETAA,VZMAT,VZA,DVZA)
      CALL ENTER(XIA,ETAA,VRMAT,VRA,DVRA)
      AA=SQRT(G*EXP(PA-RA))
      DSDTAN=.5*(VZA-AA+VZNEW(I,1)-A)
      IF(ABS(DSDTA-DSDTAN).LT.ABS(DSDTA/TOLER))
     1GO TO 16
      DSDTA=DSDTAN
      GO TO 15
   16 DSDTB=VZNEW(I,1)+A
   17 XIB=(DELNEW(1)*XI(I)+DSDTB*DLT)/DELTA(1)
      ETAB=0.0
      CALL ENTER(XIB,ETAB,PMAT,PB,DPB)
      CALL ENTER(XIB,ETAB,RMAT,RB,DRB)
      CALL ENTER(XIB,ETAB,VZMAT,VZB,DVZB)
      CALL ENTER(XIB,ETAB,VRMAT,VRB,DVRB)
      AB=SQRT(G*EXP(PB-RB))
      DSDTBN=.5*(VZB+AB+VZNEW(I,1)+A)
      IF(ABS(DSDTB-DSDTBN).LT.ABS(DSDTB/TOLER))
     1GO TO 30
      DSDTB=DSDTBN
      GO TO 17
   30 AAVEA=.5*(A+AA)
      AAVEB=.5*(A+AB)
      DVRNEW=(4.*VRNEW(I,2)-VRNEW(I,3))/(2.*DLY)
      DVRAVA=.5*(DVRNEW+DVRA)
      DVRAVB=.5*(DVRNEW+DVRB)
      UQ1=AAVEA*AAVEB*(VZA/AAVEA+VZB/AAVEB+(PB-PA)/G-DLT*(DVRAVB-DVRAVA)
     X)/(AAVEB+AAVEA)
      PQ1=PB-G*DVRAVB*DLT-G*(UQ1-VZB)/AAVEB
      IF(ABS(PQ1-PNEW(I,1)).LT.ABS(PNEW(I,1)/TOLER))GO TO 40
      PNEW(I,1)=.5*(PNEW(I,1)+PQ1)
      VZNEW(I,1)=UQ1
      DPT=(PNEW(I,1)-PMAT(I,1))/DLT
      DRT=DPT/G+(VZMAT(I,1)*DPZ)/G-VZMAT(I,1)*DRZ
      GO TO 13
   40 VZNEW(I,1)=UQ1
      PNEW(I,1)=PQ1
      DPT=(PNEW(I,1)-PMAT(I,1))/DLT
      DRT=DPT/G+(VZMAT(I,1)*DPZ)/G-VZMAT(I,1)*DRZ
      RNEW(I,1)=RMAT(I,1)+DRT*DLT
   44 CONTINUE
      RETURN
      END
```

```
$IBFTC NSL09    DECK
      SUBROUTINE NSMTH(F,JT)
      DIMENSION F(25,25)
      COMMON DUM(3),IM,JM
      IMAX=IM-1
      AIM=IMAX
      DO 10 JA=1,JT
      DO 10 IA=2,IMAX
      AI=IA-1
      F(IA,JA)=F(1,JA)+(F(IM,JA)-F(1,JA))*AI/AIM
   10 CONTINUE
      RETURN
      END
$IBFTC NSL10    DECK
      SUBROUTINE INPRT(JM)
      REAL MIN
      INTEGER EPS
      DIMENSION AC(2),AD(2),AE(2),AF(2)
      COMMON DLY,DLZ,DLT,
     X       IM,JD,RMAT(25,25),RNEW(25,25),PMAT(25,25),PNEW(25,25),
     1     VRMAT(25,25),VRNEW(25,25),VZMAT(25,25),VZNEW(25,25),
     2     XI(25),ETA(25),W(25),WNEW(25),DELTA(25),DBDY(25),COT(25),G,
     3      D2BDY(25),D2ADY(25),EPS
      COMMON /FRESTM/ VIN,RHOIN,PIN,VIN1,MIN,RL
      DATA AA,AB,AC,AD,AE,AF,AG,AH,AI/6H ZETA ,6HRADIAL ,6HMACH   ,
     X     3H   ,6HDENSIT,3HY   ,6HPRESSU,3HRE  ,6HVELOCI,3HTY  ,
     X     5HZETA ,5HETA   ,5HT(ND)/
      WRITE(6,900)
      WRITE(6,901)
      IF(EPS) 10,20,10
   10 WRITE(6,902)
      GO TO 30
   20 WRITE(6,903)
   30 WRITE(6,904) AA,IM,AB,JM
      WRITE(6,912) AC,MIN,AD,RHOIN,AE,PIN,AF,VIN
      WRITE(6,905) AG,DLZ,AH,DLY,AI,DLT
      WRITE(6,910)
      WRITE(6,906) (DBDY(J),J=1,JM)
      WRITE(6,910)
      WRITE(6,907) (D2BDY(J),J=1,JM)
      WRITE(6,910)
      WRITE(6,908) (XI(I),I=1,IM)
      WRITE(6,910)
      WRITE(6,909) (ETA(J),J=1,JM)
      WRITE(6,900)
      WRITE(6,911)
      RETURN
  900 FORMAT(1H1)
  901 FORMAT(52X16HBLUNT NOSED BODY)
  902 FORMAT(51X17HAXISYMMETRIC CASE//)
  903 FORMAT(52X16HRECTILINEAR CASE//)
  904 FORMAT(4X10HNUMBER OF A6,1X7HPOINTS I2)
  905 FORMAT(4X6HDELTA A5,E16.8)
  906 FORMAT(49X21HINVERSE OF BODY SLOPE/(3X8E16.8))
  907 FORMAT(44X31HSECOND DERIVATIVE OF BODY SHAPE/(3X8E16.8))
  908 FORMAT(48X24HXI COORDINATES OF POINTS/(3X8E16.8))
  909 FORMAT(47X25HETA COORDINATES OF POINTS/(3X8E16.8))
```

```
  910 FORMAT(/)
  911 FORMAT(53X14HINITIAL VALUES//)
  912 FORMAT(4X12HFREE STREAM A6,A3,E16.8)
      END
$IBFTC NSL11   DECK
      SUBROUTINE PRINT(JM)
      REAL MIN
      INTEGER EPS
      COMMON DLY,DLZ,DLT,
     X      IM,JD,R(25,25),RNEW(25,25),P(25,25),PNEW(25,25),
     1      VR(25,25),VRNEW(25,25),VZ(25,25),VZNEW(25,25),
     2      XI(25),ETA(25),W(25),WNEW(25),DELTA(25),DBDY(25),COT(25),G,
     3        D2BDY(25),D2ADY(25),EPS
      COMMON /FRESTM/ VIN,RHOIN,PIN,VIN1,MIN,RL
      DATA PA,RA,VZA,VRA,IA,JA/2HP ,2HR ,2HVZ,2HVR,2HI=,2HJ=/
      ICNT=4
      DO 100 I=1,IM
      J=-2
    1 J=J+3
      J1=J+1
      J2=J+2
      IF(J .GT. JM) GO TO 100
      IF(J .NE. JM) GO TO 10
      WRITE(6,900) IA,I,JA,J
      WRITE(6,901) PA,P(I,J),RA,R(I,J)
      WRITE(6,901) VZA,VZ(I,J),VRA,VR(I,J)
      GO TO 90
   10 IF(J+1 .NE. JM) GO TO 20
      WRITE(6,900) IA,I,JA,J,IA,I,JA,J1
      WRITE(6,901) PA,P(I,J),RA,R(I,J),PA,P(I,J1),RA,R(I,J1)
      WRITE(6,901) VZA,VZ(I,J),VRA,VR(I,J),VZA,VZ(I,J1),VRA,VR(I,J1)
      GO TO 90
   20 CONTINUE
      WRITE(6,900) IA,I,JA,J,IA,I ,JA,J1,IA,I ,JA,J2
      WRITE(6,901) PA,P(I,J),RA,R(I,J),PA,P(I,J1),RA,R(I,J1)
     X      ,PA,P(I,J2),RA,R(I,J2)
      WRITE(6,901) VZA,VZ(I,J),VRA,VR(I,J),VZA,VZ(I,J1),VRA,VR(I,J1)
     X      ,VZA,VZ(I,J2),VRA,VR(I,J2)
   90 WRITE(6,902)
      ICNT=ICNT+6
      IF(ICNT .LT. 54) GO TO 1
      WRITE(6,903)
      ICNT=0
      GO TO 1
  100 CONTINUE
      IF(ICNT .LT. 48) GO TO 110
      WRITE(6,903)
  110 WRITE(6,904) (DELTA(J),J=1,JM)
      WRITE(6,905) (W(J),J=1,JM)
      WRITE(6,906) (COT(J),J=1,JM)
      RETURN
  900 FORMAT(10XA2,I2,1XA2,I2,2(29XA2,I2,1XA2,I2))
  901 FORMAT(8X3(2XA2,E15.8,2XA2,E15.8))
  902 FORMAT(//)
  903 FORMAT(1H1)
  904 FORMAT(57X5HDELTA/(3X8E16.8))
  905 FORMAT(53X14HSHOCK VELOCITY/(3X8E16.8))
  906 FORMAT(53X15HSHOCK COTANGENT/(3X8E16.8))
      END
```

```
$IBFTC NSL12    DECK
      SUBROUTINE EXTRA1(G,I)
      COMMON /CORNER/ JM
      DIMENSION G(25,25)
      G(I,JM) =2.*G(I,JM-1) -G(I,JM-2)
      RETURN
      END
$IBFTC NSL13    DECK
      SUBROUTINE RANKH(I,J,W,SN,K)
      REAL MIN
      DIMENSION W(25)
      COMMON DLY,DLZ,DLT,
     X      IM,JM,RMAT(25,25),RNEW(25,25),PMAT(25,25),PNEW(25,25),
     1      VRMAT(25,25),VRNEW(25,25),VZMAT(25,25),VZNEW(25,25),
     2      XI(25),ETA(25),X(25),WNEW(25),DELTA(25),DBDY(25),COT(25),G  ,
     3      D2BDY(25),D2ADY(25),EPS,THETA(25),DELNEW(25)
      COMMON /FRESTM/ VIN,RHOIN,PIN,VIN1,MIN,RL
      COMMON /CORNER/ JT,BPPP
      COMMON /FRUS/ DUM(6),XMAX
      WINV=-W(J)
      IF(RL .GT. .00001) GO TO 50
      SN2=SN*SN
      U=((G-1.)*(VIN1-WINV)**2*SN2+2.*G)/((G+1.)*(VIN1-WINV)*SN)
     1      +WINV*SN
      V=VIN1*SQRT(1.-SN2)
      P=(2.*(VIN1-WINV)**2*SN2-G+1.)/(G+1.)
      R=((G+1.)*P+G-1.)/(G+1.+(G-1.)*P)
   10 CONTINUE
      P=ALOG(P)
      R=ALOG(R)
      DEL=ATAN(SN/SQRT(1.-SN**2))-ATAN(U/V)
      GO TO (20,30),K
   20 VZMAT(I,J)=SQRT(U**2+V**2)*COS(DEL)
      VRMAT(I,J)=VZMAT(I,J)*SIN(DEL)/COS(DEL)
      PMAT(I,J)=P
      RMAT(I,J)=R
      RETURN
   30 VZNEW(I,J)=U
      VRNEW(I,J)=V
      PNEW(I,J)=P
      RNEW(I,J)=R
      RETURN
   50 X=XMAX-B(ETA(J))-BPPP
      GO TO (60,70),K
   60 X=X-DELTA(J)
      GO TO 80
   70 X=X-DELNEW(J)
   80 ANG=ARSIN(SN)
      CALL RES(X,ETA(J)+RL,DEF,AM,SR)
      RAT1=(1.+(G-1.)*.5*MIN*MIN)/(1.+(G-1.)*.5*AM*AM)
      RM=AM*AM*G+WINV**2/RAT1-2.*AM*WINV*COS(DEF)*SQRT(G/RAT1)
      BETA=ANG-ATAN(AM*SIN(DEF)/(AM*COS(DEF)-WINV*SQRT(1./(G*RAT1))))
      U=SQRT(RAT1/RM)*((G-1.)*RM*SIN(BETA)**2+2.*G)/
     . ((G+1.)*SIN(BETA))+WINV*SIN(ANG)
      V=AM*SQRT(G*RAT1)*COS(BETA)
      P=(2.*RM*SIN(BETA)**2-(G-1.))/(G+1.)*SR*(RAT1**(G/(G-1.)))
      R=((G+1.)*P+G-1.)/(G+1.+(G-1.)*P)*SR*(RAT1**(1./(G-1.)))
      GO TO 10
      END
```

```
$IBFTC NSL14    DECK
      SUBROUTINE BP(F,YP,J,G)
      DIMENSION F(1),G(1),YP(1)
      COMMON /FRUS/ DELT,X2,X1,Y2,RSPHER,XMIN,XMAX,Y1,     IFR,RC,    STEP
      COMMON /CORNER/ JT,BPPP
      Y=YP(J)
      X=B(Y)
     . +BPPP
      IF(IFR.GT.0) GO TO 10
      F(J)=Y/X
      G(J)= (X**2+Y**2)/(X**3)
      GO TO 30
   10 IF(X .LT. (X2-X1)) GO TO 20
      F(J)=COS(DELT)/SIN(DELT)
      G(J)=0.
      GO TO 30
   20 F(J)=(RC+Y-Y2)/X
      G(J)=((RC+Y-Y2)**2+X**2)/(X**3)
   30 RETURN
      END
$IBFTC NSL15    DECK
      SUBROUTINE DERIV(H,I,J,DH)
      DIMENSION H(25,25)
      COMMON DLY,DUM(2),IM,JM
      DH=(H(I  ,J+1)-H(I  ,J-1))/(2.*DLY)
      RETURN
      END
$IBFTC NSL16    DECK
      SUBROUTINE EXTRA(F)
      DIMENSION F(25)
      COMMON /CORNER/ JM
      F(JM) = 2.*F(JM-1) - F(JM-2)
      RETURN
      END
$IBFTC NSL17    DECK
      SUBROUTINE INITL(JT,RFIT,CD)
      REAL MIN
      INTEGER EPS
      COMMON DLY,DLZ,DLT,
     X        IM,JM,RMAT(25,25),RNEW(25,25),PMAT(25,25),PNEW(25,25),
     1      VRMAT(25,25),VRNEW(25,25),VZMAT(25,25),VZNEW(25,25),
     2      XI(25),ETA(25),W(25),WNEW(25),DELTA(25),DBDY(25),COT(25),G,
     3       D2BDY(25),D2ADY(25),EPS
      COMMON /FRESTM/ VIN,RHOIN,PIN,VIN1,MIN,RL
      COMMON /BLNT/ STPP,NSTOP
      COMMON /FRUS/ DELT,X2,X1,Y2,RSPHER,XMIN,XMAX,Y1,IFR,RC,STEP
      COMMON /CORNER/ JT,BPPP
      READ(5,900) IM,JM,JT,EPS,IFR,NSTOP
      IF(JT .LT. JM) JT=JM
      READ(5,901) RMAX,DLT,RSPHER
      READ(5,901) PIN,RHOIN
      IF(IFR .GT. 0) READ(5,901) X2,Y1,Y2
      IF(IFR .EQ. 2) READ(5,901) XMIN,XMAX,DELT
      IF(IFR .NE. 2) GO TO 3
      DELT=DELT*3.1415926/180.
```

```
      RL=RSPHER
    3 Y1=Y1-RL
      Y2=Y2-RL
      RMAX=RMAX-RL
      BPPP=0.
      IF(IFP .EQ.0) GO TO 4
      ALL=(Y2-Y1)/SIN(DELT)
      RC=ALL/SIN(DELT*.5)*COS(DELT*.5)
      ETA(JM)=FLOAT(JM-1)*RMAX/FLOAT(JT-1)
      BPPP=SQRT(2.*RC*(Y2-ETA(JM))-(Y2-ETA(JM)**2))
      X1=X2-ALL*COS(DELT+1.)
    4 CONTINUE
      DLT=DLT*SQRT(PIN/RHOIN)
      DLZ=1./FLOAT(IM-1)
      DLY=RMAX/(FLOAT(JT-1))
      VIN=MIN*SQRT(G*PIN/RHOIN)
      VIN1=MIN*SQRT(G)
      ETA(1)=0.
      RB=RSPHER
      IF(IFP.NE.0) RB=Y2
      SSOD=RB*(4./MIN)*3.5/(7.*FLOAT(EPS+1))
      C1=B(0.)
      RSO=SSOD+X2
      DO 10 J=1,JT
      IF(J .EQ. 1) GO TO 5
      ETA(J)=(FLOAT(J-1)/FLOAT(JT-1)*RMAX)
      IF(J-JM) 5,5,6
    5 CALL BP(DBDY,ETA,J,D2BDY)
      DELTA(J)=(C1-B(ETA(J)))*.75+SSOD
      COT(J)=DBDY(J)/4.
      GO TO 7
    6 COT(J)=COT(JM)
      DELTA(J)=DELTA(J-1)-COT(J)*DLY
    7 CONTINUE

      IF(IFP .EQ. 0) GO TO9
    8 XSO=(RSO-SQRT(RSO**2-ETA(J)**2))*.5
      YY=AMIN1(ETA(J),ETA(JM))
      DELTA(J)=B(3.)+SSOD-XSO-B(YY)
      COT(J)=ETA(J)/SQRT(RSO**2-ETA(J)**2)
    9 CONTINUE
      W(J)=0.
   10 CONTINUE
      IF(RL .GT. .0001) CALL COFFER(XMIN,XMAX,RL,CD)
      RL=2.
      CD=0.
      DO 20 I=1,IM
   20 XI(I)=1.-FLOAT(I-1)/FLOAT(IM-1)
      DO 30 J=1,JT
      SN=SQRT(1./(1.+COT(J)**2))
      CALL RANKH(1,J,W,SN,1)
   30 CONTINUE
      PMAT(1,1)=EXP (PMAT(1,1))
      PMAT(IM,1)=PMAT(1,1)/(((2.*(2.*G*MIN**2-G+1.)*((G-1.)
     X      *MIN**2+2.))/((G+1.)**2*MIN**2*((G-1.)*MIN**2
     X      +2.)))**(G/(G-1.)))
      PMAT(IM,1)=ALOG(PMAT(IM,1))
```

```
      PMAT(1,1)=ALOG(PMAT(1,1))
      DO 35 J=1,JM
      PMAT(IM,J)=PMAT(IM,1)*SQRT(1./(1.+DBDY(J)**2))
      RMAT(IM,J)=RMAT(1,1)+(PMAT(IM,J)-PMAT(1,1))/G
   35 CONTINUE
      VRMAT(IM,1)=0.
      VZNEW(IM,1)=0.
      VRNEW(IM,1)=0.
      DO 40 J=2,JM
      V=SQRT(2.*G*(EXP(PMAT(IM,1)-RMAT(IM,1))-EXP(PMAT(IM,J)
     X      -RMAT(IM,J)))/(G-1.))
      SN2=1./(1.+DBDY(J)**2)
      VRMAT(IM,J)=V*SQRT(SN2)
   40 VZMAT(IM,J)=V*SQRT(1.-SN2)
      IF(JT-JM) 60,60,50
   50 JMP=JM+1
      DO 55 J=JMP,JT
      PMAT(IM,J)=PMAT(IM,JM)
      RMAT(IM,J)=RMAT(IM,JM)
      VZMAT(IM,J)=VZMAT(IM,JM)
   55 VRMAT(IM,J)=VRMAT(IM,JM)
   60 CALL NSMTH(PMAT,JT)
      CALL NSMTH(RMAT,JT)
      CALL NSMTH(VZMAT,JT)
      CALL NSMTH(VRMAT,JT)
      RETURN
  900 FORMAT(10I5)
  901 FORMAT(4E15.0)
      END
+00106

$IBFTC NSL18    DECK
      SUBROUTINE INDR1(G,GY,GZ,GYY,GZZ,GYZ,I,J)
      DIMENSION G(25,25)
      COMMON DLY,DLZ
      IF(J-1) 10,20,10
   10 GY=(G(I,J+1)-G(I,J-1))/(2.*DLY)
      GZ=-(G(I+1,J)-G(I-1,J))/(2.*DLZ)
      GYY=(G(I,J+1)+G(I,J-1)-2.*G(I,J))/(DLY**2)
      GZZ=(G(I+1,J)+G(I-1,J)-2.*G(I,J))/(DLZ**2)
      GYZ=-(G(I+1,J+1)+G(I-1,J-1)-G(I+1,J-1)-G(I-1,J+1))/(4.*DLZ*DLY)
      RETURN
   20 CONTINUE
      GY=0.
      GZ=-(G(I+1,J)-G(I-1,J))/(2.*DLZ)
      GYY=2.*(G(I,J+1)-G(I,J))/(DLY**2)
      GZZ=(G(I+1,J)+G(I-1,J)-2.*G(I,J))/(DLZ**2)
      GYZ=0.
      RETURN
      END

$IBFTC DMP      DECK
      SUBROUTINE KIKOFF
      X=-2.
      Y=X**3.79
      RETURN
      END
```

```
$IBFTC MSL61    DECK
      SUBROUTINE RES (X,Y,AA,BB,CC)
      DIMENSION TOT(3),F(3),COEF(6,4,40),XX(40)
      COMMON /CHAR/ COEF,KK
      DO 20 K=1,KK
      SUM=COEF(1,1,K)
      NFIT=4
      DO 10 N=2,NFIT
   10 SUM=SUM+COEF(N,1,K)*(Y**(N-1))
   20 XX(K)=SUM
      DIFF=1.E16
      DO 30 K=1,KK
      DIR=ABS(XX(K)-X)
      IF(DIR .GT. DIFF) GO TO 40
   30 DIFF=DIR
      K=KK
   40 K=K-2
      IF(K.LT.1)K=1
      U1=X-XX(K)
      U2=X-XX(K+1)
      U3=X-XX(K+2)
      U4=XX(K)-XX(K+1)
      U5=XX(K)-XX(K+2)
      U6=XX(K+1)-XX(K+2)
      F(1)=U2*U3/(U4*U5)
      F(2)=-(U3*U1)/(U4*U6)
      F(3)=(U1*U2)/(U5*U6)
      DO 70 I=1,3
      TOT(I)=0.
      DO 60 N=1,3
      NN=K +N-1
      NFIT=5
      SUM=COEF(1,I+1,NN)
      DO 50 L=2,NFIT
   50 SUM=SUM+COFF(L,I+1,NN)*(Y**(L-1))
   60 TOT(I)=TOT(I)+SUM*F(N)
   70 CONTINUE
      AA=TOT(1)
      BB=TOT(2)
      CC=TOT(3)
      RETURN
      ENTRY SHSHP(X,ANS)
      ANS=COEF(1,1,KK+1)
      DO 80 I=2,6
   80 ANS=ANS+COEF(I,1,KK+1)*(X**(I-1))
      RETURN
      END
```

```
$IBFTC NSL62    DECK
      SUBROUTINE COFFER(XMIN,XMAX,RFIT,CD)
      DIMENSION X(20),Y(20),P(20),DEL(20),AM(20)
      DIMENSION X1(20),Y1(20)
      DIMENSION HOL2(72)
      COMMON /CHAR/ COEF(6,4,40),KK
      LL=0
      KK=0
      READ(4) RFIT
      READ(4) HOL2
    5 READ(4) NNNN, NPTS ,NNNM
      DO 10 J=1,NPTS
      N=NPTS+1-J
10    READ (4) X(N),Y(N),DEL(N),P(N),AM(N)
      READ(4) CD
      NPTP=NPTS
      IF(X(NPTS).GT.XMAX)GO TO 50
      IF(X(1).LT.XMIN) GO TO 5
      IF(NPTS.LT.5) GO TO 5
      DO 20 K3=1,NPTS
      K1=NPTS+1-K3
      IF(X(K1) .GE. XMIN) GO TO 30
   20 CONTINUE
      GO TO 5
   30 DO 40 K2=1,NPTS
      IF(X(K2) .LE. XMAX) GO TO 45
   40 CONTINUE
      GO TO 50
   45 NPTS=K1-K2+1
      IF(NPTS.GE.5) GO TO 48
      K2=K1-4
      IF(K2.LT.1) K2=1
   48 KK=KK+1
      NFIT2=4
      X1(LL)=X(NPTR)
      Y1(LL)=Y(NPTR)
      LL=LL+1
      CALL POFIT(Y(K2), X(K2),NPTS,NFIT2,COEF(1,1,KK),ERR)
      NFIT2=5
      CALL POFIT(Y(K2), AM(K2),NPTS,NFIT2,COEF(1,2,KK),ERR)
      CALL POFIT(Y(K2),DEL(K2),NPTS,NFIT2,COEF(1,3,KK),ERR)
      CALL POFIT(Y(K2),  P(K2),NPTS,NFIT2,COEF(1,4,KK),ERR)
      GO TO 5
   50 REWIND 4
      LL=LL-1
      WRITE(6,900)(X(I),I=1,LL)
  900 FORMAT(4X6E16.8)
      NFIT1=MIN0(LL-1,5)
      CALL POFIT(X1,Y1,LL,NFIT1,COEF(1,1,KK+1),ERR)
      RETURN
      END
```

```
$IBFTC NSL63    DECK
       SUBROUTINE POFIT(X,Y,NPTS,NFIT,COEF,RRR)
       DIMENSION X(1),Y(1),COEF(1),C(30)
       CALL LSQPF(X,Y,0,NPTS,NFIT,C,IERR)
       WRITE(6,900) IERR,C
C       C 3,7,12,18,25
       J=0
       DIF=100.
       II=0
       DO 10 I=1,NFIT
       II=II+2+I
       IF(C(II) .GT. DIF) GO TO 10
       DIF=C(II)
       J=I
   10  CONTINUE
       DO 20 I=1,6
   20  COEF(I)=0.
       IBG=((J+1)*(J+2))/2-3
       II=J+1
       DO 30 I=1,II
       IBGN=IBG+I
   30  COEF(I)=C(IBGN)
       WRITE(6,901) COEF(1),(COEF(N+1),N=1,NFIT)
       RETURN
  900  FORMAT(10XI4/(4X6E16.8))
  901  FORMAT(15X6E16.8)
       END
```